ECONOMICAL ASSESSMENT OF HYDROGEN SHORT-RANGE AIRCRAFT WITH THE FOCUS ON THE TURNAROUND PROCEDURE

Master's Thesis
by
Jonas Mangold

Institute of Aircraft Design
University of Stuttgart

and

Institute of System Architectures in Aeronautics
German Aerospace Center (DLR)

Stuttgart, April 2021

University of Stuttgart
Germany

Institute of Aircraft Design

Head of Institute
Prof. Dr. Peter Middendorf
Prof. Dr. Po Wen Cheng
Prof. Dr. Andreas Strohmayer

Contact
Pfaffenwaldring 31
D-70569 Stuttgart
T +49 (0)711 685-62402
F +49 (0)711 685-62449

University of Stuttgart
Institute of Aircraft Design • Pfaffenwaldring 31 • D-70569 Stuttgart

Jonas Mangold
Karl-Stirner-Str. 17
73494 Rosenberg
Student No.: 2940456

Master's Thesis

Economical assessment of hydrogen short-range aircraft with the focus on the turnaround procedure

In order to achieve a long-term sustainable aviation, the energy carrier plays the most important role because it not just influences the economical behaviour of aircraft but also the climate impact and the required resources. Green liquid hydrogen produced via electrolysis and liquefaction procedures is one potential candidate, mainly driven by the lowest production costs of all electricity-based energy carrier. However, there are several questions to be answered. The most urgent ones are the liquid hydrogen tank design and integration, the climate impact of burning hydrogen at high altitudes and the ground handling/operation at the airport. The latter one especially focuses on the achievable turnaround times mainly driven by the refuelling rates and tank cooldown procedures. This constitutes an important factor influencing the economic competitiveness of the energy carrier liquid hydrogen.

The aim of this work is to investigate the limiting phenomena of the refuelling and cooldown process and their effect on the turnaround time and hence the impact on aircraft design and behaviour of the air vehicle.

Work Items

- Literature research of the conventional, Jet A-1 refuelling process and the relevance on the turnaround times
- Literature research of cryogenic fuel properties and cryogenic refuelling process and its influence on the turnaround times
- Work out the driving physical phenomena of the refuelling procedure and define possible future potentials
- Derive design recommendations for refuelling vehicles, aircraft concepts and airport infrastructure for various airport sizes and market penetration scenarios
- Define the impact of the cryogenic fuel properties, refuelling procedure and turnaround times on aircraft design
- Assessment of the economic behaviour and the influence as well as the sensitivity of the turnaround times driven by the refuelling and tank related variables using a cash-operating cost (COC) model

Thesis issued on	19 October 2020
Thesis submitted on	18 April 2021
Advisors	Nicolas Moebs (IFB) Daniel Silberhorn (DLR)

Stuttgart, 27 October 2020

Prof. Dr.-Ing. Andreas Strohmayer

IFB
Institute of Aircraft Design

Abstract

In order to achieve a long-term sustainable aviation, the energy carrier plays the most important role because it not just influences the climate impact and the required resources but also the economical behaviour of aircraft. Green Liquid Hydrogen (LH2) produced via electrolysis and liquefaction procedures is such a potential energy carrier. However, there are several questions to be answered, such as the operation at the airport. In this regard, the main focus is on the achievable turnaround times mainly driven by the refuelling rates and procedures. This constitutes an important factor influencing the economic competitiveness of the energy carrier LH2. The investigation of limiting phenomena of LH2 refuelling and its effects on the turnaround times, impact on aircraft design and hence the operational economic behaviour of the air vehicle is the aim of this thesis. Based on a comparison to Jet A-1 refuelling, new LH2 refuelling procedures are described and evaluated. Process steps that are considered are connecting/disconnecting, purging, chill down and refuelling.

Two methods for connecting and purging the refuelling system are developed, and their technical feasibility is investigated to enable coupling by a disconnect to the aircraft. Therefore, the avoidance of expensive helium for the purging process is targeted. In the next step, a lumped capacitance method is used to calculate the cooling process of warm pipelines in order to investigate the temporal influence under a reduced mass flow for low thermal stress. New limitations for LH2 refuelling are derived by applying dimensionless numbers of the Space Shuttle Loading and determining the dimensions and mass flow of the pipeline.

For the assessment of impacts on LH2 aircraft operation, changes on the level of ground handling vehicles are compared to current procedures with Jet A-1 refuelling of short-, medium- and long-range aircraft. In addition, the technical challenges at the airport for refuelling trucks as well as pipeline systems and dispensers are presented. Solutions are shown on how to handle vaporised hydrogen to generate minimal losses.

In addition to the technology solutions, explosion protection and applicable safety regulations are analysed and the overall refuelling process is validated including the influences on the turnaround process and cash operating costs. The comparison in terms of time needed is shown with the help of a Gantt chart and potentials for optimisation are described. The thermodynamic properties of LH2 as a real, compressible fluid are considered to derive implications for airport-side infrastructure. The advantages and disadvantages of a subcooled liquid are evaluated and cost impacts are transferred. Problems such as cavitation and two-phase flows are addressed.

Finally, implications on LH2 aircraft design are investigated. By understanding the thermodynamic properties, three calculation methods for the aircraft tank volume are shown. Losses of LH2 for a constant tank pressure in flight are derived, and thus an theoretical optimal insulation quality for the respective flight phase is defined. For longer ground or standstill times at the airport, the losses and the necessary procedure for a return flight without refuelling are presented.

Kurzfassung

Um die Luftfahrt der Zukunft nachhaltig zu gestalten, spielt der genutzte Energieträger die wichtigste Rolle, denn er beeinflusst nicht nur die Klimabelastung und die benötigten Ressourcen, sondern auch das wirtschaftliche Verhalten von Flugzeugen. Ein besonders vielversprechender Energieträger ist grüner Flüssigwasserstoff (LH2), der durch eine Elektrolyse und ein Verflüssigungsverfahren hergestellt wird. Es gibt jedoch noch einige offene Fragen in Hinblick auf die Nutzung von LH2, etwa bezüglich des Betriebs am Flughafen. Hierbei stehen vor allem die erreichbaren Turnaround Zeiten im Vordergrund, die hauptsächlich von den Betankungsraten und der Betankungsprozedur bestimmt werden. Diese Größen stellen bedeutende Einflussfaktoren für die wirtschaftliche Wettbewerbsfähigkeit des Energieträgers LH2 dar. Das Ziel dieser Arbeit ist deshalb die Untersuchung von begrenzenden Phänomenen der LH2 Betankung und deren Auswirkungen auf die Turnaround Zeiten, auf den Flugzeugentwurf und schließlich auf das betriebswirtschaftliche Verhalten des Flugzeuges. Basierend auf einem Vergleich zur Jet A-1 Betankung werden neue LH2 Betankungsprozeduren beschrieben und bewertet. Die betrachteten Prozessschritte sind An- und Abkoppeln (connecting/disconnecting), Spülen (purging), Abkühlen (chill down) und Betanken (refuelling).
Zwei Methoden zum Anschließen und Spülen des Betankungssystems werden entwickelt und ihre technische Machbarkeit untersucht, um ein Ankoppeln durch eine Schnellkupplung zu ermöglichen. Dabei wird die Vermeidung von teurem Helium für den Spülvorgang angestrebt. Im nächsten Schritt wird mit einer Lumped Capacitance Methode der Abkühlvorgang von warmen Rohrleitungen berechnet, um den zeitlichen Einfluss bei reduziertem Massenstrom für eine geringe thermische Belastung zu untersuchen. Es werden neue Begrenzungen für die LH2 Betankung abgeleitet, indem dimensionslose Zahlen des Space Shuttle Loadings verwendet und die Abmessungen und der Massenstrom der Pipeline bestimmt werden.
Für die Bewertung der Auswirkungen auf den Betrieb von LH2 Flugzeugen werden die Änderungen auf der Ebene der Bodenabfertigungsfahrzeuge mit den derzeitigen Verfahren bei der Jet A-1 Betankung verglichen. Darüber hinaus werden die technischen Herausforderungen für Betankungsfahrzeuge sowie Pipelinesysteme und Dispenser am Flughafen dargestellt.
Es werden Lösungen aufgezeigt, wie mit verdampftem Wasserstoff umgegangen werden kann, um lediglich minimale Verluste zu generieren. Neben den technischen Lösungen werden auch der Explosionsschutz und die geltenden Sicherheitsvorschriften analysiert und der gesamte Betankungsprozess inklusive der Einflüsse auf den Turnaround Prozess und die Betriebskosten validiert. Der zeitliche Vergleich wird mit Hilfe eines Gantt Diagramms dargestellt und Optimierungspotenziale werden erörtert. Die thermodynamischen Eigenschaften von LH2 als reales, kompressibles Fluid werden betrachtet, um daraus Implikationen für die flughafenseitige Infrastruktur abzuleiten. Des Weiteren werden die Vor- und Nachteile einer unterkühlten Flüssigkeit bewertet und deren Kostenauswirkungen bestimmt. Auftretende Probleme wie Kavitation und Zweiphasenströmungen werden beleuchtet.
Schließlich werden die Auswirkungen von LH2 auf den Flugzeugentwurf untersucht. Durch das Verständnis der thermodynamischen Eigenschaften werden drei Berechnungsmethoden für das Tankvolumen im Flugzeug aufgezeigt. Verluste von LH2 für einen konstanten Tankdruck im Flug werden abgeleitet und damit eine theoretisch optimale Isolationsgüte für die jeweilige Flugphase definiert. Die auftretenden Verluste und das notwendige Vorgehen für einen Rückflug ohne Betankung bei längeren Boden- oder Stillstandszeiten am Flughafen werden dargestellt.

Contents

Nomenclature

Abbreviations

ASK	Available Seat Kilometer
APU	Auxiliary Power Unit
BT	Block Time Supplement
COC	Cash Operating Cost
COP	Coefficient of Performance
DOC	Direct Operating Cost
ET	External Tank
EU	European Union
GH2	Gaseous Hydrogen
H2	Hydrogen (independent of the aggregate state)
HHV	Higher Heating Value
LFL	Lower Flammability Limit
LH2	Liquid Hydrogen
LHV	Lower Heating Value
LOX	Liquid Oxygen
LPFTP	Low Pressure Fuel Turbo Pump
MLM	Maximal Landing Mass
MTOM	Maximal Take-Off Mass
MZFM	Maximal Zero Fuel Mass
NBP	Normal Boiling Point
NPSH	Net Pressure Suction Head
$NPSH_a$	Net Pressure Suction Head available
$NPSH_c$	Net Pressure Suction Head critical
O2	Oxygen
OEM	Operating Empty Mass
ppm	parts per million
QD	Quantity Distance
SEC	Specific Energy Consumption
SFC	Specific Fuel Consumption
SLH2	Slush Liquid Hydrogen
SSME	Space Shuttle Main Engine
ST	Storage Tank
TRBS	Technical Rule for Operational Safety
TRGS	Technical Rule for Hazardous Substances
UFL	Upper Flammability Limit

Symbols

Latin

A	m^2	Area
Bi	–	Biot number
C	–	Coefficient
d	m	Diameter
D	N	Drag
g	$\mathrm{m/s}^2$	Gravitational acceleration
h	J/kg	Specific enthalpy
h	$\mathrm{W/m}^2\mathrm{/K}$	Heat transfer coefficient
H	m	Height
k	W/m/K	Thermal conductivity
L	m	Length
m	kg	Mass
M	–	Mach number
n	min^{-1}	Rotational speed
n_s	–	Specific speed
n_{ss}	–	Suction specific speed
Nu	–	Nusselt number
p	Pa	Pressure
P	W	Power
Pr	–	Prandtl number
Q	W	Heat
q	$\mathrm{W/m}^2$	Heat flow
Re	–	Reynolds number
S	m^2	Surface
T	K	Temperature
v	m/s	Velocity
V	m^3	Volume
x	–	Vapour Fraction
Z	–	Compressibility factor

Greek

α	min^{-1}	Refuelling factor of Jet A-1
Δ	–	Delta (Difference)
κ	–	Heat capacity ratio
λ	–	Friction factor
μ	$\mathrm{Pa} \cdot \mathrm{s}$	Dynamic coefficient of viscosity
ρ	$\mathrm{kg/m}^3$	Density
σ	N/m	Surface tension

Subscripts

a	absolute
b	bulk
c	characteristic
d	discharge
g	gauge
i	inner
l	liquid
o	outer
sat	saturated
s	suction
v	vapour
avg	average
boil	boiling
conv	convective
el	electrical
min	minimum
spl	single phase liquid
spv	single phase vapour

List of Figures

List of Tables

1 Introduction

The European Commission's Green Deal with the goal of carbon neutrality by 2050, also challenges the aviation industry to break new ground [91]. Considering the worldwide increasing air-travel demand, it becomes clear that the goal of decarbonisation can only be achieved through new energy sources and innovative aircraft configurations. In addition to carbon dioxide (CO2), the harmful greenhouse gases emitted during kerosene combustion include water vapour (H2O), carbon monoxide (CO), oxidise of nitrogen (NOX), soot, aerosols and unburned hydrocarbons (UHC) [74, 152, 62]. Two-thirds of the emitted CO2 comes from short and medium-range aircraft, which account for 70 % of the global fleet [91].

Hydrogen (H2) is a versatile and clean energy carrier that can be produced renewably by electrolysis. Green H2 thus offers enormous potential to contribute to sustainable development and growth in aviation. In addition, H2 holds great promise for addressing the challenges of climate change, energy supply and distribution. Due to its higher gravimetric specific energy than kerosene (factor 2.8), H2 is a natural choice as a fuel for aviation. When H2 is burned, the primary combustion product is only water, and the secondary emissions are nitrogen oxides. Other emissions, such as CO2, are eliminated because H2 is not a hydrocarbon fuel. H2 is also a fuel with few contaminants, greatly reducing particulates in the engine exhaust. Moreover, in addition to combustion, H2 offers the possibility of conversion to electrical energy through a fuel cell. Given the increased public awareness of the problem of global warming and greenhouse gas emissions, the question arises to what extent the expansion of aviation should be limited without the use of renewable energy.

Sustainable aviation fuels are the main competitors of H2. Synthetic kerosene produced by the power to liquid (PtL) process, assuming electric energy as the power source as well as CO2 captured from the air and water as primary resources [129], is one possibility. Using PtL, the aircraft design does not change, and the airport does not need new infrastructure. In contrast, the energy required for production is greater, which means that the fuel price is higher than LH2. In addition, CO2 is produced during combustion, which was previously filtered out of the air at great expense.
However, H2 has a disadvantage when used as a fuel, especially in aviation, because its density is much lower than kerosene. This difference leads to larger tank volumes, which have a negative effect on the wetted area and increase aerodynamic drag. In principle, H2 can be stored in different aggregate states and different pressure ranges. Gaseous hydrogen (GH2) is stored under ambient temperature and high pressures of up to 700 bar, although the volume required for the same energy amount is still seven times higher than that of kerosene. To obtain a higher density and reduce the pressure to an acceptable level, the H2 is liquefied by cooling it to 20 K at ambient pressure. Liquid hydrogen (LH2) requires only four times the volume to store the same amount of energy compared to kerosene. Another densification method is Slush Liquid Hydrogen (SLH2), where a part of the mixture consists of frozen H2. However, this method is not investigated further because the physical properties would change too much and several additional challenges arise.

Due to the cryogenic temperatures of LH2, the tank needs insulation to keep the heat input low. The heat input causes LH2 to heat up, which leads to evaporation and pressure build-up in the tank. This also defines the dormancy time, which describes the period between closing the tank and reaching the maximum operating pressure and venting. The maximum pressure must be increased to extend the dormancy time, or the insulation quality must be increased. The pressure build-up due to the heat input is also called self-pressurisation.
LH2 has been used as a fuel in astronautics for quite some time because its properties are well suited as rocket fuel, regardless of the climatic effect. There are also research initiatives in the automotive industry to use H2 as a fuel for a fuel cell or an internal combustion engine. For duty transport, which accounts for a large share of pollutant emissions, H2 is suitable because of its zero greenhouse gases in case of a fuel cell.

For the use of LH2 as a fuel in aviation, it must be possible to implement the turnaround and refuelling at the airport. This process should be carried out without any safety risk and without any time extension, as otherwise the operating costs would increase and the economic competitiveness would not be guaranteed. The main objective of this thesis is to investigate the refuelling process of LH2 for short-range aircraft. The investigation of the refuelling process refers to the analysis of different processes necessary due to the use of LH2. Another question to be answered is the feasibility of implementation at the airport through a required infrastructure. Initial assertions indicate that the refuelling process could be two to three times longer than with Jet A-1 [160]. This claim is based on the questionable assumption of a volume flow of 900 l/min, which is supposedly the same as with Jet A-1 [91].
This significant extension of the refuelling process would have a far-reaching impact on the annual utilisation of the aircraft. Therefore, an economic assessment of the impact on a change in turnaround time is considered. In the investigation of the refuelling process, the comparison to conventional refuelling with Jet A-1 is particularly needed, as boundary conditions and limitations can be analysed and derived for LH2. Therefore, a comparison with the aerospace and automotive industries is also helpful, as the application is already taking place there. Daimler and Linde have already developed a refuelling system with LH2. A much faster refuelling is made possible by subcooled LH2 [41].

The energy carrier LH2 requires other aircraft configurations because the classic arrangement with the tank in the wing no longer works. Studies on the overall aircraft design and airport infrastructure have been made since the 1970s [147, 25, 27]. The Tupolev Tu-155 was an experimental aircraft used to test alternative fuels from 1988 to 1989 [132]. The characteristic of the aircraft configuration was the chimney on the vertical tailplane, which was used for safe venting. Brewer [26, 28, 29] and Airbus [10] with Cryoplane have demonstrated the potential of LH2 as a fuel in aviation and provide the basis for further research and development towards LH2-fuelled aircraft.

2 State of the Art

This chapter introduces technologies that are relevant for LH2-fuelled aircraft and its turnaround. Firstly, the general properties of H2 with a focus on the liquid state are presented. Secondly, the fuelling of other comparable non-aircraft applications is considered. Thirdly the refuelling process of Jet A-1 is analysed to have a comparable basis for the influence of an LH2 aircraft. Finally, an introduction to the state of the art cash operating cost calculation method is introduced.

2.1 Properties and Operation of Hydrogen

Hydrogen is the most abundant chemical element in the universe, but on earth, especially in the atmosphere, free diatomic hydrogen can be found only in negligible amounts. H2 exists in almost all organic compounds as well as in water in a combined state. Sufficiently large quantities on the earth's surface are available as a chemical component of water. Whereas in gaseous form, it cannot be held within the atmosphere by the earth's gravity. [110, 81]

The basic properties and handling of hydrogen are described in the following section. Hydrogen has a Higher Heating Value (HHV) of 141.78 kJ/kg and a Lower Heating Value (LHV) of 119.95 kJ/kg during combustion [80]. These values differ due to the aggregate state of the combustion product. The HHV is determined with liquid water and the LHV with vapour as the combustion product. The distinction between these values becomes relevant in consideration of the manufacturing process later on. However, useful energy refers to the LHV.

When mixed with air, the ignition limits of hydrogen are between the Lower Flammability Limit (LFL) of 4 vol.% and the Upper Flammability Limit (UFL) of 75.7 vol.%. This concentration range changes in pure oxygen (O2) to a UFL of 94 vol.%. A further distinction can be made between the detonation limits, where the concentration limits are between 18.3 and 58.9 vol.%. [105]
The difference between a detonation and an ignition is forming a shock front with supersonic velocity, which is associated with a distinctive pressure shock. The minimum ignition energy of H2 is 0.017 mJ [105], which is more than an order of magnitude lower than other fuels.

The zero-emission production of H2 is done by electrolysis, in which water is chemically split. In this process, electrical energy is converted into chemical energy. However, the electrical energy must be generated from renewable energy sources to ensure the electrolysis and production of emission-free hydrogen. The splitting of water into oxygen and hydrogen requires a high theoretical energy input of 286 MJ/kmol, which corresponds to the HHV [68]. The efficiency of electrolysers is also defined in comparison to the HHV. Depending on the system design and size, efficiencies of 60 to 85 % (related to the HHV) result [80, 112, 110]. For the subsequent energy consumption, a required energy input for electrolysis of 180 MJ/kg H2 is assumed, which corresponds to an efficiency of 78.8 %.

The liquefaction of the GH2 after electrolysis is principally achieved by isothermal compression followed by isenthalpic expansion. For the different systems, a reference is made to Cardella [34]. For the liquefaction of GH2, a further 18 to 45 MJ/kg of energy is required. [80, 85, 139, 34, 32]
The system's efficiency refers to the work of an ideal reversible Carnot process, which in turn depends on the system properties, such as the pressure. In the following work, a liquefaction energy of 30 MJ/kg H2 is considered in further analysis. Conversely, 25 % of the later usable energy (LHV) must be applied to liquefy hydrogen. The addition of the energies required for the emission-free production of LH2 results in a value of 210 MJ/kg, used in the following work as the basis for cost evaluation.

For the storage of H2 in vessels, the diffusion property must be considered. However, the permeation of hydrogen molecules is negligible in metallic tank walls. The volatilisation of H2 is prevented in composite materials by an internal metallic liner. In pure composite materials, however, the permeation rate is not negligible in practical applications. [161]
A distinction is made between four types of tanks for mobile use, in which the wall construction differs. Type 1 is the typical steel tank. A liner made of metal (steel or aluminium), which is partially (type 2) or completely (type 3) wrapped with a fibre reinforced composite material, is used. Type 4, on the other hand, is the liner itself made of carbon fibre reinforced polymer.

Diffusion causes hydrogen embrittlement in the material, where ionised hydrogen enters the crystal structure and causes stresses. This effect leads to accelerated crack growth and material failure. The susceptibility to hydrogen embrittlement depends on various boundary conditions, such as the type of crystal structure, surface properties and load. Hard high strength steels are susceptible to embrittlement. In contrast, soft low carbon steels, austenitic steels and certain aluminium alloys are not. [80, 161]
For the choice of materials, the following work limits the selection to aluminium alloy 6061 and stainless steel X5CrNi18-10 (AISI 304), which are suitable for GH2, LH2, and SLH2 [105].

The hazardous substances ordinance of H2 is based on the chemicals directive, where GH2 is classified as an extremely flammable gas. No toxic effect or harm to the environment is defined, which means that no maximum permissible working concentration is specified. For LH2, additional cold burns or injuries due to the cryogenic temperatures have to be considered. [80]

2.1.1 Thermodynamic Properties

A hydrogen molecule can occur in two different energetic states characterised by the orientation of the spins in the atomic nucleus. The spin denotes the rotation of an elementary particle around its own axis. In orthohydrogen, the nuclear spins are oriented in parallel. In the case of opposite spins (anti-parallel or paired), one refers to parahydrogen. This distinction is relevant because the energy level differs. Parahydrogen has lower rotational energy and thus a lower energy level. A transition from orthohydrogen to parahydrogen releases energy, which must be taken into account in the calculation. Above a temperature of 220 K, a mixture of 75 % orthohydrogen and 25 % parahydrogen is present, see Figure 2.1, which is referred to as normalhydrogen. During liquefaction, this additional energy to be dissipated must be considered. At equilibrium, LH2 consists of 99.8 % parahydrogen. Equilibrium hydrogen refers to a mixture in thermodynamic equilibrium. [81, 80, 110]

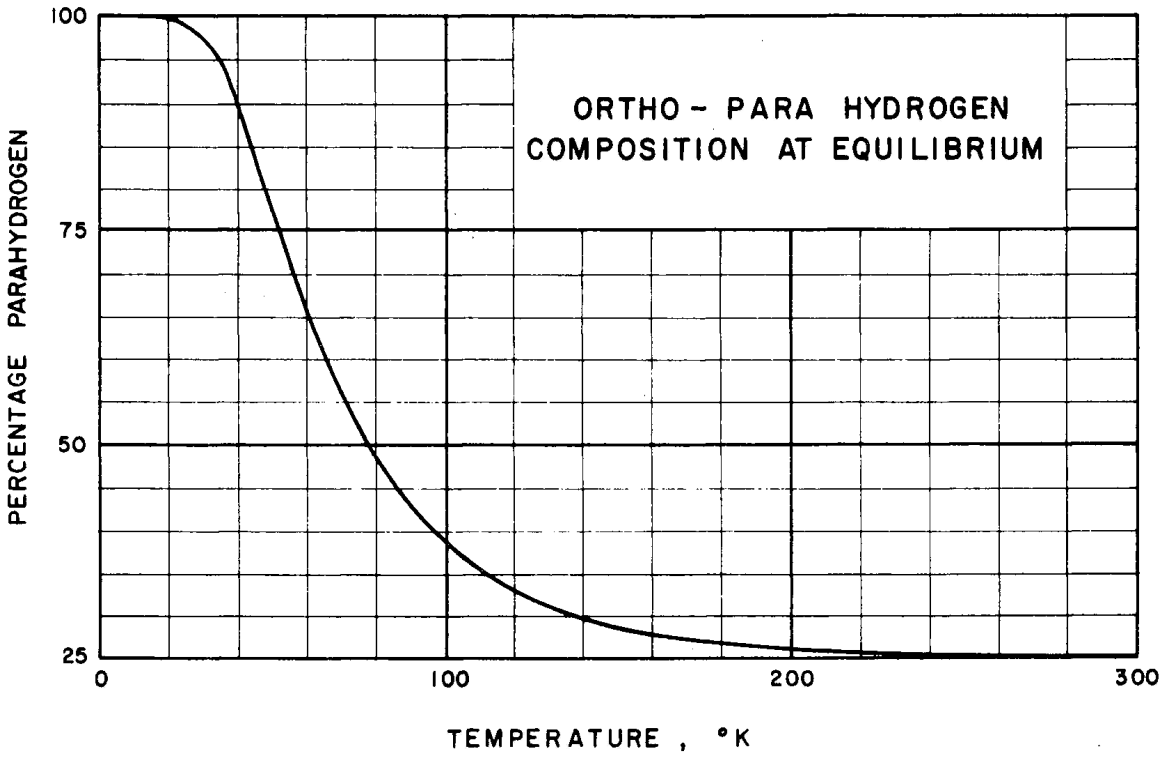

Figure 2.1: Ortho-para hydrogen composition at equilibrium [22]

Due to the high proportion of parahydrogen in the equilibrium state, the physical values of parahydrogen are used in the following work. Table 2.1 shows important fixed points for parahydrogen.

	Temperature K	Pressure bar_a	Density kg/m^3
Triple Point	13.80	0.0704	$\rho_{solid} = 86.50$
			$\rho_{liquid} = 77.03$
			$\rho_{vapour} = 0.13$
Normal Boiling Point	20.39	1.01325	$\rho_{liquid} = 70.78$
			$\rho_{vapour} = 1.34$
Critical Point	32.94	12.86	$\rho = 31.43$

Table 2.1: Fixed points for parahydrogen [81, 90, 117]

Figure 2.2 shows a phase diagram of hydrogen. The fixed points shown in Table 2.1 can also be seen. Furthermore, the sublimation line, melting line, and vapour-liquid saturation line show the different phase regions of hydrogen.

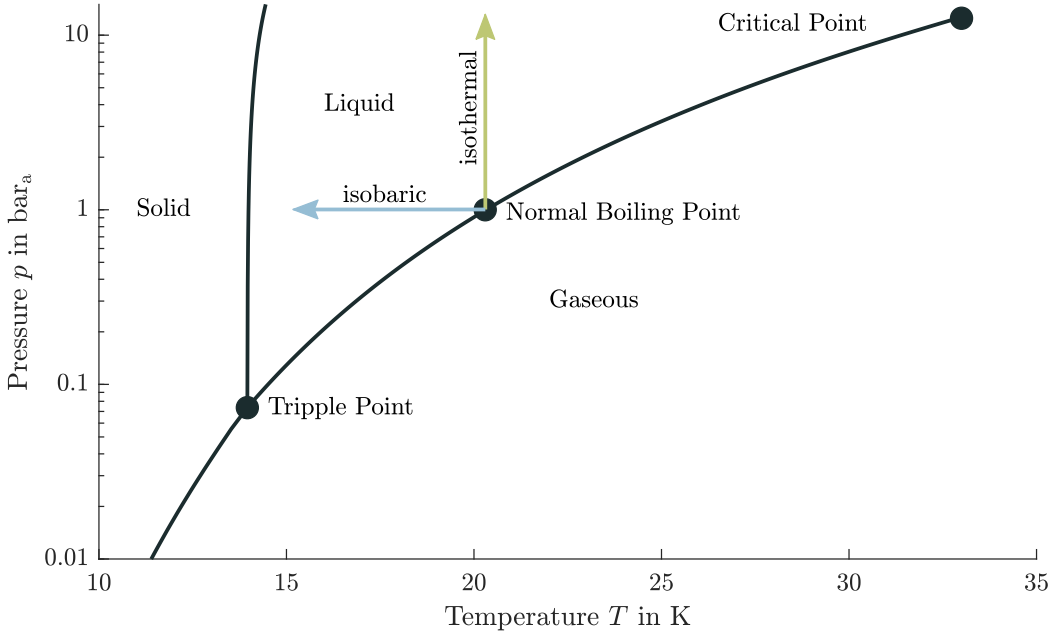

Figure 2.2: Phase diagram of parahydrogen [83]; isothermal and isobaric subcooling starting from Normal Boiling Point (NBP)

A distinction must be made between two regions: the ideal gas and the real gas when determining the gaseous phase's state variables. At pressures significantly lower than the critical pressure and temperatures significantly higher than the critical temperature, the state variables can be calculated using the ideal gas equation [80]. On the other hand, at low temperatures and high pressures, the ideal gas equation is no longer sufficient to account for real gas effects, such as the attractive forces and interactions between molecules and their own volume. One possibility to take the real gas behaviour into account is the compressibility factor Z, see Equation 2.1. This represents the deviation from the ideal gas state and is an empirical function of temperature and pressure. Diagrams for the compressibility factor can be found in [80, 90].

$$p \cdot V = Z \cdot m \cdot R \cdot T \tag{2.1}$$

In the liquid phase, however, the ideal or real gas law no longer applies. With a 14-term fundamental equation of state, the liquid phase can also be calculated [81]. However, there is a significant difference between a saturated liquid and a subcooled liquid.
First, the saturated liquid is explained, which describes the state on the saturated liquid line and in the temperature-entropy diagram with a vapour content of $x = 0$. In this case, the density can be calculated by the temperature or the pressure and does not require both state variables. The saturation line thus represents the beginning of the wet vapour region, which is a two-phase region of vapour and liquid. By reaching this state, for example, by heat input, the liquid is boiling. Further energy inputs at this point cause the liquid to vaporise and increase the vapour content. The enthalpy of vaporisation or latent heat Δh_v results from the enthalpy difference between the saturated liquid line (boiling line) ($x = 0$) and the saturated vapour line ($x = 1$). This parameter describes the amount of energy required to vaporise the liquid and is a function of the pressure.

Secondly, the explanation of the properties of a subcooled (or compressed) liquid: The term subcooled describes a liquid in the single-phase region and therefore not on the saturated liquid line. There are two ways to generate a subcooled liquid, see Figure 2.2, starting from the saturated liquid line [21]:

1. By removing heat, the degree of subcooling can be specified by the removed enthalpy (ΔH). This change of state takes place under constant pressure and is therefore isobaric.

2. By increasing the pressure of the liquid. An isothermal change of state occurs, defined by overpressure (Δp) to the saturation line.

Due to the subcooling of the liquid, the state variables deviate from the saturation line. Thus, the temperature of the subcooled fluid is below the equilibrium temperature. The first advantage of this state is that the H2 can thus absorb heat until thermodynamic equilibrium is reached, without any vaporisation losses [80].
The calculation of the state variables, such as density, enthalpy and entropy, are a function of temperature and pressure. Due to the much more complex equations for determining the quantities, a database should be used to calculate changes of state. In this work, these data come from the tool RefProp [83]. Basic tables and diagrams on substance properties can be found at McCarty et al. [90] to get an overview of LH2. To summarise these properties, LH2 must be treated as a real compressible fluid.

Another parameter for the design of short-time tanks is the characteristic curve of vapour pressure over temperature, as shown in Figure 2.3. This diagram is a modified representation of the saturated liquid line from Figure 2.2. The increasing curve of vapour pressure reflects the behaviour over time for cryogenic tanks. If the temperature of the fluid increases due to environmental influences, the vapour pressure will also increase. This, in turn, means that if a certain subcooled level is maintained, the liquid pressure must also increase. Therefore no subcooled level also means a two-phase regime, which leads to considerable problems.

Similar to the subcooled level, there are two simplified ways to enter this two-phase region, see Figure 2.3. As just explained, on the one hand by a temperature rise of the liquid in the tank due to environmental influences. On the other hand, by a pressure drop under isothermal conditions. This scenario can be divided into two cases. A sudden pressure drop in the tank, for example, due to the failure of a valve, would cause the liquid to boil out (flash evaporation) until the saturated state is reached. Additional information on thermodynamics and the calculation of two phases can be found in Baehr et al. and Bostock et al. [14, 21].

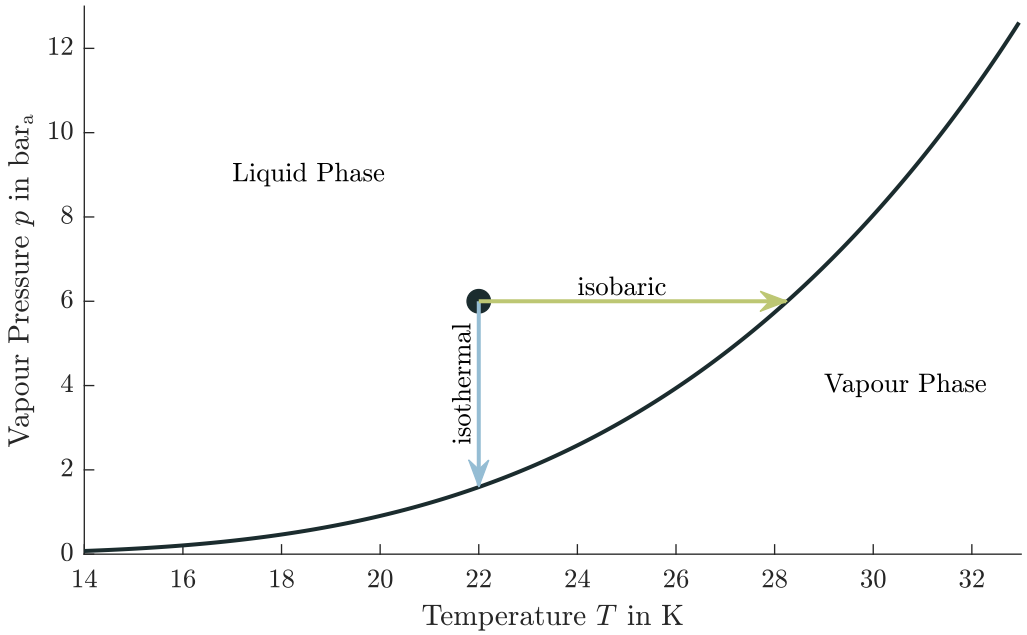

Figure 2.3: Vapour pressure of parahydrogen as a function of temperature [83, 22]; reaching two-phase condition with isobaric temperature increase and isothermal pressure drop

Flow cavitation also corresponds to a pressure drop but through a local increase in velocity. Therefore, the fluid is expanded or accelerated, and the static pressure drops below the saturation pressure and evaporates ($p < p_{\mathrm{vapour}}$). The fundamental difference of cavitation from flash evaporation lies in the further consideration of the vapour bubble. There is again a higher static pressure downstream of the pressure drop due to the deceleration of the flow, which causes the vapour bubbles to implode ($p > p_{\mathrm{vapour}}$). [63]
These impinging vapour bubbles can cause cavitation erosion, vibration, or pressure pulsation [63]. Damage to the material mainly occurs in pumps, more precisely in pump impellers, which leads to the next chapter.

Furthermore, for the liquid storage of hydrogen in tanks, it must be noted that there must always be a gas layer above the liquid phase.
The ullage above the liquid in sealed tanks is the extra gas volume. This additional volume is needed to allow for thermal expansion of the liquid, accumulation of gases initially dissolved in the fuel, or gaseous products from slow reactions within the fuel during storage. [143]
Therefore, a two-phase mixture must always be present in the tank at all times to avoid excessive pressure fluctuations [153]. However, this statement does not mean in general that the contents of the tank must be in the two-phase (liquid vapour saturation) region in the T-s diagram and must become a saturated state. There must only be a gaseous component to absorb the density changes of the liquid due to the compressibility of the gas. As a result of the compressibility of the gas, the pressure in the tank does not increase excessively. Hence, in non-thermodynamic equilibrium, there can be a subcooled liquid and a hotter gas in the tank. However, when thermodynamic equilibrium is reached, the ullage and liquid temperatures are equal, and the vapour pressure curve balances out.

2.1.2 Cryogenic Pump System and Design Parameters

In principle, there are two ways of feeding the fuel to the engine to ensure the required mass flows and pressures through a suitable system. On the one hand, expelling or displacing can be achieved by pressurising the tank with a high-pressure system. On the other hand, the mass flow can be moved by pumps divided into a low-pressure pump near the tank and a high-pressure pump near the engine. [143, 70]
A pressurised gas feed system is discussed in Section 3.3.1. According to Huzel et al. [70], there is no simple rule that justifies system choice. Instead, a variety of parameters, such as the vehicle's mission, size and weight, thrust level and duration, and space available for the propulsion system, are decisive on reliability considerations. However, both feed systems always require some pressurisation gas system.

Cavitation leads to the diminution and fluctuation of the pump discharge mass flow due to excessive vapour formation. In rocket engines, this vapour bubbling can reduce thrust and make combustion erratic and dangerous. [143]
Additionally, cavitation can degrade pump performance or other systems [119]. Furthermore, it can result in flow instabilities, and substantial damage [70]. Therefore, pumps without vapour formation are necessary and are described below based on significant pump parameters.

The pressure head H of a fluid pump is the added energy transferred from the pump to the fluid. This can be derived from the incompressible energy head equation of Bernoulli's equation:

$$H = \frac{p_\mathrm{d} - p_\mathrm{s}}{\rho \cdot g} + \frac{{v_\mathrm{d}}^2}{2 \cdot g} \tag{2.2}$$

The head and the volume flow are independent of the density of the type of medium by expressing them as the energy head method. Whereas the pressure rise, and mass flow are dependent on the medium. [131]
Considering compressibility, the pressure head is typically defined as an isentropic enthalpy rise from inlet conditions to discharge pressure. Therefore, the specific head depends on the thermodynamic condition, because in an isentropic pressure increase the temperature rises, too. The incompressible relationship can generally be used as a first approximation for small pressure changes below 70 bar. [71]
The difference between the incompressible and isentropic approach for calculating the pump power is the temperature rise of the isentropic change of state. Considering that the state variables of LH2 are close to the vapour pressure curve, this increase in temperature becomes relevant to prevent two-phase flows.

Volume flow Q, pressure head H and rotational speed n are the three parameters that characterise a pumping performance and thus largely determine the type of impeller and pump design. The specific speed n_s is a key figure derived from the similarity conditions, making it possible to compare impellers of different sizes and operations. Moreover, it can be used to classify their optimum design and the shape of the associated characteristic curves in different operating data. [63]

Because the specific speed is a dimensional parameter, the magnitude varies depending on the units used. In the following equation, the common variants in metric and imperial units are listed. In the following work, metric units are used.

$$n_s \left(\mathrm{min}^{-1}, \mathrm{m}^3/\mathrm{s}, \mathrm{m}\right) = n \cdot \frac{\sqrt{Q}}{H^{3/4}} \tag{2.3}$$

$$N_s \left(\mathrm{min}^{-1}, \mathrm{gpm}, \mathrm{ft}\right) = n \cdot \frac{\sqrt{Q}}{H^{3/4}} = 51.64 \cdot n_s \tag{2.4}$$

Values for the specific speed ranging in the literature between 1 (radial impeller) and 400 (axial impeller) [63, 143, 70]. Low values of the specific speed characterise pumps with low volume flow and high head rise. The indication for high volume flow and low-pressure rise is a higher specific speed [71].
An increase in rotational speed raises the pump specific speed. It can also increase the pump efficiency, which can reduce the number of stages. This makes the pump lighter, which in turn has advantages in the design. On the negative side, there is an increase in the pump inlet requirements to avoid cavitation and higher wear of the pump and an increase in costs. [131]

The second important parameter in the pump design is the suction specific speed n_{ss}, which is used to characterise the suction behaviour of the pump. This parameter makes it possible to compare pumps that are not geometrically similar. It is defined as follows [63]:

$$n_{ss} \left(\mathrm{min}^{-1}, \mathrm{m}^3/\mathrm{s}, \mathrm{m}\right) = n \cdot \frac{\sqrt{Q}}{\mathrm{NPSH_c}^{3/4}} \tag{2.5}$$

$$N_{ss} \left(\mathrm{min}^{-1}, \mathrm{gpm}, \mathrm{ft}\right) = 51.64 \cdot n_{ss} \tag{2.6}$$

The suction specific speed is derived from similarity conditions for cavitation states and is calculated in the same way as the specific speed. For rocket propellant pumps, the design values of suction specific speeds range from 200 without inducers to values over 2000 for certain propellants with inducers [71].
The specific speed refers to the critical Net Positive Suction Head $\mathrm{NPSH_c}$. To avoid cavitation or limit it to an acceptable level, the pressure upstream of the impeller must be above the vapour pressure of the fluid by a certain value. This pressure head difference or minimum suction head above the vapour pressure head describes the $\mathrm{NPSH_c}$ and is, therefore, a pump-specific value. Therefore, the $\mathrm{NPSH_c}$ value is also a measure of the level at which a subcooled liquid must be present. The increase does not exceed the saturated liquid line in velocity and the drop in static pressure.

If the impeller or inducer operates above its suction specific speed limit, excessive cavitation will occur, and the pump will not deliver the required pressure rise. In other words, a reduction of inlet NPSH below $\mathrm{NPSH_c}$ results in a rapid decrease of the developed head and causes nonsteady flow. Furthermore, it can cause physical damage to the hardware and increase oscillations. [131, 71]

To prevent these phenomena and avoid cavitation during a pump's operation, the pump-inlet available Net Positive Suction Head $\mathrm{NPSH_a}$, must be higher than the critical NPSH.

$$\mathrm{NPSH_a} > \mathrm{NPSH_c} \tag{2.7}$$

The $\mathrm{NPSH_a}$ is the difference between the pump inlet total pressure head and the liquid vapour pressure, expressed as follows [143]:

$$\mathrm{NPSH_a} = H_{\mathrm{tank}} + H_{\mathrm{elevation}} - H_{\mathrm{friction}} - H_{\mathrm{vapour}} \tag{2.8}$$

$$\mathrm{NPSH_a} = \frac{p_{\mathrm{t,ullage}}}{\rho \cdot g} + H_{\mathrm{elevation}} - \frac{\Delta p_{\mathrm{friction}}}{\rho \cdot g} - \frac{p_{\mathrm{vapour}}}{\rho \cdot g} \tag{2.9}$$

The inlet total pressure head is determined from the absolute ullage gas pressure in the tank above the liquid level, the elevation of the propellant level above the pump inlet, friction losses in the line and the vapour pressure of the fluid [143]. In Figure 2.4, these various heads are defined.

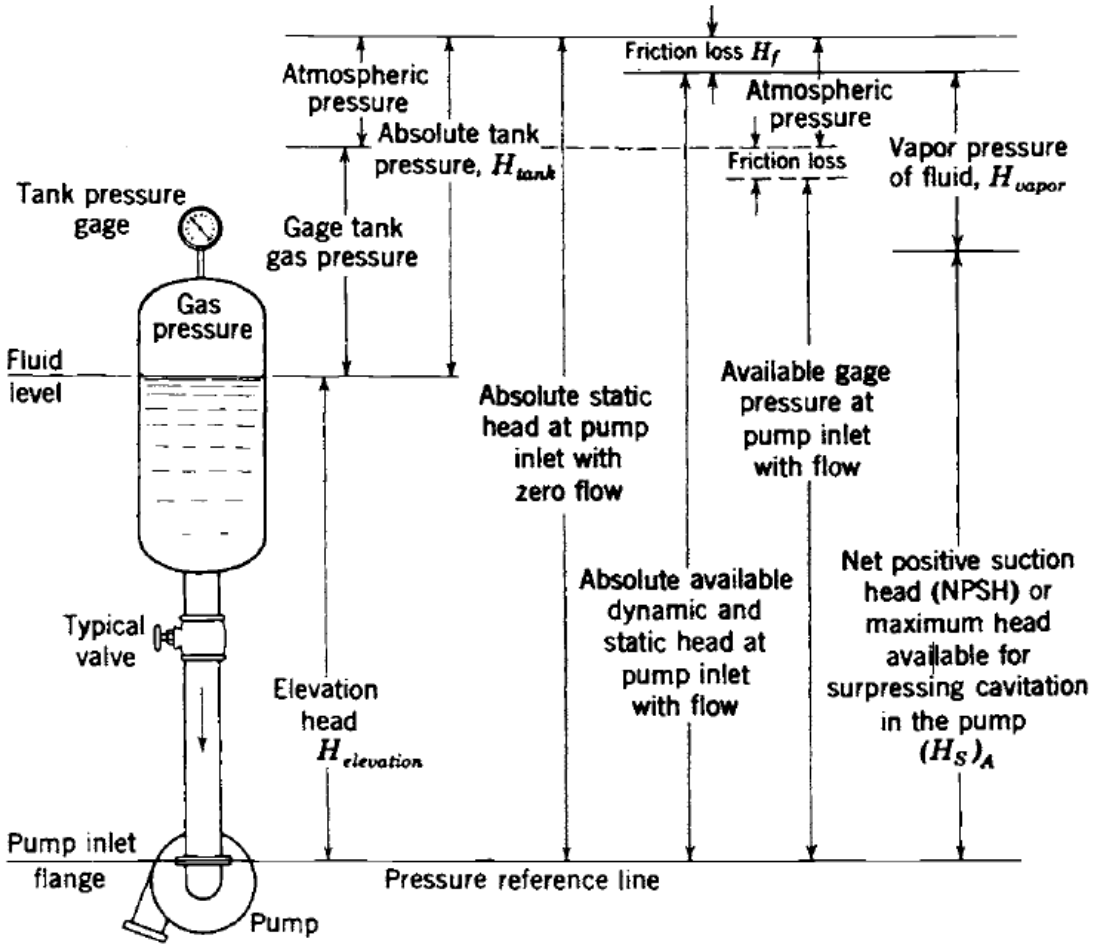

Figure 2.4: Definition of $\mathrm{NPSH_a}$ [143]

According to Sobin et al. [131], there are three methods to correct the problem of an insufficient NPSH for the pump to meet design requirements:

1. Increasing tank pressure, which increases the supplied pressure head but also raises the required tank wall thickness and weight
2. Decreasing the rotational speed to meet the requirements for a suction specific speed but also decreasing pump efficiency and increase pump weight
3. Redesigning the inlet of the pump by using a larger diameter and reducing friction losses, but pump efficiency can decrease

As already described in Section 2.1.1, LH2's vapour pressure is a function of temperature. Thus, this means that the $NPSH_a$ value of the tank is also a function of the fluid's temperature. This has strong effects during the flight phase since the temperature changes due to a variety of influences. Furthermore, the conditions at the tank inlet can be reduced by refuelling with subcooled LH2. The lower temperature of LH2 reduces the vapour pressure and, at constant NPSH, the absolute pressure in the tank is also reduced. The refuelling of subcooled LH2 is analysed in Section 4.1 and its effects in Section 4.2.

For rockets, with short launch phases, this influence plays a minor role but is also considered. In the tank design, this increasing vapour pressure with temperature is taken into account. With a liquid temperature increase from 22 to 23 K, the tank pressure must increase by 0.46 bar [71]. With a usual nominal pressure in space applications of 2.2 bar_a when feeding with pumps [143, 134], this is a significant additional pressure increase. From the higher pressure follows a larger wall thickness and hence an increase in structural mass. Or, conversely, in a reduction of the payload.

Values of $NPSH_c$ for LH2 pumps range from 5 to 178 m [70, 119, 126]. Two values that have proven themselves in reality are particularly interesting. The Space Shuttle Main Engine (SSME) has an $NPSH_c$ value of 56 m for LH2 [52]. In addition, the engine of the second stage of the Saturn V has a value of 100 m [126].

However, the pumping of saturated liquids can also be accomplished with a Zero-NPSH pump. In this case, the $NPSH_c$ of the pump will be 0. This approach means that there does not have to be any subcooled liquid in the tank. Zero-NPSH means that the liquid is in a saturated state, i.e. the tank pressure corresponds to the vapour pressure. Suction at the pump inlet causes the static pressure to fall below the vapour pressure, and a certain amount of the liquid vaporises. With specially designed low-pressure pumps that allow a volume fraction of 30% to 50%, a pressure rise of up to 7 bar can be realised without surging, pressure drop, or damage [45]. On the other hand, for an effective Zero-NPSH pump, a phase separator must be fitted [112]. A subcooled liquid is created in the pump outlet due to the pressure build-up [33].
By pumping a saturated liquid, a pressurisation system can be eliminated in the vehicle. In addition, the requirements for the start preparation are minimised. [138]

Therefore, the possibility of using a Zero-NPSH pump has extensive consequences for the tank and fuel system because a pressurisation system becomes unnecessary. This system simplification, which also entails reducing the tank and fuel system mass, has significant consequences for the overall aircraft design, which are further examined in Section 4.2.

2.1.3 Boiling Heat Transfer

LH2 only exists at temperatures under 20.4 K at ambient pressure. These low or cryogenic temperatures create a high temperature difference concerning ambient temperature, which affects the heat transfer from the wall to the fluid. Convective heat transfer assumes a single-phase fluid, which has no change of phase. Due to low temperature differences, depending on the fluid properties, this boundary condition is also fulfilled. However, at cryogenic temperatures, high temperature differences are quickly reached, and two-phase phenomena must be considered. This approach is essential when cooling tank and transfer line hardware. Vapour-free flow is the goal of the cooling process. The motivation behind this is described in Section 4.4. In the following section, the effects of high temperature differences and multiphase heat transfer are explained.

In multiphase heat transfer, two processes can occur at an interface. The liquid to vapour phase change referred to as boiling, and condensation, the phase change from vapour to liquid. The phase change and the associated enthalpy of vaporisation lead to higher heat transfer, and the heat transfer coefficient also increases compared to conventional single-phase convection. Intensification of heat transfer is thereby possible. In addition, there is the possibility of increasing the heat transfer by superimposing a flow (forced convection boiling) and/or a subcooled liquid.

Starting with the basic form of a boiling process: pool boiling. Here, the liquid is at quiescence in a pool with a higher wall temperature than the saturated fluid. The heat transfer behaviour can be divided into four different regimes, which depend on the superheat temperature ΔT_{sat}. The superheat temperature (or excess temperature) is defined as the temperature difference between the wall temperature T_{wall} and the temperature of the saturated fluid T_{sat}:

$$\Delta T_{\mathrm{sat}} = T_{\mathrm{wall}} - T_{\mathrm{sat}} \tag{2.10}$$

Figure 2.5 shows a schematic representation of the Nukiyama diagram of the different boiling regimes, plotted against the wall superheat and the heat flow. As the superheat temperature increases, the four regimes are natural convention, nucleate, transition and film boiling. There is a maximum (CHF) and minimum heat flow (Leidenfrost Point) due to transient conditions of rising vapour bubbles. A detailed explanation of each regime can be found in Barron et al. [18].

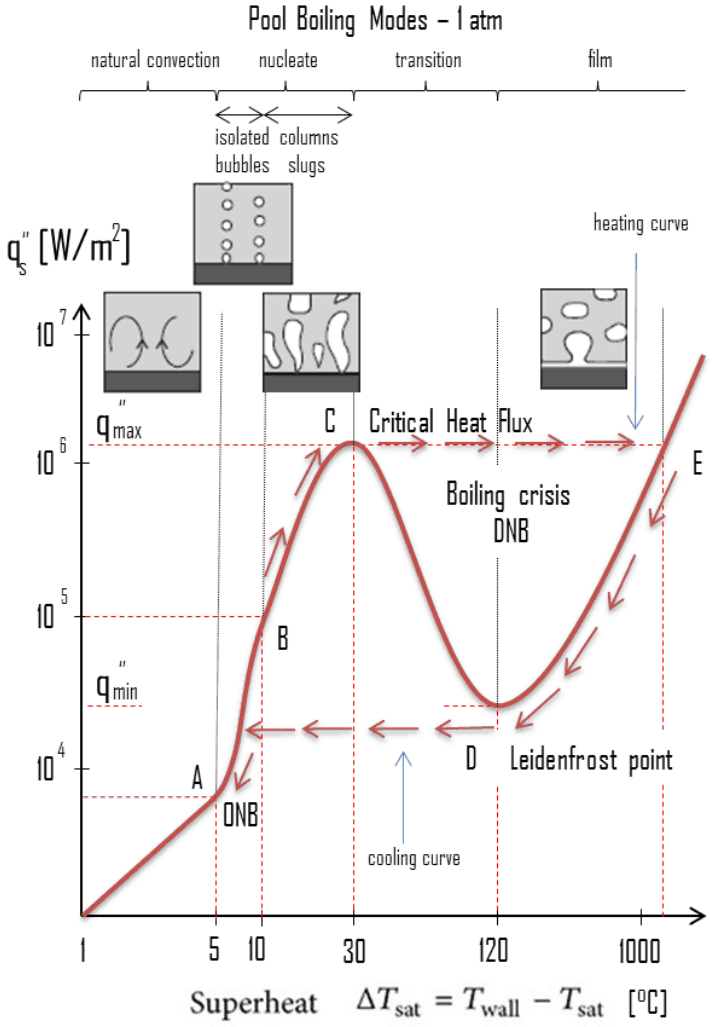

Figure 2.5: Schematic Nukiyama curve; heating and cooling route hysteresis, different boiling regions [39]

In addition, the effect of wall superheating has a hysteresis in power-controlled methods. The heating and cooling lines run on different lines if the wall temperature is not an independent variable. In a heat transfer where the temperature is an independent variable, no hysteresis occurs. [19]

In real cooling processes, without additional heating power, the wall temperature is an independent variable. Thus, the Nukiyama curve has no hysteresis and no sudden temperature drop in the transition boiling [162, 64]. Figure 2.6 shows the individual boiling regimes of nitrogen. A sudden, rapid temperature jump occurs in Figure 2.6 a) in the transition region, which can be seen in Figure 2.6 b) as a peak in the heat flow over time. To escape this exact modelling of the process and define a conservative case for the heat transfer, the sudden increase of the heat flow in the transition region is neglected in further consideration.

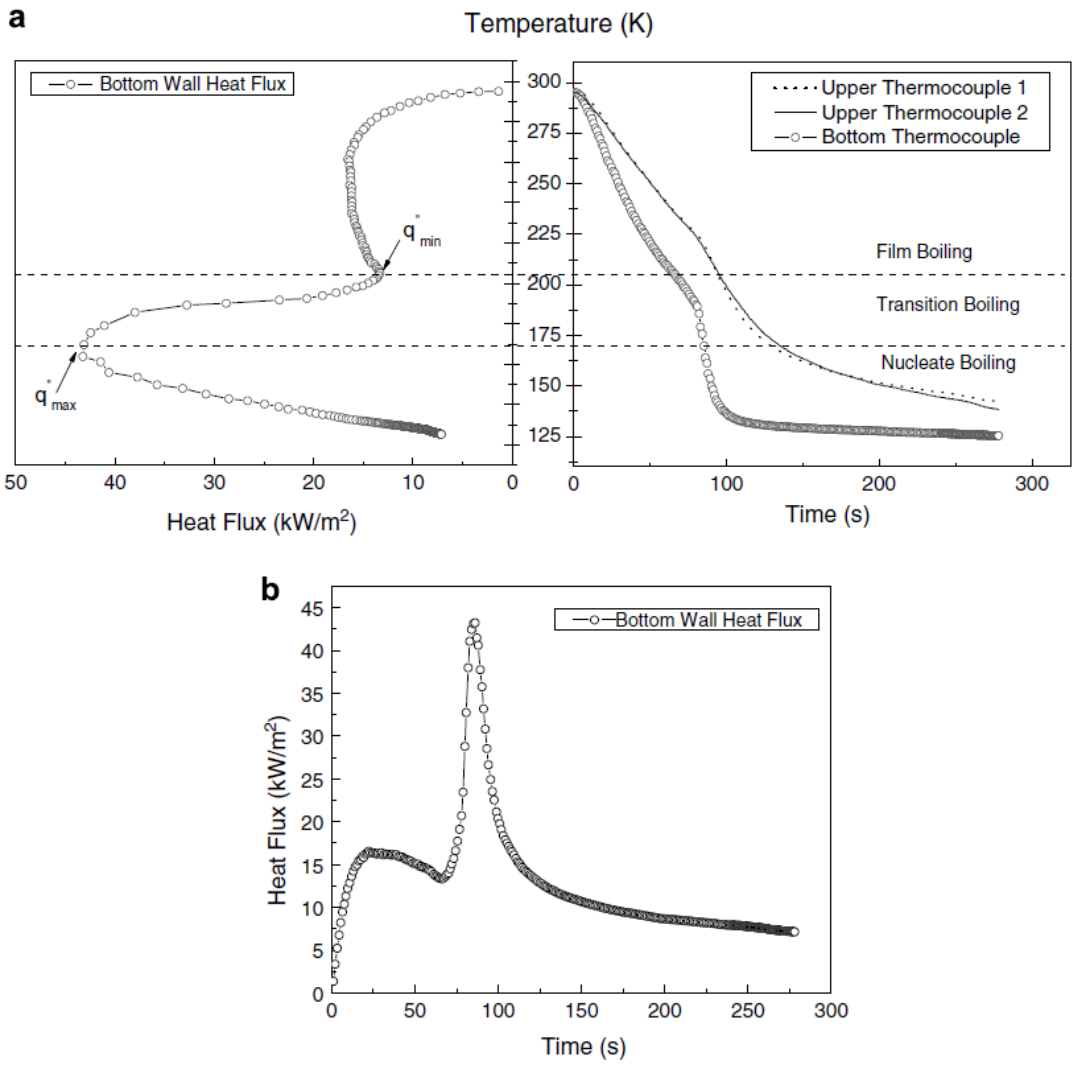

Figure 2.6: Heat flow during chill down of a pipe: a function of the temperature and time [162]

The calculation of the heat flow is possible through a variety of equations. Experimental values for the heat flux and superheated temperature of the nucleate boiling and film boiling are shown in Figure 2.7. This diagram shows that the majority of the temperature range above a wall temperature of 40 K belongs to the film boiling regime [23, 24]. The nucleate boiling regime can be classified in a range of 20 to 23 K. Due to the extensive wall temperature range of the film boiling regime, this has the most considerable impact on the cooling process [155, 24].

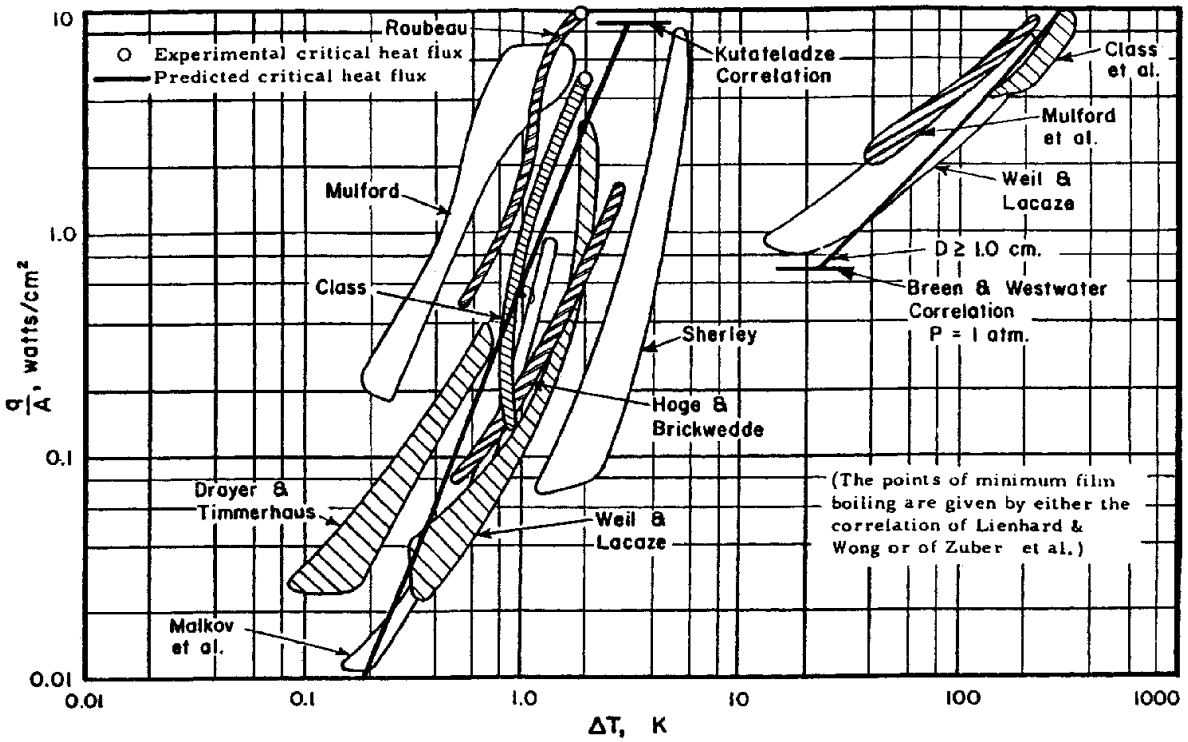

Figure 2.7: Experimental Nukiyama diagram for LH2, adapted from BRENTARI et al. [24]

Another way to influence the heat transfer is through a superposition by a flow. Like free and forced convection in single-phase fluids, the heat transfer is increased by combining the boiling regime with forced convection, which is called forced convection boiling. The influence of forced convection also depends on the superheat temperature and thus the boiling regime [135]. A simple approach to combine both methods is the superposition principle, in which the individual components of the heat flow $\dot{Q}$ or heat transfer coefficient h are added [61]:

$$\dot{Q} = \dot{Q}_{\mathrm{boil}} + \dot{Q}_{\mathrm{conv}} \tag{2.11}$$

$$\dot{Q} = \left(q_{\mathrm{boil}}(T) + h(T)_{\mathrm{conv}} \cdot (T_{\mathrm{wall}} - T_{\mathrm{sat}})\right) \cdot A \tag{2.12}$$

$$h = h_{\mathrm{boil}} + h_{\mathrm{conv}} \tag{2.13}$$

The heat transfer for film boiling regime can be expressed after Breen and Westwaster equation [24] for wall temperatures above 40 K [23]:

$$q_{\mathrm{boil,film}}(T) = \frac{0.37 + 0.28 \cdot \dfrac{l_{\mathrm{c}}}{D}}{\left(\dfrac{l_{\mathrm{c}} \cdot \mu_{\mathrm{v}} \cdot (T_\infty - T)}{{k_{\mathrm{v}}}^3 \cdot \rho_{\mathrm{v}} \cdot (\rho_{\mathrm{l}} - \rho_{\mathrm{v}}) \cdot g \cdot h'_{\mathrm{v}}}\right)^{\frac{1}{4}}} \cdot (T_\infty - T) \tag{2.14}$$

$$l_{\mathrm{c}} = \left[\frac{\sigma}{g \cdot (\rho_{\mathrm{l}} - \rho_{\mathrm{v}})}\right]^{\frac{1}{2}} \tag{2.15}$$

$$h'_{\mathrm{v}} = \frac{\left(\Delta h_{\mathrm{v}} + 0.34 \cdot c_{\mathrm{p,l}} \cdot (T_\infty - T)\right)^2}{\Delta h_{\mathrm{v}}} \tag{2.16}$$

The additional heat transfer coefficient due to forced convection can be calculated using a modified Dittus-Boelter equation or Sieder-Tate correlation [24]. The Reynolds number and Nusselt number are calculated with the single-phase vapour (spv) properties of the bulk saturation conditions and the velocity of the mixture [65]:

$$h_{\mathrm{conv,film}} = 0.023 \cdot Re_{\mathrm{spv}}^{0.8} \cdot Pr_{\mathrm{v}}^{0,33} \cdot \left(\frac{\mu_{\mathrm{v}}}{\mu_{\mathrm{wall}}}\right)^{0.14} \cdot \frac{k_{\mathrm{v}}}{d} \tag{2.17}$$

$$Re_{\mathrm{spv}} = \frac{\rho_{\mathrm{v}} \cdot v_{\mathrm{avg}} \cdot d}{\mu_{\mathrm{v}}} \tag{2.18}$$

$$v_{\mathrm{avg}} = \frac{\dot{m}}{\rho_{\mathrm{b}} \cdot A} \tag{2.19}$$

$$\rho_{\mathrm{b}} = \left(\frac{x}{\rho_{\mathrm{v}}} + \frac{1-x}{\rho_{\mathrm{l}}}\right)^{-1} \tag{2.20}$$

$$x = \frac{m_{\mathrm{v}}}{m_{\mathrm{v}} + m_{\mathrm{l}}} = \frac{q(T) \cdot A}{\Delta h_{\mathrm{v}}} \cdot \frac{1}{\dot{m}} \tag{2.21}$$

Due to the simplification by neglecting the transition boiling, the second temperature range of 20 to 40 K follows. This heat transfer is also calculated using a superposition method. Here, the convective heat transfer is calculated with the Dittus-Boelter relation. In contrast to film boiling, however, the Reynolds number and the Nusselt number and the heat transfer coefficient are calculated using the single-phase properties of the liquid (spl) [65].

$$h_{\mathrm{conv,spl}} = 0.023 \cdot Re_{l}^{0.8} \cdot Pr_{\mathrm{l}}^{0.4} \cdot \frac{k_{\mathrm{l}}}{d} \tag{2.22}$$

$$Re_{\mathrm{l}} = \frac{\rho_{\mathrm{l}} \cdot v_{\mathrm{avg}} \cdot d}{\mu_{\mathrm{l}}} \tag{2.23}$$

The Leidenfrost point is calculated with a modified Zuber relation [163, 24]:

$$q_{\mathrm{boil,minheat}} = 0.16 \cdot \rho_{\mathrm{v}} \cdot \Delta h_{\mathrm{v}} \cdot \left[\frac{g \cdot \sigma \cdot (\rho_{\mathrm{l}} - \rho_{\mathrm{v}})}{(\rho_{\mathrm{l}} + \rho_{\mathrm{v}})^2}\right]^{\frac{1}{4}} \tag{2.24}$$

Additional information on heat transfers and other calculation methods can be found in [155, 151, 84, 79].

A further possibility to increase the heat transfer is to subcool the liquid, which increases the temperature difference. The resulting vapour bubbles on the wall surface condense again in the liquid, which leads to no net vapour generation [57]. Formulations for subcooled boiling can be found in [24, 35, 19, 145].

2.2 Handling Options for Hydrogen

H2 is already used in industry or research, where it is stored and transported in gaseous, liquid, chemical or physical composition. Typical pressures for compressed GH2 are 350 and 700 bar, used in the automotive industry [121]. The adapters for refuelling in the automotive industry are standardised under the SAE2600 [120] standard. However, the real gas behaviour for GH2 during the transfer or refuelling process must also be considered based on the Joule Thompson effect: Due to the isenthalpic expansion, the hydrogen heats up, which affects the system.

LH2, on the other hand, has no standardised industry norm for transfer. Depending on the manufacturer, the diameters of the lines and the connections differ. In addition, the purging process will also be performed on a manufacturer-specific basis. The purging process after connecting and before disconnecting the hoses is based on the fact that no foreign gases may remain in the hoses. On the one hand, this is for reasons of safe handling and compliance with explosion protection. On the other hand, at the cryogenic temperatures of 20 K of the LH2, all substances except helium would freeze and block the pipe. At a contamination level of 1 part per million (ppm) or less, the transfer process can be started for LH2 [98]. For GH2, the guidelines are not as strict. The oxygen content should be less than 1 % by volume [105]. This difference exists due to the risk of explosion because of blockage since freezing oxygen cannot occur in GH2. After all, the temperatures in the system are higher than the freezing temperature of oxygen.

First, the uniform definition of adapters and couplings is set. The following definition, according to Stuck [141] is used:

- Disconnects provide quick action separation of system interfaces
- Couplings are mechanical connections of a fluid system, which are capable of disassembly but not in quick action
- Fixed joints are connected elements without the requirement of replacement, removal or disassembly

One possibility that allows the handling of LH2 is the Johnston or Johnston-Cox coupling [110, 16]. According to the definition just introduced, this is a disconnect and allows a pipe to be connected and disconnected quickly, see Figure 2.8. Due to the additional vacuum insulation, there is no significant heat input at the connection interface that could lead to liquid evaporation.

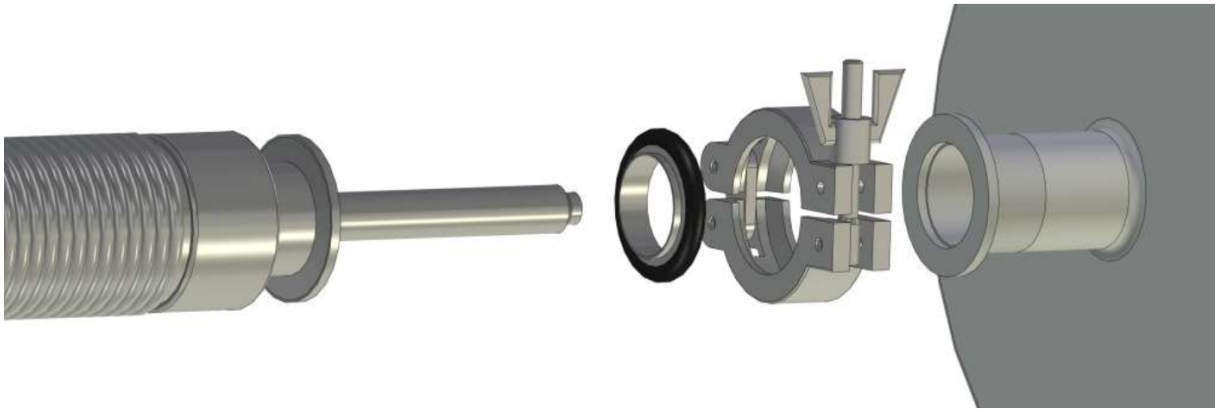

Figure 2.8: Johnston coupling for LH2 transfer line connection [78]

Due to the open connection point, the Johnston coupling represents a disconnect where a purging process must be performed after connection to remove foreign particles. This procedure has the disadvantage of requiring a certain amount of time and a purging system with an inert gas.

Another possibility of a connection is a clean break disconnect. In this type of disconnect, a small amount of spillage is released during connection and disconnection [141]. The volume of spillage occurs between the two valve seals, which is minimised by design in this type of coupling. A two-valve disconnect designed for minimum spillage is shown in Figure 2.9.

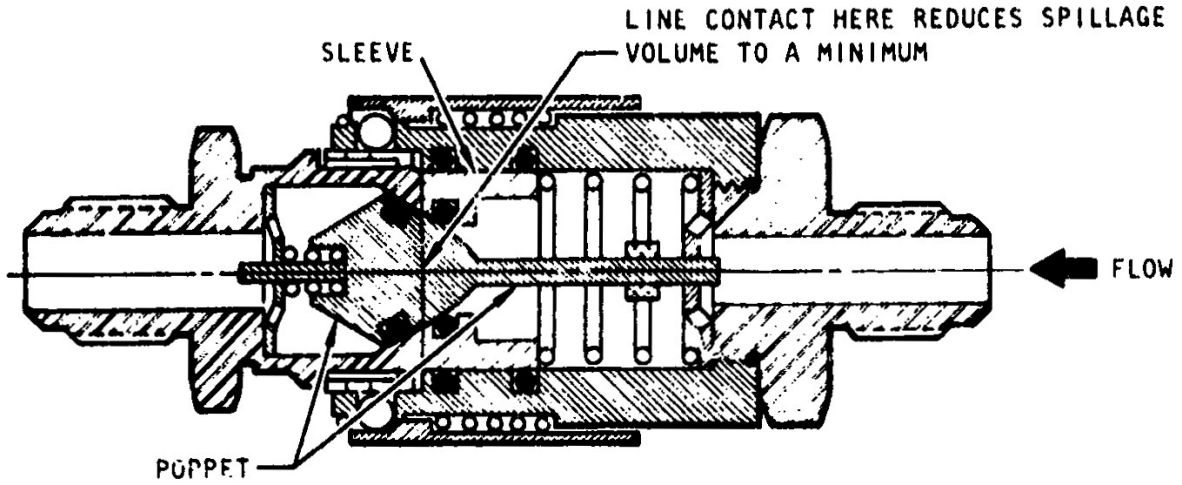

Figure 2.9: Two valves disconnect designed for low spillage; spillage volume less than 0.05 ml for 0.5 in disconnect [141]

The overpressure in the hose prevents penetration of the atmosphere into the piping system. As a result, no foreign particles are absorbed when the two connections are connected, and the H2 system remains free of contamination. For LH2 systems, the overpressure is at minimum 0.2 bar_g [98]. For GH2 in storage vessels, an overpressure of 1.7 bar_g is specified as a minimum [98, 105].

For the transportation of LH2 by trucks, there are important aspects which are described below. Due to the low density compared to hydrocarbons, a LH2 container can transport only 3000 to 5000 kg of LH2 [73, 60].
The loading time is 3 to 6 h and is carried out with an overpressure of 1 bar_g. During the transportation, a pressure of 1.5 bar_a is maintained in the tank. [60, 144]
Subsequently, at the delivery point, the LH2 can be unloaded using two methods [73]:

- The first option is to build up the pressure in the tank, whose overpressure to the storage tank then feeds the LH2. The pressure build-up occurs either by self-pressurisation due to the heat input from the environment or by vaporisation through a heat exchanger. The disadvantage of this method is the long operation time and high pressures that can lead to venting
- The second method consists of transfer through a pump. The main disadvantage of this variant is the pump's cost and frequent maintenance due to cavitation occurring. In addition, a vaporiser must be attached to the transport tank to keep the pressure in the tank constant when LH2 is withdrawn.

For conventional road tank trucks the following properties are given:
Mass flows of 500 to 4000 kg/h can be achieved when feeding at an overpressure of 1-2 bar. Unloading LH2 from the delivery trucks takes between 0.5 and 2 h [16, 144, 60]. Helium is required for the purging process. [60, 144]
The transport tanks operate between 1 and 12 bar. The connection between the storage tank and truck is made with a flexible transfer line. [73]

It can be concluded from this that no clean break disconnect is used for the connection. This means that air enters the filling hose through the connection, and it must therefore be inerted. Explicit descriptions of the type of connection and procedure are manufacturer-specific and not public. The two methods for transferring LH2 corresponds with statements from Section 2.1.2. Pump cavitation is also mentioned here as one of the most important criteria, making a pump solution prone to failure and expensive [73]. The time required for refuelling and unloading is very large for this conventional industrial application. Therefore, the question arises why a faster solution is not applied. On the one hand, if LH2 is delivered, the time required is not a significant issue. A larger mass flow would also imply a more technically complex system, which would cause more costs. On the other hand, the maximum pressure of the transport tank is limited by the total mass of the truck. A higher pressure difference is therefore only possible to a limited extent.

2.3 Non-Aircraft Liquid Hydrogen Applications

In the following chapter, comparable refuelling applications are discussed, and their specifications are analysed. The comparison with the automotive industry is based on large batches and numbers of refuellings, which are handled without any safety concerns. On the other hand, astronautics is characterised by large individual quantities, which are only required in a certain time interval.

2.3.1 Automotive Industry

The automotive refuelling process of LH2 is interesting so far as the safety regulations are high, and any person who is allowed to drive a motor vehicle should be able to execute the procedure. The comparison of mass flow from cars to airplanes is not meaningful here since scale effects can occur. Additional information on possible dimensions can be found in Stewart [137]. The volume flow for refuelling cars is between 50 and 80 l/min [13, 109]. For comparison purposes, the LH2 tank volume can be assumed with a typical gasoline tank volume and the volumetric energy density. A car would have a capacity of 120 l, a bus of 1500 l, and a truck of 3000 l.

Design considerations for LH2 refuelling include bulk LH2 storage, a transfer system, instrumentation, controls, safety equipment and a GH2 recovery system. Following processes result in vaporisation and therefore in losses of LH2 during the transfer from the supply tank to receiving tank: [137]

- Flashing of the liquid using pressure differential method to lower pressure of the receiving tank as the saturated liquid pressure
- Addition of heat as pump work and other heat leaks associated with a pump
- Chill down of the supply tank pressurisation gas (hydrogen or helium)
- Chill down of initially warm transfer lines, refuelling station, and receiving tank

- Remaining of warm gas or liquid from the previous filling
- Heat leak through other parts like supports, connections, thermal insulation, and the transfer lines

Some of the losses associated with a pressure differential transfer could be avoided by using a pump. However, pump transfer leads to other problems like cavitation, and the operation is more complex and expensive. [137]
From the point of view of simplicity, a pressure difference method is better. A more detailed consideration that significantly influences the refuelling time is the phase transition when passing through the saturated line. If the receiving tank's pressure is too low, a portion of the liquid phase vaporises and must be removed again through the recovery line. As a result, adequate mass flow is reduced, and refuelling takes longer. The recovery line must be adjusted in dimension, which is only designed for losses due to environmental heat input and chill down. A more detailed consideration of this effect is calculated in Section 3.2.3.

Conventional cryogenic disconnects contain several additional restrictions that the public cannot use. These systems have two significant disadvantages. Firstly, conventional equipment handling is complicated, and only experienced and qualified personnel should handle it. Personal protection like gloves and goggles are indispensable during operation. Secondly, thermal losses appear with weak insulation equipment. Additionally, through cryogenic temperatures, ice formation can occur and impedes or prevents dismounting. Therefore, the coupling has to be heated and cleaned adequately before reuse. [159]

A solution to the problems just described is offered by the hermetic clean break disconnect from Linde [159]. This disconnect meets all essential requirements for public use. A schematic illustration of this tight disconnect is shown in Figure 2.10. Each counterpart has ball valves that close the respective system. After connecting and opening the ball valves, the cold finger is extended into the vehicle part. This type of connection establishes a coaxial, isolated, and hermetically sealed connection. The coaxial design has the advantage that LH2 is transferred in the inner line to the tank, and the outer line returns the vent gas. After the refuelling process, the cold finger is retracted, the ball valves close, and the adapter can be dismounted.

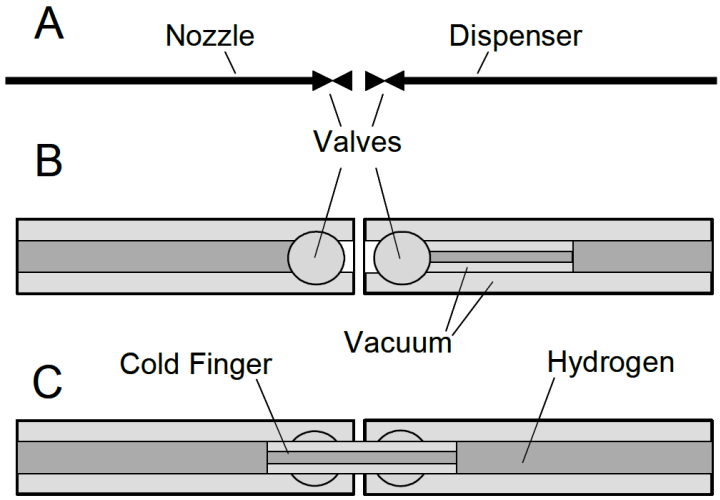

Figure 2.10: Principle of automotive LH2 refuelling disconnect; two valves disconnect with coaxial pipe design; additional double walled vacuum insulated pipe which will be pushed forward after engagement, called cold finger [13]

A manual docking of this disconnect and transfer hose by a person is possible in the automotive sector. Thereby the volume between the connected counterparts (spillage volume) is flushed with gaseous helium for cleaning. Manual operation is possible with this clean break disconnect, but a robot operation would be a future method to avoid specially trained people. [159]

A fully automatised refuelling robot for LH2 was being used at Munich Airport in 1999. The system renders any personal operation, and the customer does not need to leave the vehicle. In 2-3 min, the automatic refuelling process is executed. The robot could reach all necessary points to be approached through 4-axis kinematics. The drive technology consists of electric servo actuators with an absolute measuring system. Furthermore, the disconnect contains sensors for docking and the mechanism for connecting. The system is designed for different vehicle types that can be refuelled but with the prerequisite that the vehicle type is once learned. [109]
A detailed refuelling sequence for the operation of an automatic refuelling station is described in Stewart [137]. Simplified, the procedure of refuelling is divided into four sequences [109]:

1. Signalling, entry and initial position recognition
2. Communication and authorisation
3. Docking procedure and refuelling
4. Undocking procedure, receipt issue and exit

Safety aspects with H2 are, especially for automotive use, important. In direct comparison, LH2 shows advantages over GH2 due to the lower storage pressure, which has a favourable effect on leakage characteristics. In terms of a sealed clean break disconnect, no explosive atmosphere can occur through the low spillage disconnects. Nevertheless, monitoring and detecting H2 by a gas sensor is essential and follows a system for a power supply shutdown and emergency stop. [109]

The purging and evacuation process has two significant disadvantages. This process takes time that would extend the refuelling process, which should be done as quickly as possible. Second, helium is an expensive, non-renewable inert gas that should not be used in regular operation. Due to a limited amount of available helium, a massive increase in helium consumption could raise the price to such an extent that LH2 as a fuel would become uneconomical. Evacuation and purging before and after refuelling would be eliminated with the use of a self-sealing quick disconnect [137, 66, 86].

Filling hoses with tight sealing cryogenic disconnects can refuel without purging cycles because the clean break device lets no air or humidity into the system. However, for commissioning, the system must be purged three times with helium to prevent an explosive atmosphere. Furthermore, time-consuming heating of the disconnect can be dropped. Additionally, this device prevents dangerous situations due to incorrect handling because no H2 can emerge if the connection is suddenly disconnected or removed. [66]

The effect of the clean break disconnect and the optimisation of the refuelling process can be demonstrated by the reduction in time required, as seen in Figure 2.11, from more than an hour to less than 3 min. In addition, the losses of LH2 are minimised since continuous heating and cooling results in an evaporating amount of H2. The bayonet disconnect is connected in 20 s and disconnected in 10 s. The improvement in time compared to the non-clean break Johnston disconnect is more than 30 % [156].

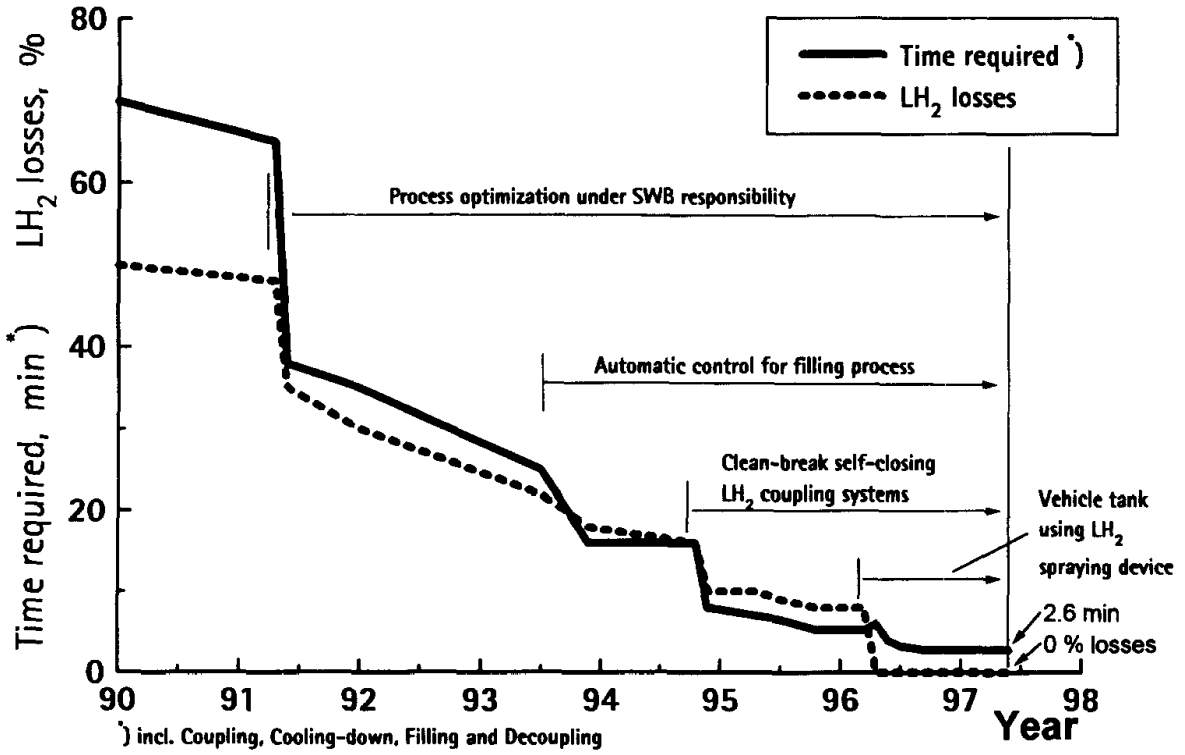

Figure 2.11: Development of the time duration and losses of an automotive LH2 refuelling process under the influence of new processes [156]

In addition to the time benefit of the clean break disconnect in Figure 2.11, a further improvement is made by a spraying device. Here, the subcooled LH2 is sprayed into the upper part of the tank. This process has the great advantage that a recovery line is no longer needed to return the vaporised hydrogen. [156]
Therefore, the subcooled H2 cools down the remaining warm gas phase and lets it condense. If the LH2 was fed into a liquid phase at the bottom, the tank's pressure would increase until no pressure differential remained. Condensation occurs at the interface between the liquid and gas phases but not to the same extent as the spraying device.

Consequently, a recovery line is needed to keep the tank's pressure constant or prevent it from rising. The advantage of the spraying device also has a disadvantage. The cooling and condensation of the warm gas-phase heat up the subcooled H2. However, this subcooling in the refuelling system was subjected to a considerable amount of energy. Besides, the density of the LH2 decreases due to the temperature increase caused by heat absorption. This influence of the effective tank conditions must be taken into account in the tank design and the volume calculation, see Section 4.1.

Pressure differential and pump refuelling can thereby be further subdivided [94]: Pressure differential system into one or two flow systems and pressure raise (pump) systems in saturated and subcooled liquid phase. In addition, a combination of these variants is conceivable.

Through pressure limitations in tank design, according to breaking stress, H2 has to be released when exceeding a defined pressure, defined as venting pressure. Venting pressure for automotive applications is ranging between 4 and 7 $\mathrm{bar_a}$ [13, 159, 66, 156]. Therefore the question is, what happens with vented GH2 after refuelling and disconnecting.

One possibility, which disposes of H2 without usage, is to release it into the atmosphere. This approach has the disadvantage that it could form an explosive atmosphere, and therefore it is not optimal. Closed areas such as a garage have to be considered with cars. A catalytic converter might be a suitable and reliable solution to eliminate the release in the air. This reaction releases energy in the form of heat, which avoids combustible H2-air mixtures. [111]
In a venturi pipe, H2 is mixed with air and oxidise into water in a following catalyst [20]. Both variants do not use the vented H2 which is uneconomical. Therefore, feeding a small H2 on board fuel cell to produce electricity for battery charging is an attractive and convenient opportunity [111].

2.3.2 Astronautics

Space programs have enabled the development and successful implementation of large-scale LH2 production, storage, transfer, transportation, and distribution systems. In this context, the desirable properties of LH2, particularly its high heat of combustion and high specific impulse, make it particularly well suited for rocket propellant. Successful usage dates back to the upper stage of the Centaur in 1963. The Centaur has a tank capacity of $32\,m^3$ of LH2, which increased to $1287\,m^3$ in the Saturn V. These programs demonstrated the feasibility of LH2 as a rocket propellant and improved its handling of other potential applications. [16]

At Kennedy Space Center LH2 storage is in $3217\,m^3$ sphere, see Figure 2.12. The stainless steel inner shell has a diameter of 18.8 m and the outer shell is carbon steel and 21.3 m in diameter. The annular space, used as insulation, is filled with perlite and is evacuated. The experimental boil-off loss rate is about 0.02 % per day. A vaporiser heat exchanger is used to pressurise the sphere. This vaporiser has to convert the LH2 to GH2 at a temperature of 88 K. The maximum allowable internal working pressure is $6.2\,bar_g$. [16]

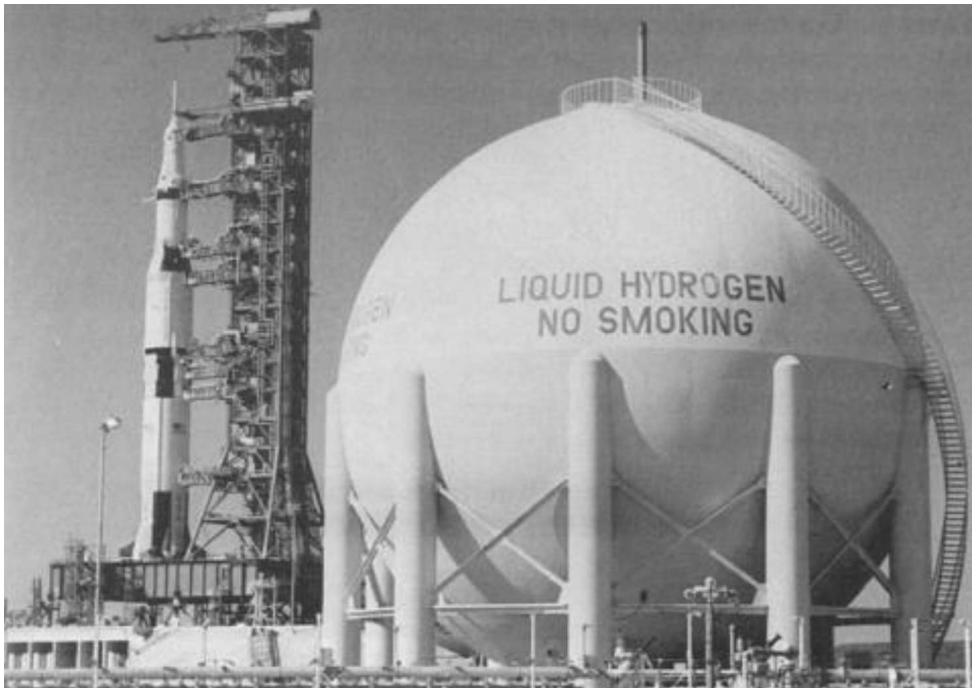

Figure 2.12: Storage Tank (ST) of LH2 at Kennedy Space Center; maximal operating pressure of $6.2\,bar_g$; volume of $3217\,m^3$ [16]

Through the pressurisation, the transfer of LH2 is carried out by the pressure differential method. The advantage of this variant is the simplicity of the system. For a loading operation, the storage system requires only a few components that are not susceptible to failure. This transfer has the advantage, especially for irregular rocket loading, of keeping system failure to a minimum.

The storage system consists of a vent system, vaporiser as a heat exchanger, liquid level sensors, fill manifold and manual and remote-controlled valves [16]. For propellant loading, additional components like control valves are necessary. Figure 2.13 shows the loading schematic of the External Tank (ET) from the Space Shuttle.

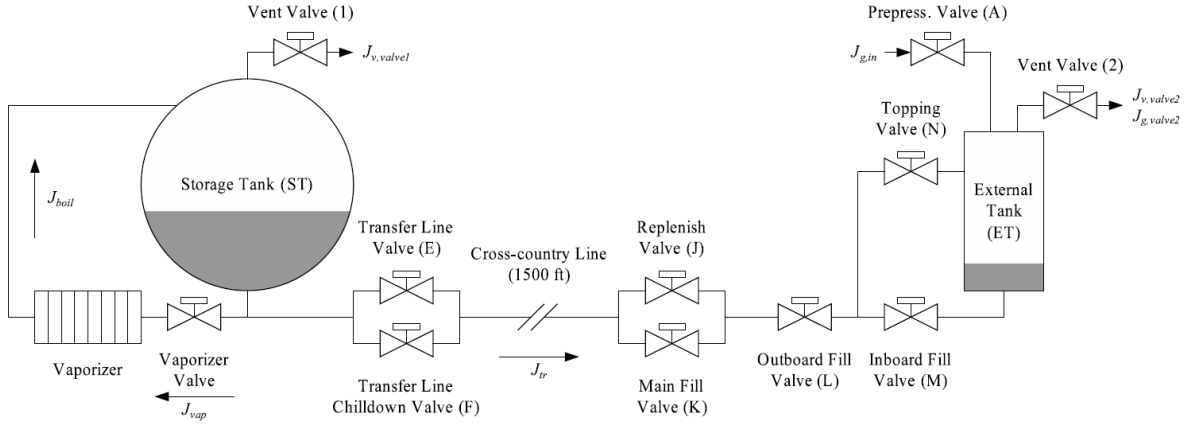

Figure 2.13: Space Shuttle LH2 loading schematic [107]

Another interesting parameter is the temperature of the recirculated GH2 after the heat exchanger or vaporiser. According to the ideal gas law, a higher temperature at the same pressure and volume means a lower mass needed for pressurisation. Hence, a higher temperature in the ullage means a lower mass flow of LH2 that must be removed and sent through the vaporiser. The mass flow subsequently affects the power and dimensions of the heat exchanger. On the other hand, the tank components, i.e. the liquid and gaseous fractions, strive for thermodynamic equilibrium. As a result, the warm gas phase at the top of the tank releases energy to the cold liquid. This heat transfer heats the liquid, which should remain as cold as possible to maintain the desired density.
Furthermore, in the interface, in addition to the energy exchange, a mass transfer also occurs. The warm GH2 condenses, and the liquid phase evaporates. In conclusion, a hot gas temperature and a large mass flow oppose each other, for which an optimum is determined. Moreover, this study presupposes a detailed consideration of the thermal behaviour, which requires temperature gradients and temperature differences in a non-thermodynamic equilibrium. Mathematical modelling of thermodynamics can be found in [107, 115, 40].

The basic rocket loading process and the various sections that depend on each other are shown in Figure 2.14 for the second stage of the Saturn V. The actual loading process is divided into several sections, which can be distinguished on the mass flow.
In principle, each loading process begins with the purging of all components to remove foreign particles. For rocket loading, this is followed by initial pressurisation of the tank with helium, which is provided by ground support. This pre-pressurisation is required to control the mass flows, maintain the pressure above ambient pressure, and prevent air and oxygen ingress.

The tank's pressure must be selected to ensure that the inflowing LH2 is in the subcooled region. In other words, the pressure in the tank must be above the vapour pressure. The temperature of LH2 at the inlet conditions to the tank dictates the vapour pressure in this case. If the vapour pressure is lower than this, a fraction will vaporise, and the effective LH2 mass flow would be reduced, increasing the loading time. For a calculation, refer to Section 3.4.

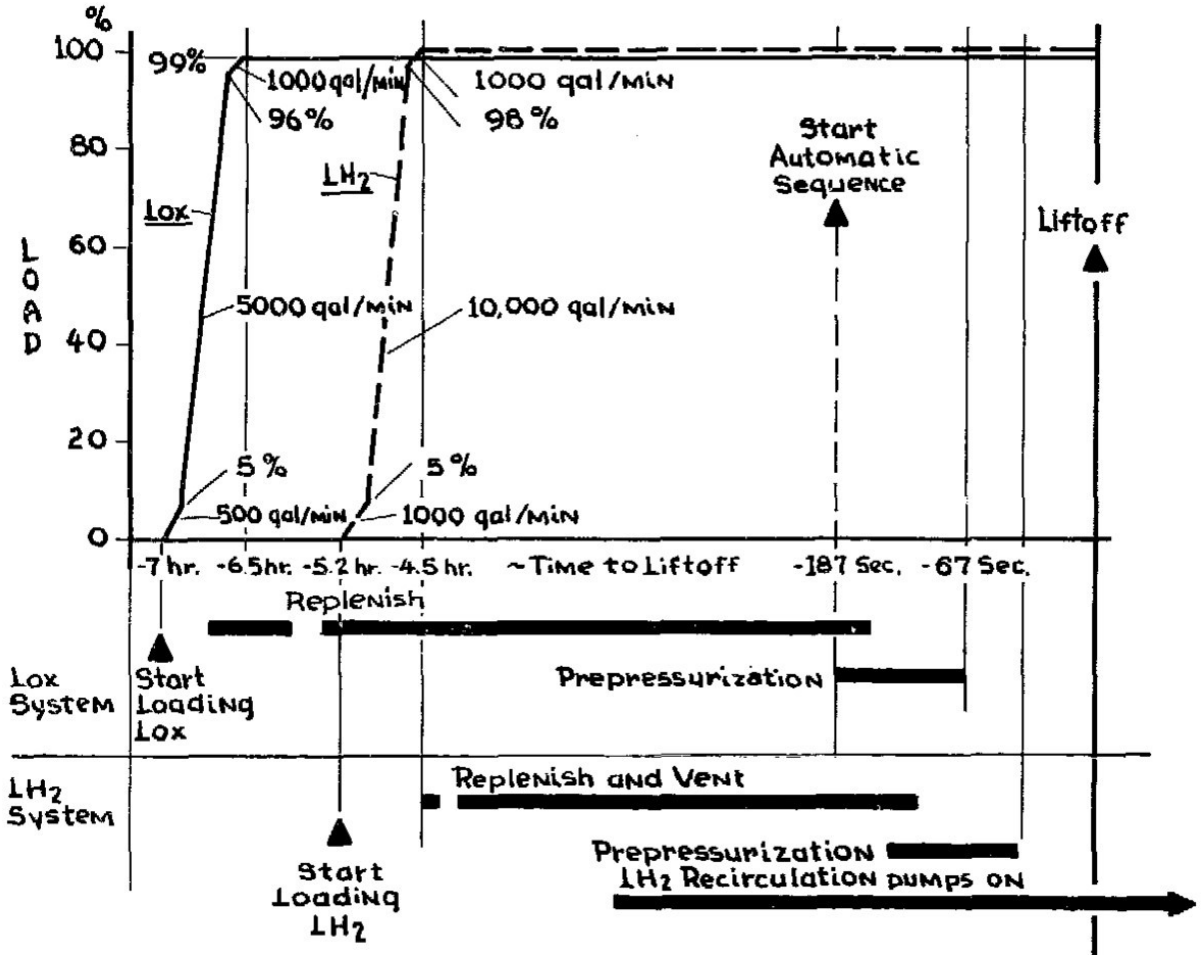

Figure 2.14: Propellant loading of Saturn V [89]

After pressurisation, slow fill begins, characterised by a reduced or small mass flow necessary to chill down the system. Usually, the rocket and its components have an ambient temperature or higher. Through the large temperature differences to cryogenic LH2, the first transferred LH2 will vaporise. Due to the liquid's heat dissipation, primarily due to the enthalpy of vaporisation, the transfer components, such as lines, valves, and the tank itself, chill down. A reduced mass flow in this first loading section follows for several reasons. During the cooling process, the large temperature gradients create thermal stress, affecting component strength and fatigue properties. Thus, the cooling process should be uniform and at an acceptable rate for the material. Due to the density difference between liquid and vapour, higher flow velocities are achieved, which bring an additional limitation in the mass flow. Because of vaporisation losses caused by the phase transition, the fuel level in the tank will also not increase linearly with the mass flow. Therefore the effective liquid mass flow will decrease. This slow filling is maintained up to a fill level of 5 % to ensure that all components are sufficiently cooled down.

With fast fill, LH2 is transferred with the maximum mass flow. Due to the already cold lines, no significant amount is evaporated anymore, and the process is not affected. Compared to the slow fill, the fast fill has a ten times higher mass flow. This section is maintained up to a fill level of 85 % to 98 %. Further distinctions in the loading sections up to 98 % fill level are in fast fill with reduced pressure and reduced flow [107]. Reducing the mass flow at high fill levels avoids overfilling and flooding.

Replenish and topping ensure that the required fill level is maintained and continues until shortly before the liftoff. Moreover, the tank pressure is reduced through a vent valve to 0.01 $\mathrm{bar_g}$ [107]. The reason for this step is to get NBP conditions back. That means that the temperature of the LH2 in the tank decreases through flash evaporation. Environmental heat during flow and tank duration raises the liquid temperature. The temperature could rise without boiling in the subcooled region within a pressure in the tank of about 2.7 $\mathrm{bar_a}$ [107]. Through the pressure drop when opening the valve, the liquid boils back to the saturated conditions at a pressure of 1.02325 $\mathrm{bar_a}$ with the appropriate temperature of 20.3 K.

Space Shuttle Loading

The Space Shuttle was operated from 1981 to 2011 by NASA as a reusable low earth orbit spacecraft. It includes the Orbiter Vehicle, a pair of solid rocket boosters and the ET containing Liquid Oxygen (LOX) and LH2. [92]
The ET has a LH2 volume of about 1500 $\mathrm{m^3}$ [134, 92]. An operating ullage pressure of 2.2 to 2.35 $\mathrm{bar_a}$ and venting pressure of 2.5 $\mathrm{bar_a}$ [134].
The ET is fuelled, in space applications called propellant loading, with a pressurised system, [107]. Figure 2.13 shows a schematic of the loading system for the ET. To maintain the storage tank's pressure level, some of the liquid flow is vaporised and injected into the ullage. According to Bernoulli's equation, the pressure in the ST must be high enough to compensate dynamic pressure, hydrostatic pressure and friction losses through valves and pipes.
The diameter of the transfer pipe is $d_{\mathrm{pipe}} = 0.254\,\mathrm{m}$ with a length of $l_{\mathrm{pipe}} = 457\,\mathrm{m}$. Table 2.2 gives a summary about the mass flow and pressure levels. Additionally, the Reynolds number and a simplified Reynolds number $v \cdot d$ are calculated. As a dimensionless number it provides a comparability for the aircraft refuelling, see Section 2.5.

Section	p_{ST}	p_{ET}	$\dot{V}$	v	$v \cdot d$	Re
	$\mathrm{bar_a}$	$\mathrm{bar_a}$	$\mathrm{m^3/min}$	$\mathrm{m/s}$	$\mathrm{m^2/s}$	-
Slow fill	5.56	2.7	5.68	1.87	0.47	$24.3 \cdot 10^5$
Fast fill	5.56	2.7	28.40	9.34	2.37	$122.3 \cdot 10^5$

Table 2.2: Flow regime of loading LH2 for the Space Shuttle ET; Reynolds number is calculated with a kinematic viscosity of $\nu(T = 20\,\mathrm{K}, p = 2\,\mathrm{bar_a}) = 1{,}937 \cdot 10^{-7}\,\mathrm{m^2/s}$

The Reynolds number is well above the critical Reynolds number of 2300 at slow and fast fill. Thus, there is a turbulent flow in the pipe. As mentioned before, the tank's pressure is increased during the loading process to prevent the LH2 from boiling. The pressure is maintained at 2.7 $\mathrm{bar_a}$ during this process. The corresponding saturated temperature would be 24.09 K. To make these values easier to interpret: With the enthalpy difference at the maximum mass flow, a heat input of 1.2 MW would be added to the system to reach the saturated state. The mass flow is controlled by the opening degree of the valves.

SpaceX Falcon 9 Loading

SpaceX introduces a different loading procedure for their rockets. The rocket is just 35 min loaded before liftoff [58], in contrast to the Space Shuttle and Saturn V, which are refuelled several hours before launch. On SpaceX, the astronauts are already on board during the loading process for a human-crewed mission. This scenario is called Load and Go because immediately after the loading procedure, the rocket has to lift off. The fundamentally different sequence must be done because of a densification process. SpaceX uses LOX and Rocket Propellant-1 (RP-1) as the propellant. The LOX is thereby subcooled below the saturated temperature of the NBP by 24 K [53]. This subcooling has the effect of increasing the density, making the tank's volume smaller and reducing overall mass. This advantage of the greater density of the oxidiser implies the disadvantage that the conventional loading process can no longer be applied. Any heat input into the fluid would increase temperature and decrease the density [133]. With Space Shuttle loading, these long periods of standstill before liftoff are not a problem. Vaporised H2 is replenished as the heat input is immediately converted to latent heat. The sensitive heat input on a SpaceX rocket, on the other hand, is very disadvantageous and must be reduced by the short time between loading and liftoff.

Space programmes have demonstrated the handling of LH2 as an energy carrier and fuel. The knowledge gained from this experience and rockets' design with cryogenic fluids can be adapted to aviation. Design aspects for rockets, such as the tank architecture, the fuel system and the calculation methods, can be found in the three fundamental aerospace books by Sutton [143], Ring [115] and Huzel et al. [71]. The problem in borrowing the assumptions and equations developed for rockets, and launch systems is flight duration. Because of the short operating times during a rocket flight mission, simplifications can be made in space flight vehicles' design. However, adopting these simplifications in aircraft design can lead to incorrect interpretation of calculation results since the wrong boundary conditions have been adopted, considering a ten hour long-range flight.

2.4 Conventional Turnaround With Jet A-1

IATA Aircraft Handling Manual defines the time an aircraft occupying a stand or a gate at the airport as the turnaround time [59]. An alternative definition that describes the surface's blocking is the time difference between the positioning and removal of the wheel chocks, respectively, on and off block time. The turnaround, in its typical time sequence, is defined between the Actual Time of Arrival (ATA) and its Actual Time of Departure (ATD) [123]. Turnaround time is generally represented as a bundle of processes whose sub-processes run in parallel or sequentially, see Figure 2.15. The influence of the process sequence can be derived from legal or logistical requirements. These sub-sections can be isolated in general key processes: deboarding, unloading, fuelling, cleaning, catering, loading and boarding [123]. Additional information on individual processes and their impact on turnaround and analysis on delay influences and improvements can be found in Schlegel [123].

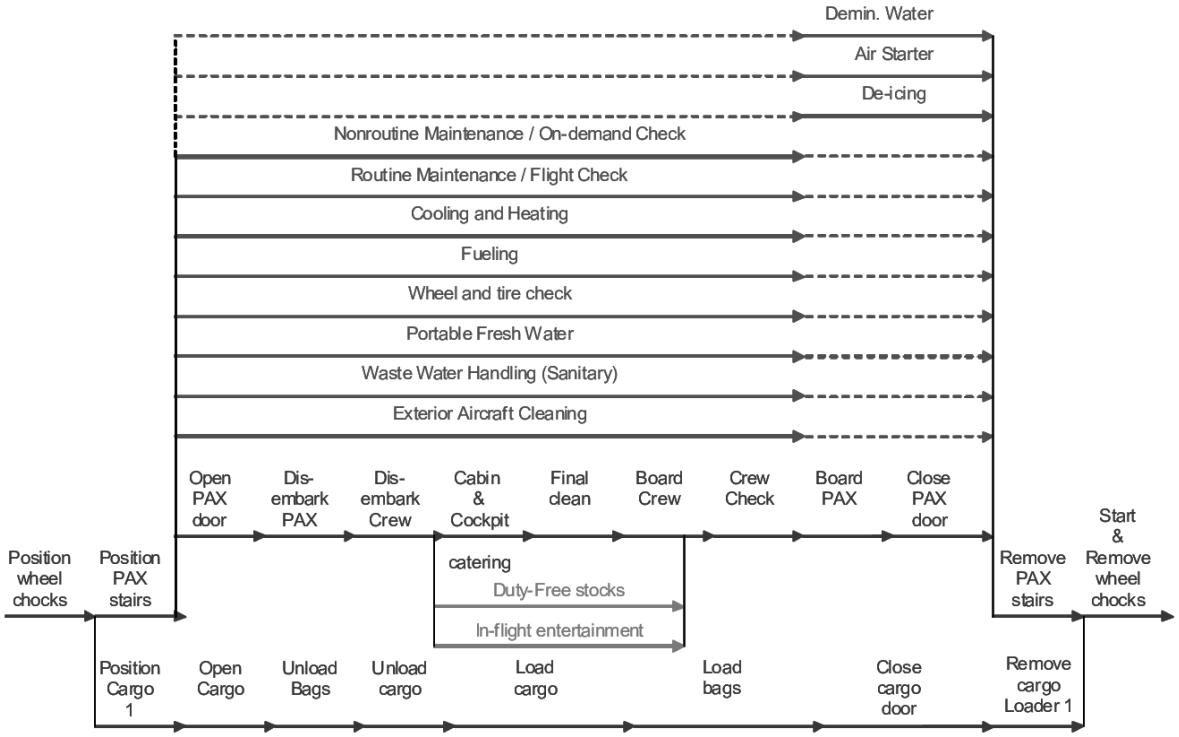

Figure 2.15: Sequential and parallel turnaround processes [106]

The critical path of the turnaround represents the sequence of processes that take the longest time. The turnaround time becomes crucial for short-haul aircraft because it limits the number of possible flights per day. If the turnaround time can be reduced, the aircraft can be used for more flights per day. However, the decisive factor for a short turnaround time is a reduction in the critical path. Conversely, there is no advantage in decreasing a process that is not time-critical. This improvement makes the aircraft more profitable and reduces the Direct Operating Costs (DOC). For the calculation method, please refer to Section 2.6.

Figure 2.16 shows the typical sequence of a turnaround for an A320 with a Gantt chart. The critical path is shown, which reflects the dependencies and independence of individual processes. Processes such as catering, cleaning and unloading are independent and can be performed in parallel. On the other hand, cleaning and boarding are dependent on each other and can only be executed sequentially. The critical path is typically formed by deboarding, catering and boarding [59]. The critical path also depends on the airport. A distinction must be made for the stochastic estimation between the airport types: hub, non-hub and supply base [106]. At the gate or in the apron, the aircraft's parking position is another influencing variable that determines the turnaround time. Boarding and deboarding are accomplished at the terminal with a passenger bridge and in the apron with two boarding stairs, which have a time influence.

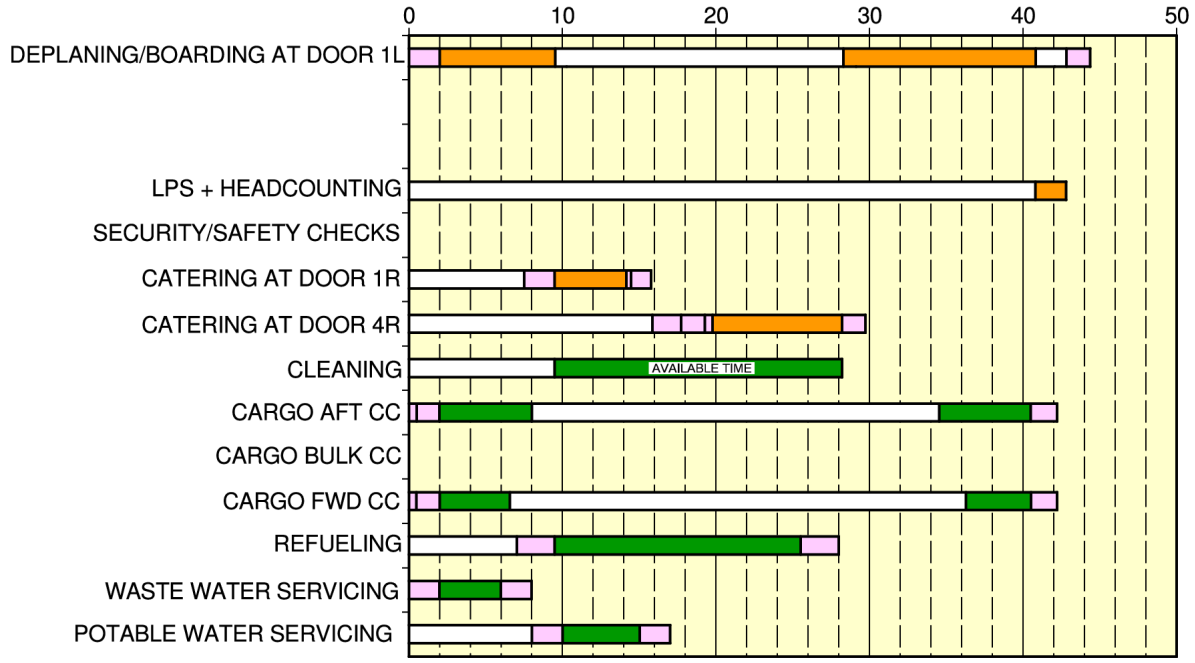

Figure 2.16: Airbus A320 full-service turnaround Gantt chart; turnaround time is 44 minutes; critical path (in orange): deboarding, catering, boarding [11]

In principle, Jet A-1 refuelling and defuelling with passengers embarking, on board or disembarking are possible. However, an increase in safety precautions is provided for this process. Avgas or wide-cut fuels, such as Jet B, or a mixture of these types may not be refuelled if passengers are boarding, on board, or deboarding at the same time. [50]
This regulation can significantly shorten the turnaround process when refuelling is on the critical path. The additional cost, such as an extra person being on the aircraft for a few minutes to support in an emergency case, will not outweigh the time saved.

Due to the complexity of the process and the variety of possible variants, Sanz [122] has defined four different scenarios. These scenarios involve an aircraft, between B737 and A320, with a 500 NM mission. Refuelling with passengers on board is not considered. The scenarios differ simply by the business model of the airline (conventional or low cost) and the parking position (terminal or apron). Furthermore, a half ground handling service is considered for low cost carrier because some airlines do not clean the cabin, refill potable water, and remove wastewater every flight. A detailed description of the different influences considered can be found in Sanz [122]. The results of the turnaround time simulation show that with full ground handling service, the critical path consists of disembarking, cleaning and embarking. Just in case of half service refuelling substitutes cleaning.

In summary, the results from Sanz [122] can be summarised that for conventional Jet A-1 turnarounds at short-range missions, the refuelling of the aircraft is only on the critical path if non-essential operations for each flight are neglected. Besides, this simulation does not consider simultaneous refuelling and boarding/deboarding. By simultaneous operation, the critical path no longer contains refuelling. It would only consist of disembarking and embarking and the waiting time in between, until new passengers are transported to the aircraft by buses or the boarding bridge is completely cleared.

According to the simulation results of Fricke [59], the critical path consists of refuelling in 56 % of the simulated cases. Catering is in 36 % and cleaning in 8 % the limiting process. Furthermore, by parallelizing refuelling and boarding, the conclusion is that turnaround time can be reduced, and catering becomes the critical path.
The critical path depends on 80-90 % of all turnarounds from refuelling, catering or cleaning as the limiting process between deboarding and boarding. The conclusion is also drawn that parallel fuelling and boarding would reduce the turnaround time and could be a solution for delayed flights. [51]
The prediction or determination of the turnaround time is affected by several variables. Based on original equipment manufacturer data [125], the actual statistical turnaround time is shown versus the number of passengers in Figure 2.17. A distinction is also made between aircraft categories to provide a more accurate classification. For regional aircraft, the average turnaround time is determined to 17 min. For single-aisle aircraft, such as the A320, the average time is 35 min, and for twin-aisle aircraft 61 min. [124]

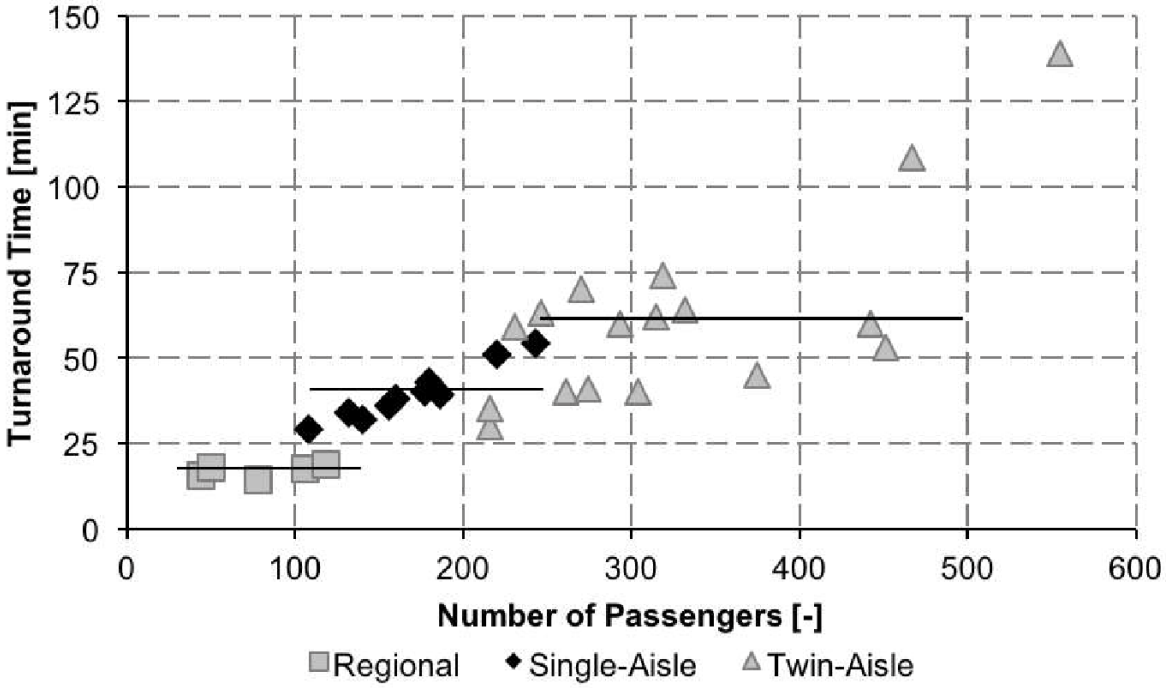

Figure 2.17: Correlation for the turnaround time based on the number of passengers for regional, single-aisle and twin-aisle aircraft; horizontal lines define respectively average turnaround time [124]

As a conclusion to this section, it can be said that refuelling is no longer commonly on the critical path when parallel refuelling and boarding are taken into account. For transit or half ground handling service, refuelling would only become a limiting process for short turnarounds ($<$ 18 min for 150 passengers [122]) if the safety requirements for parallel refuelling cannot be fulfilled. Consequently, it can be concluded that if the refuelling time with LH2 is similar or smaller to Jet A-1, no influence on the turnaround time can be perceived. However, the space requirements of ground vehicles may still affect and influence the turnaround. Besides, the vehicles could interfere with each other and obstruct each other.

2.5 Refuelling of Jet A-1

In the previous chapter, an aircraft's turnaround has been analysed, and it is shown that refuelling does not lay on the critical path. Thereby, refuelling with LH2 should take the same amount of time to have no impact on the turnaround. By this conclusion, the conventional refuelling process of Jet A-1 is the authoritative reference. Therefore, the refuelling process with Jet A-1 is analysed in the following section, considering the procedure, the time required, and the safety precautions.

Commercial aircraft are always refuelled from the lower side of the wing. This procedure is also called pressure or underwing refuelling. The refuelling process requires a ground vehicle connected to the aircraft with one (single) or two (dual) points. Thus, the flow rate or refuelling rate depends on the number of hoses connected. Ground vehicles can be divided into two types. A dispenser is needed when a pipeline is implemented in the airport infrastructure, and a hydrant connection is available at each parking position. The main task of a dispenser is to reduce the operating pressure of the pipeline system from 20 bar to the maximum permissible static pressure of 3.5 bar [77]. The second way to refuel an aircraft is with a refuelling truck. This tank truck does not require a pipeline system but instead acts as a connection between the storage tank and the aircraft. The fuel delivery is carried out by pumps on the truck, which means that the tank truck is independent of external support and can be used on the apron. The time required for positioning and connecting as well as disconnecting and removing the ground vehicle is taken from the Airbus Airport and Maintenance Planning of an A320 with 2.5 min each [11].
Manufacturer-specific specifications for the volume flow are possible up to 4000 l/min with a dual point connection for dispensers and refuelling trucks. The inner diameter of a hose is specified as 2.5 in. [118]
If fuelling shall be faster in time, it is necessary to refuel on both sides of the wing. Hence, a second fuelling vehicle is required. In the case of a long-range aircraft, each side of the wing has dual-point connectors which allow to refuel with two refuelling vehicles. As a consequence, the volume flow doubles which leads to a volume flow of 8000 l/min.

In contrast, short-medium-range aircraft are typically refuelled only on the right side of the wing. Furthermore, only one hose is used for refuelling, i.e. with a single point connection, as faster refuelling is not needed because it is not on the critical path. Therefore, dual point refuelling is not needed, as the refuelling time for continental flights is relatively short. For example, a refuelling time of 15 min is scheduled for an A320. [123]

To be able to define the refuelling process for LH2, the question arises which limitations there are in the refuelling of Jet A-1. Jet A-1 has the property of an accumulator, which is characterised by a low electrical conductivity of less than 50 pS/m. As a result, static electricity builds up as it flows through a pipe due to friction. The discharge of this static electricity can cause ignition of the fuel in explosive mixtures. Therefore, there is a limitation in the flow conditions of Jet A-1 [12, 128, 77]:

$$v \cdot d \leq 0.5\,\mathrm{m^2/s} \tag{2.25}$$

$$v \leq 7\,\mathrm{m/s} \quad | \text{ short pipe} \tag{2.26}$$

$$v \leq 3\,\mathrm{m/s} \quad | \text{ long pipe} \tag{2.27}$$

The limitation in the flow velocity differs in the length of the pipe through which the flow passes. For short pipe sections, such as the deck hose of a refuelling vehicle, a maximum speed of 7 m/s is prescribed. The limitation for longer sections, on the other hand, is stricter and is limited to 3 m/s. Another limitation is the term $v \cdot d$, which can be interpreted as a simplified Reynolds number and thus describes and limits the flow regime. This simplified Reynolds number $v \cdot d$ cannot be used for comparison because it is dimensionally dependent. To evaluate the comparison of the flow regime independent of the fluid, this simplified term of $v \cdot d = 0.5\,\mathrm{m}^2/\mathrm{s}$ can be converted into a Reynolds number with the kinematic viscosity of $\nu(T = 288.15\,\mathrm{K}) = 1.75 \cdot 10^{-6}\,\mathrm{m}^2/\mathrm{s}$ [38] into a Reynolds number of $Re = 2.86 \cdot 10^5$. It is clear that there is turbulent flow in the pipe, but it can still be in the transition area between hydraulically smooth and hydraulically rough in the Moody diagram.

Through Equations 2.25 and 2.27, a diameter of 2.5 in can be calculated using the maximum boundary conditions. This characteristic is probably one reason for choosing this hose diameter. Another reason could be airport refuelling personnel's handling characteristics, as the deck hose has to be manually connected to the aircraft. The mass to be lifted for ground personnel is 24 kg for a hose filled with fuel. The deck hose has a mass of 3.4 kg/m [108] at a length of 3.5 m [118], and the underwing refuelling nozzle has a mass of 3.3 kg [47]. Therefore it is manageable stress for airport staff during a working day [31].
A change in limitations can be made with an antistatic additive [77]. This consideration of an additive is not taken into account, since a reduction of the refuelling time has no influence on the turnaround, see Section 2.4.

Recalculating of single-point fuelling under static electricity restrictions results in a maximum volume flow of a 2.5 in hose of 1500 l/min and of a 3.0 in hose of 1800 l/min. This contemplation means that a volume flow of up to 3600 l/min is possible when refuelling an aircraft with a dual-point connection. To make this volume flow comparable with the refuelling of LH2, it can be expressed as an energy flow of 2100 MJ/s.
The following equation describes the transferred refuelled volume to be able to use these results of the maximum volume flow [69]:

$$\dot{V} = \dot{V}_{t=0} \cdot e^{\alpha \cdot t} \tag{2.28}$$

$$V = \int_0^t \dot{V}\,\mathrm{d}t = \dot{V}_{t=0} \cdot \frac{e^{\alpha \cdot t} - 1}{\alpha} \tag{2.29}$$

$\dot{V}_{t=0}$ defines the initial volume flow, which corresponds to the maximum flow rates calculated with the static electricity limitations. The value for the resistance of the tank and other components involved during refuelling is denoted by the factor α [124].

According to Equation 2.28, the volume flow decreases exponentially for $\alpha < 0$. This decrease is due to the rising liquid level in the tank, leading to an increase in hydrostatic pressure and the increasing pressure losses due to closing valves in the connection between the separated tanks [69]. However, this characteristic can be explained based on the pump capacity and Bernoulli's equation. With a constant pump power, the pump can deliver a higher volume flow at the beginning of the refuelling process because the back pressure due to a low liquid head is still low. As the liquid level rises, the pump must always apply a higher pressure, which leads to a lower volume flow at constant performance. This specific characteristic is represented in factor α and varies depending on the aircraft type. The refuelling process α values are $-0.022\,\mathrm{min}^{-1}$ for a B747 [69], $-0.0145\,\mathrm{min}^{-1}$ for an A380 [69], and $-0.036\,\mathrm{min}^{-1}$ for an A320 [122].

The maximum volume flow varies significantly from the source of specification. The manufacturer-specific specifications are correspondingly high, e.g. 4000 l/min [118], which is technically possible due to a suitable pump design but does not correspond to the limitations. On the other hand, the maximum volume flows still vary from the airport infrastructure [69], which is why there is no clearly defined value. Therefore, a comparable sizeable initial flow rate $\dot{V}_{t=0}$ of 1800 l/min for a single-point and 3600 l/min for dual-point refuelling is used further. At an inner diameter of 2.5 in at the beginning of refuelling, they infringe the limitations due to static charging, but the exponential reduction recaptures this. Nevertheless, these maximum values serve for the time critical comparison with LH2.

Figure 2.18 shows the effect on the refuelling time by aircraft type and the number of hoses. For the same amount of fuel, the α values significantly influence the refuelling time.

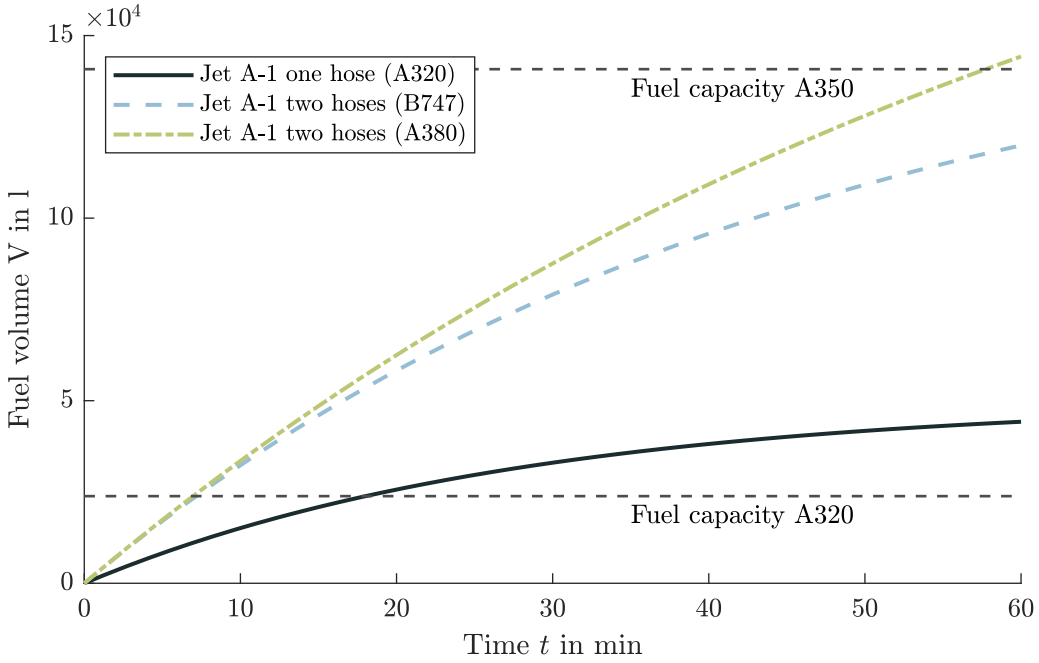

Figure 2.18: Refuelling time comparison between aircraft types; differentiation between short/medium and long-range by the number of connected hoses; same volume flow available at refuelling vehicle level

A variety of regulations regulate the operation and execution of a refuelling procedure with Jet A-1. The safety-relevant aspects relate to the safety distances to the refuelling equipment and the fuel system vent openings on the aircraft. A safety distance of 15 m applies for none aircraft servicing functions. A distance of 3 m for aircraft servicing functions. No ignition spark may occur in these safety zones to prevent the fuel's ignition. [99]
A detailed examination of explosion protection is given in Section 3.1.

2.6 Calculation of Cash Operating Costs

The Thorbeck [148] method is used to calculate the operating costs. To exclude uncertainties in estimating the cost of capital, the Cash Operating Costs (COC), the DOCs without the capital costs, are used in the further analysis. Equation 2.30 shows the basic structure of the Thorbeck calculation method [148]:

$$COC = C_{\text{crew}} + C_{\text{fuel}} + C_{\text{fees}} + C_{\text{main}} = C_1 + C_2 \tag{2.30}$$

Therefore, the COC depends on a fix, route independent costs C_1 expressed through the crew's cost. Secondly, on the variable, route dependent costs C_2 which consists of fuel, fees, and maintenance costs.

$$C_2 = FC \cdot (c_{\text{fuel}} + c_{\text{fees}} + c_{\text{main}}) \tag{2.31}$$

The variable costs C_2 are scaled with the flight cycles per year FC to include the costs per year and an average annual utilisation period. The flight cycles per year can be determined with the following equation:

$$FC = \frac{OT_{p.a.}}{FT + BT} \tag{2.32}$$

The flight cycles per year are calculated through the flight time FT and an additional time called Block Time Supplement BT. The BT defines additional time or duration when the aircraft is not flying. Thereby the turnaround time is also part of this section. As a statistical average, Thorbeck [148] gives a value of 1.83 h.

The sensitivity of block time to COC is shown in Figure 2.19. Especially for short-range flights, a change in block time has a significant impact on operations' costs. A reduction by half would result in a 5.4 % decrease in COC for a 500 NM mission. For longer flights, this effect becomes smaller as the aircraft flies proportionately longer.

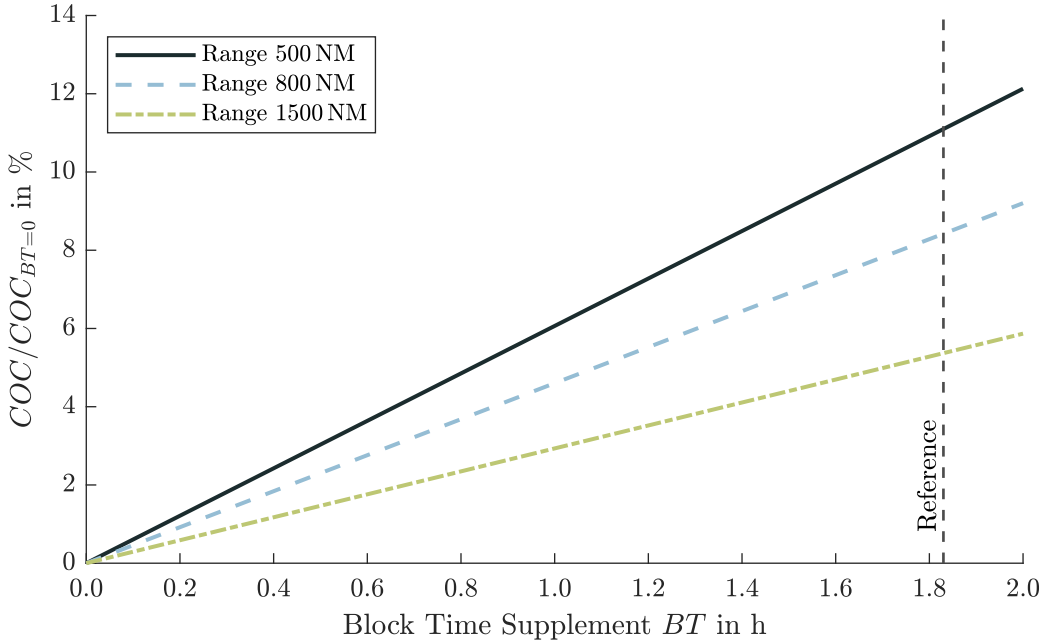

Figure 2.19: Sensitives of COC depending on BT for different flight routes; reference case: $BT = 1.83\,\text{h}$ [148]

However, no direct influence of the turnaround time on the costs can be derived from this sensitivity analysis since there is no correlation between block time supplement and turnaround time. Figure 2.20 shows the relationship between turnaround time and flight distance, which influences the annual flight cycles.

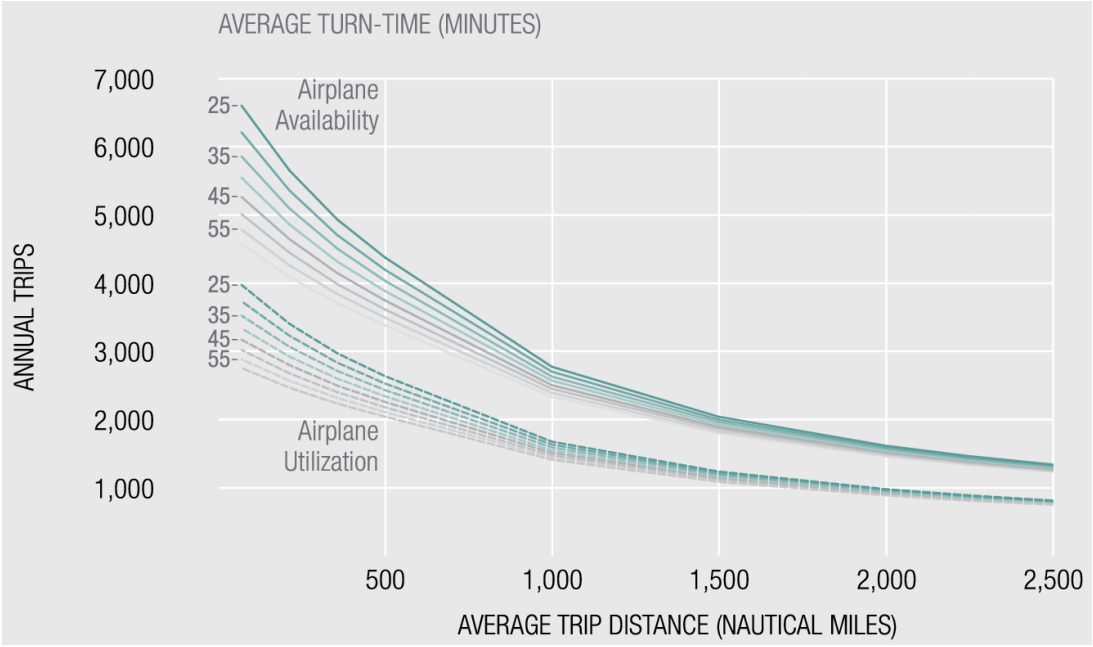

Figure 2.20: Airplane availability and utilisation as a function of average trip distance and turnaround time [96]

The curves are derived from typical mission profiles, and speed schedules [96]. This statement is relevant because the annual flight cycles also depend on the flight time, see Equation 2.32. The flight time can also be expressed in terms of distance and speed and is consequently aircraft type dependent. Based on the findings and the correlations of Mirza [96], a function is derived that converts the turnaround time into a block time supplement, as shown in Figure 2.21.

By transferring and iteratively calculating the turnaround time and range, the block time supplement becomes independent of aircraft type, mission profile, and speed schedule. A similar approach is taken by Schmidt [124], but the turnaround time is directly converted to the annual flight cycles and thus dependent on the aircraft type. There is no considerable variation in aircraft characteristics at long ranges anymore, and therefore the type of aircraft does not affect the flight time significantly. However, at short ranges, there are a variety of possible configurations that vary greatly in altitude and speed. Thus, the separate consideration of flight cycles from turnaround time through block time supplement is particularly relevant at short ranges.

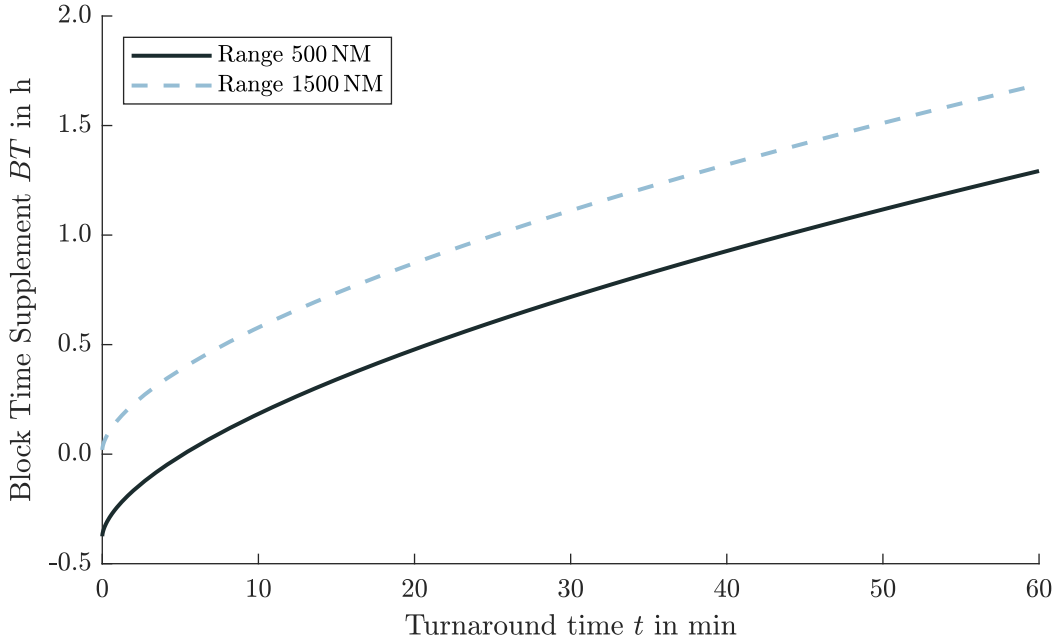

Figure 2.21: Transfer of the turnaround time into the BT for the calculation of the annual flight cycles

Figure 2.21 represents a statistic that describes the effect of the turnaround time on the annual flight cycles. With a longer flight route, which is characterised by a longer flight time, with the same turnaround time, there is subsequently also an increased BT. Alternatively, in other words, the FCs show a nonlinear behaviour since the BT also depends on the flight distance. A possible reason for this nonlinear effect is that the critical path also changes with the flight distance. On short flights, where only carry-on baggage is carried onto the aircraft, the deboarding/boarding and turnaround time are shortened. In contrast, much baggage is carried or must be loaded by the ground crew on the typical vacation flight, which takes more time. Thus, the critical path would depend on various variables and explain the nonlinear influence of Figure 2.21 and 2.20.

The results of the nonlinear correlation on the COCs can be seen in Figure 2.22. Like Figure 2.19, the COCs increase with a longer turnaround time and depend on the flight distance. Differences can be seen in the quantitative values of the costs. By implementing the conversion of turnaround time to the block time supplement, the cost increase becomes smaller for longer turnarounds. Therefore it has less impact on the airline's profit forecast.

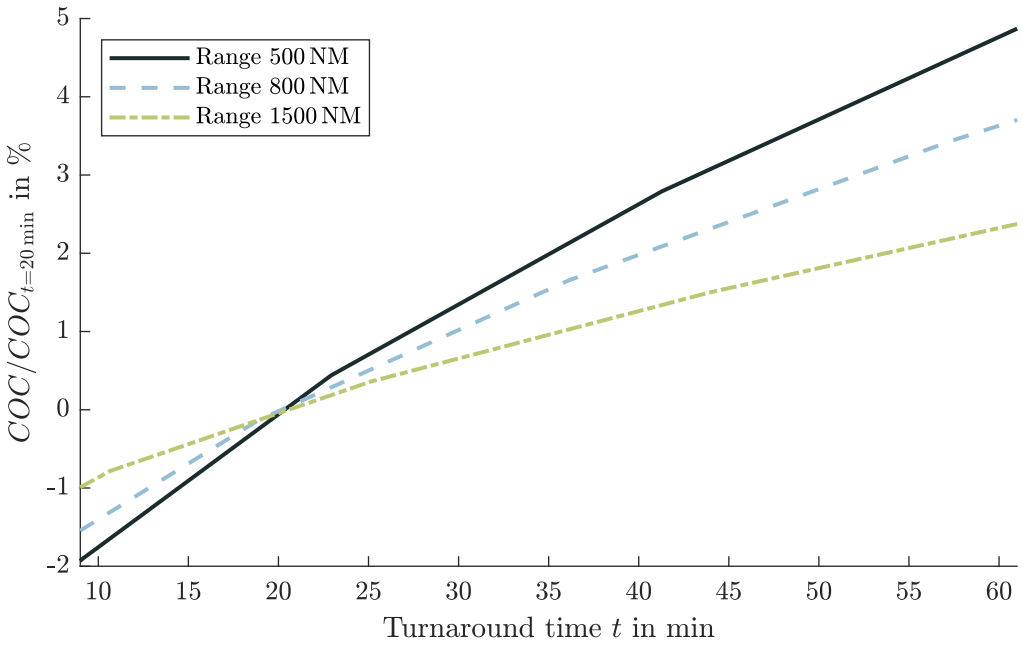

Figure 2.22: Transferred sensitivities of the direct turnaround time to the COC; related to the respective COCs from a 20 min turnaround

3 Turnaround and Refuelling With Liquid Hydrogen

This chapter examines the turnaround and refuelling process with LH2. The safe handling of H2 as a fuel is always in the context of ensuring explosion protection. Due to legal regulations, the basic measures required for handling H2 at the airport are analysed first. The avoidance of a dangerous explosive atmosphere is considered essential. The refuelling procedure with LH2 is defined, and the temporal influence of the individual sequential steps is determined. This procedure consists of positioning and connecting, purging, chill down, fuelling, purging, disconnecting and removing. This process's feasibility at the airport is analysed using two ground vehicles, and the necessary infrastructure is defined. A comparison is made with the refuelling time of Jet A-1 for different fuel quantities and aircraft configurations. Finally, the cost increase of LH2 is determined by the different refuelling systems with the required infrastructure.

3.1 General Safety Regulations

The safety regulations and laws can have a major impact on the handling of H2. Therefore, the conditions should be shown, analysed, and the necessary conditions for their implementation determined in the following section. Basically, explosion protection can be presented in a methodical, common-sense approach that consists of the following three measures: Starting with primary explosion protection, which includes avoiding an explosive atmosphere. The secondary protection describes the avoidance of an ignition source, but an explosive atmosphere can occur. Finally, tertiary explosion protection, which is intended to limit the effects of an explosion to a harmless level.

In the European Union (EU), minimum requirements for explosion protection of workers are documented in the ATEX directives [3, 1]. Furthermore, the minimum safety and health requirements for workers [2] must be observed. The member states of the EU convert these minimum requirements into national laws [82]. In this work, therefore, only German legislation is taken into consideration. Nevertheless, there are guidelines that can be complied with, which give more stringent recommendations, but are not legally binding. In Germany, the EU guidelines have been transferred to the Ordinance on Industrial Safety and Health (BetrSichV) [7] and Ordinance on Hazardous Substances (GefStoffV) [5].
In Germany, the ordinances are further broken down by technical rules. They show the current state of the art and specify the requirements. If the technical rule is complied with, it can be assumed that the ordinances' relevant requirements are met. However, the current state of technology does not have to be complied with, as the technical rules are not statutes. With a well-engineered concept for explosion protection, own rules can be defined, which must then be checked. [6]

The Technical Rules for Hazardous Substances (TRGS) 720 [9] describes the procedure for assessing and avoiding explosion hazards under atmospheric conditions. Hence, no explosion protection measures are required without any explosive atmosphere. According to the Technical Rules for Operational Safety (TRBS) 2152 Part 2/ TRGS 722 [6] a permanently technical tight system prevents a dangerous explosive atmosphere in the area of the system. In the case of a permanent technical system, no releases are to be expected if it is designed accordingly and guaranteed by maintenance and monitoring.

Section 2.2 already describes explosion protection that can prevent foreign particles' ingress by overpressuring the system relative to the environment. The minimum overpressure for LH2 systems is $0.2\,\mathrm{bar_g}$. In the methodological approach, this measure can be classified as primary explosion protection since it prevents an explosive atmosphere. In further work, this principle is adopted as the minimum requirement for H2 systems.

In addition, the release of a hazardous substance and the creation of an explosive atmosphere are not always a reason for a safety area. There must be a dangerous amount (dangerous explosive atmosphere) which is defined above a volume of 10 l. This means that protective precautions are only required if persons are at risk in the event of ignition with a hazardous quantity. [4]

For GH2 and LH2 storage and handling, some safety standards are considered in the following part. These regulations are not legally binding but reflect the experience and the technical status. The relationship between distance separation and quantity of explosive material is expressed in the Quantity Distance (QD) [103]. Furthermore, these guidelines are dependent on the source of ignition and type of use [103, 105, 100]. For example:

- Nonpropellant use: The minimum distance to air compressor intakes, air conditioning inlets, or ventilating equipment shall be 23 m (75 ft) measured horizontally for all quantities of LH2 [105]
- Propellant use: Quantity LH2 $m_{\mathrm{LH2}} < 4536\,\mathrm{kg}$ unprotected distance 182.9 m [103]
- Distances between bulk gaseous oxygen storage and LH2 stored above ground 23 m [100]

This acquired knowledge of explosion protection can hence be transferred to an aircraft and the airport. Brewer [25, 26] suggests that a spark free area with a radius of 27.43 m (90 ft) might be restricted to vehicles with ignition systems that have not been fully bonded or pressurised to prevent exposure to ignitable mixtures of GH2 and air, see Figure 3.1. This conservative approach considers a mechanical failure of the fuelling system. Additionally, slight pressurisation of the cabin and cargo is recommended to prevent GH2 from entering. Through the spark free zone, Brewer [25] applies for secondary explosion protection. In this perspective, explosive atmospheres are permitted in regular operation, protected by avoiding ignition sources. Finally, Brewer [26] argued that with a properly designed process and appropriate safeguards, the hazards during fuelling are not greater. Indeed, the hazards may be lower than the equivalent Jet A-1 fuelling process.

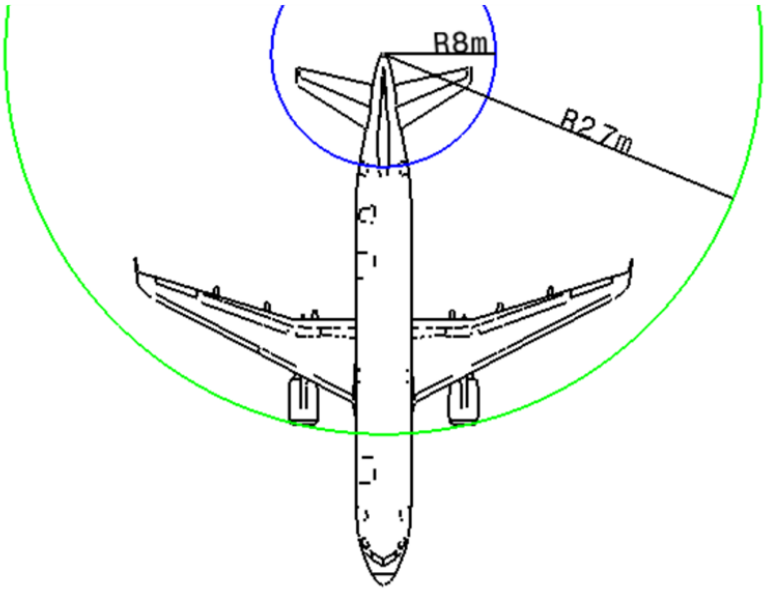

Figure 3.1: Spark free areas around the refuelling connection for a 180-passenger aircraft; considering radius of 27.43 m from Brewer [25]; radius of 7.6 m based on a hose rupture

On another side of view, Boeing [147] shows that leakage of H2 should be prevented because of its low ignition energy. Therefore a potential ignition is always present. Hence, a H2 system must be designed to minimise potential leakage because the elimination of ignition sources is not practical. This safety concept is based on primary explosion protection. Therefore, no safety radius or Ex-Zones are introduced because the system is designed that no dangerous explosive atmosphere exists.

Primary explosion protection is the most sensible protection for H2 because the minimum explosion energy is only 0.017 mJ, see Section 2.1 Jet A-1 requires a ten times higher ignition energy of 0.2 mJ [38]. A single spark, electrostatic charge of clothing through movement has an energy of 10 mJ up to 15 mJ, which already exceeds the minimum energy [30, 17]. Other ignition sources like mechanical sparks and electrical discharges may be in the order of 0.1 mJ [17]. In addition, a tool that falls to the ground can already provide the required ignition energy and trigger an ignition [56]. However, the energy of electric or electrostatic sparks is sufficient for the ignition of most fuel mixtures [161].
Therefore, despite significant safety measures, such as spark free areas, there is a chance that a deflagration will occur if there is an explosive atmosphere. For these reasons, the handling and explicitly the refuelling process with H2 must be part of the primary explosion protection. An explosive atmosphere must not form in normal operation. Conversely, from a legal point of view, no Ex-Zones need to be defined.

The diffusion coefficient of H2 is twelve times higher than gasoline vapour. Therefore H2 tends to disperse more rapidly than other fuels because of the high buoyancy. In an outdoor environment, the rapid dispersion rate of H2 is its greatest safety asset. [17]
Through the high buoyancy, H2 rises rapidly. This effect poses a minimum risk to areas surrounding a spill. Other fuels form flammable clouds which are blown on the ground. Through the non-buoyant behaviour for extended periods, conventional fuels have a great risk of conflagration or detonation if an ignition source is encountered. [26]

The resulting flame during the burning of H2 is relatively nonluminous. The low density and high liquid volatility lead to the rapid dissipation of H2 spills. These properties reduce the damage potential of a major liquid spill. Experience with the Saturn Launch Vehicle shows that damage from a tank rupture is significantly less than with comparable quantities of conventional fuels. Furthermore, the risk to personnel outside the spillage is low due to the fire's low radiative heat transfer. [147]

H2 detection devices are required to strengthen further the safety measures that have been worked out so far. These are attached to all connectors and hoses. According to Bain [16], the gas detector type of sensors must trigger an alarm from a H2 content in the air. Concentration of 0.4 % by volume is therefore chosen for triggering because this H2 content corresponds to 10 % of the LEL and is a condition for safe welding [98].
Two other ways to detect burning H2 are a thermal imaging camera that detects the heat radiation or a thermal wire fire detector to detect a temperature rise above ambient [16]. These options for triggering an alarm help localise the source of a fire. However, when these detecting devices are triggered, H2 is already burning, which indicates a failure of the H2 sensor. Therefore, the use of sufficient sensors is recommended to ensure redundancy in the detection system. The alarm's triggering triggers a rapid automatic shutdown of the refuelling process [147]. With this, the supply of LH2 is stopped in a sudden discharge by closing all valves.

Another conservative approach can be defined by introducing a safety radius of 7.6 m around the refuelling vehicle and vents, see Figure 3.1. The safety radius of 7.6 m corresponds to the QD for a quantity of 150 l [105], which corresponds to the refuelling hose's content. This solution can be traced back to the methodological approach of explosion protection to prevent an ignition spark. This additional provision would prevent ignition in the unlikely scenario of a hose rupture. However, this case is not further considered in this thesis, as the refuelling hose of Jet A-1 has a significant safety factor in the design, which is adopted for LH2.

In summary, the primary explosion protection guidelines are used for the legal safety concept. In other words, a dangerous explosive atmosphere must be avoided. This safety concept allows parallel refuelling with passengers on board. The feasibility and implementation are explained in the following sections.

3.2 Procedure of Refuelling With Focus on Time

Refuelling an aircraft with LH2 requires additional steps compared to Jet A-1. The cryogenic temperatures and the different safety concept have an impact on the procedure and steps required for refuelling. The duration of the refuelling process could increase by a factor of two to three [160] and would thus have a significant influence on the utilisation of the aircraft. The refuelling process can be divided into the following steps: Connecting, purging, chill down, refuelling, purging and disconnecting. This chapter defines and evaluates the steps required for refuelling a LH2-powered aircraft, considering the time influence.

3.2.1 Docking Manoeuvre

The refuelling process begins with the positioning of the ground vehicle that has to execute the refuelling. The positioning and connecting process are divided for LH2, as the hose's connection to the aircraft requires further processes. First, the docking manoeuvre will be specified in this section. For the fuel deck hose connection, airport personnel have so far been required for Jet A-1 to lift the hose with an adapter under the wing and connect it. This procedure does not make sense with LH2 because the hose is not made of synthetic material but stainless steel. As a result, this hose and pipe combination weighs considerably more than a Jet A-1 deck hose and can no longer be handled by one person. Moreover, manual handling of hoses with cryogenic liquids is a safety issue. Manual handling should be carried out in the buddy system, with two qualified persons who are electrostatically protected and should wear protective face shields, goggles and suitable clothing [98]. Thus, manual handling poses difficult-to-perform requirements that can be significantly simplified by a (partially) automated docking system.

A fully automated docking system that can validate the exact position through a sensor system without human interference would offer the highest safety level. This automated system with LH2 is already used on a smaller scale in the automotive industry (see Section 2.3.1). Thus, this approach can also be transferred to aircraft size, where a robotic boom is attached to the ground vehicle. Another example of an automated charging system is the Tesla robotic snake charger [146], which carries out the connecting process without human intervention. The bionic soft arm from Festo [55] demonstrated the required accuracy and mobility, enabling free movement in three-dimensional space.
However, the development of a fully automated process requires expertise, and the duration of implementation and testing must be taken into account, which can lead to problems. Another possibility to perform the docking manoeuvre without direct contact of personnel with the hose is a semi-automated process in which ground personnel control the robotic arm. With this method, there is no need for complex sensor technology and not every aircraft type has to be registered in the system. A similar application of the semi-automated process is the deicing of aircraft. Thereby, a person controls the spray arm on the vehicle because high altitudes have to be reached, and the system weight is too high for manual execution. Therefore, this system design of a deicing vehicle could be used for a semi-automated LH2 refuelling system.

The execution in the (semi-) automated process is expected to be faster to perform than the previous manual process at Jet A-1. Therefore, the conservative approach is assumed that the docking manoeuvre will be carried out at the same time as Jet A-1 of 2.5 min.

3.2.2 Connecting and Purging

When connecting an LH2 disconnect, other measures are required than for Jet A-1. The reason for this is that, as described in Section 3.1, no explosive atmosphere may develop, and, in addition, no foreign gases may enter the tank and fuel system. Due to the cryogenic temperatures, all substances freeze except for helium, which has a lower melting point of 0.95 K and a boiling point of 4.15 K. As a result, helium always remains in a gaseous state and cannot lead to pipeline blockages. Helium has the further advantage of being an inert gas that does not form chemical reactions and dissolves only slightly [143]. Nitrogen also offers the properties of inert gas. However, with a melting point of 63 K and a boiling point of 77.1 K, nitrogen would freeze in the system with LH2 and clog thin lines, such as the injection into the combustion chamber. In principle, therefore, the use of nitrogen in combination with LH2 is not recommended. The use of nitrogen will be considered later on.

As described in Section 2.2, the system requires that the system's contamination of oxygen must not be higher than 1 ppm [98] and that only a spillage of a maximum of 50 ml [8] may occur when connecting the disconnect, which does not cause a dangerous explosive atmosphere. Two methods can meet these requirements. The first method is to connect a disconnect to the aircraft, which is flooded with ambient air and which must then be purged to reduce the foreign gas concentration to the desired level. This connection option is feasible with a Johnston coupling. The second option can be used to eliminate the purging procedure. In this case, the disconnect is designed to release a minimum spillage during coupling and decoupling. Both possibilities have advantages and disadvantages in terms of feasibility and taking into account the time aspect. Therefore, both methods will now be analysed in more detail.

Johnston Disconnect

The first way to perform the connecting process with the Johnston disconnect requires a sequential process sequence to remove foreign gases from the system. There are foreign gases between the first aircraft-side valve and the valve for separation in the hose to the LH2 through the air-flooded Johnston coupling. This gas mixture must be purged out before LH2 is refuelled. There are two basic ways of carrying out this process. On the one hand, pressurisation with inert gas and subsequent depressurisation, called pressure purging: air to inert gas to H2.
On the other hand, alternating vacuuming and pressurisation with an inert gas, called vacuum purging: air to inert gas to vacuum to H2. The advantage of the first variant is that only an additional gas reservoir with high pressure needs to be provided to purge the system. The resulting overpressure in the hose then escapes by opening a valve. The advantage of the second system, which implies a disadvantage of the first variant, is the reduction of the required amount of inert gas [98]. A second disadvantage of pressure purging is the difficulty to determine if all voids and dead-legs have been adequately purged [98].
For these reasons, only vacuum purging is considered for the application on the aircraft. This procedure requires the following steps before H2 can be introduced into the system:

1. Venting the system to atmosphere and evacuation to relatively low-pressure
2. Pressurisation of the system with inert gas to positive gauge pressure

By repeating the cycles, the desired contamination level can be achieved and calculated as follows [105]: The calculation for the required number of vacuuming and pressurisation repetitions can be determined using the ideal gas law in molecular notation, see Equation 3.1. The starting point is the initial volume filled with air (20 % O2) under ISA conditions with a temperature of 288.15 K and pressure of 101.3 kPa. The vessel's total volume to be purged is irrelevant for the number repetitions, as the percentage expressed by the mass concentration c is decisive.

$$n = \frac{p \cdot V}{\Re \cdot T} \tag{3.1}$$

$$c = \frac{n}{V} = \frac{p}{\Re \cdot T} \tag{3.2}$$

The calculation assumes that the temperature remains constant and that the inert gas also has 288.15 K. Therefore, the pressure is reduced to 1200 Pa during the evacuation, which means that the oxygen concentration (c_{O2}) stays constant and is then pressurised to 1.2 bar, which means the amount of substance (n_{O2}) is constant.

The first cycle results in an oxygen concentration of 0.2 %, after the second repetition of 20 ppm and after the third repetition of 0.2 ppm. Conversely, at least three repetitions must be performed until the oxygen contamination is below 1 ppm to add LH2 to the system. Furthermore, pressurisation pressure can be increased, which entails a reduction in the number of repetitions. However, the maximum pressure of the system should not be exceeded. The example case thereby shows a conservative number of cycles. In addition, it must be ensured that the system does not collapse due to vacuuming because additional forms of failure can occur. Furthermore, before disconnecting, a Johnston coupling first requires a purging process to avoid an explosive atmosphere.

Calculation of Time Required for Evacuation

Determining the time required for purging affects the refuelling time and consequently the turnaround. The purging process is an extension of the refuelling time because this is not required for Jet A-1. For the calculation of the evacuation, which is performed with a vacuum pump, reference is made to the following equation [76]:

$$t = \frac{V}{S} \cdot \ln\left(\frac{p_{\text{start}}}{p_{\text{end}}}\right) \tag{3.3}$$

The pump's pumping speed S defines the volume that can be evaluated per unit of time and is selected as $300\,\text{m}^3/\text{h}$ [113] in the thesis.

Calculation of Time Required for Pressurisation

The calculation of the time required for the vessel pressurisation is based on the continuity equation. This formulation results in the following differential equation, which assumes a constant volume flow $\dot{V}$.

$$\begin{aligned}
\mathrm{d}m &= \dot{V} \cdot \rho \,\mathrm{d}t && (3.4)\\
\mathrm{d}\,\frac{pV}{RT} &= \dot{V} \cdot \rho \,\mathrm{d}t && (3.5)\\
\mathrm{d}p &= \frac{\dot{V}}{V} \cdot \rho RT \,\mathrm{d}t && (3.6)\\
\mathrm{d}p &= \frac{\dot{V}}{V} \cdot p \,\mathrm{d}t && (3.7)\\
\frac{1}{p}\,\mathrm{d}p &= \frac{\dot{V}}{V}\,\mathrm{d}t && (3.8)\\
\int_{p_1}^{p_2} \frac{1}{p}\,\mathrm{d}p &= \int_0^t \frac{\dot{V}}{V}\,\mathrm{d}t && (3.9)\\
\ln\left(\frac{p_2}{p_1}\right) &= \frac{\dot{V}}{V} \cdot t && (3.10)\\
t &= \frac{V}{\dot{V}} \cdot \ln\left(\frac{p_2}{p_1}\right) && (3.11)
\end{aligned}$$

According to the isentropic outflow, a constant volume flow results with the following equation. The Mach number in the tightest cross section is set to $M = 0.3$ to exclude compressible effects and prevent choking in the duct. The narrowest cross section is set to a diameter of $d_{\min} = 20\,\mathrm{mm}$.

$$\dot{V} = \frac{\dot{m}}{\rho} = v \cdot A = const. \tag{3.12}$$

$$\dot{V} = \frac{v}{a} \cdot a \cdot A \tag{3.13}$$

$$\dot{V} = M \cdot \sqrt{\kappa \cdot R \cdot T} \cdot A \tag{3.14}$$

$$\dot{V} = M \cdot \sqrt{\kappa \cdot R \cdot \frac{T}{T_0} \cdot T_0} \cdot A \tag{3.15}$$

$$\dot{V} = M \cdot \sqrt{\kappa \cdot R \cdot T_0} \cdot \left(1 + \frac{\kappa - 1}{2} \cdot M^2\right)^{-\frac{1}{2}} \cdot \frac{\pi}{4} \cdot {d_{\min}}^2 \tag{3.16}$$

With helium as the inert gas, $R = 2077\,\mathrm{J/kg/K}$ and $\kappa = 1.67$, a volume flow of $334\,\mathrm{m^3/h}$ is calculated.
A standard disconnect, such as the Johnston disconnect, flooded with air, requires considerable time and resources to enable refuelling with LH2. However, through a vacuum pump and helium provision, it is possible to handle the Johnston disconnect safely. This method is the safest option, as there is no risk of foreign gases entering or creating a dangerous explosive atmosphere.

After the refuelling process, a purging process follows, which then proceeds in reverse order: The remaining LH2 is flushed out of the hose by starting to pressurise it with helium. The next step is evacuation with the vacuum pump, followed by pressurisation with helium until enough cycles have been performed for the H2 concentration to fall below 0.25 %. This concentration of H2 is below the LEL by a factor of 15 and is therefore safe, see Section 3.1. In a conservative view, purging can also be repeated three times, as in the first purging when connecting.

Nitrogen, which also has inert gas properties, is not suitable for direct contact with LH2 because of its high melting and boiling point. For cryogenic substances below 80 K, helium should be used, and above 80 K, nitrogen can also be used [105]. However, there is a possibility to use nitrogen even with LH2. In this case, the ambient air is first removed from the vessel with nitrogen by a purging process until the desired concentration is reached. Then, using GH2, a second purging process must occur until nitrogen is removed from the system. Finally, LH2 can be introduced into the GH2 environment. This procedure offers the same safety aspects as the previous ones. However, twice the number of purging operations, i.e. evacuation and pressurisation, must be executed because the atmosphere is changed twice. Since this time aspect can be decisive, especially for short ranges, when only small quantities are refuelled, this procedure is not considered further. However, in the event of an extraordinary increase in helium's price, it may be considered.

Clean Break Disconnect

As described in the introduction to purging, there is a possibility that does not require purging. Using a clean break disconnect, as shown in Section 2.2, it is possible to connect the subsystems without foreign gases entering or a large amount of H2 escaping. This feature can be attributed to design measures that have been applied to enable a low spillage or clean break disconnect.

Finally, this type of disconnect has the advantage that the purging process's time is eliminated, and LH2 can be refuelled immediately after the connection. This type of disconnect is also used in the conventional refuelling with Jet A-1. Dry break quick disconnects also have no (low) spillage, making them accessible and safe to use. All in all, the clean break disconnect is a feasible application that no longer requires a purging process and thereby allows a time advantage and, on the other hand, does not require inert gas, which offers an economic advantage.

With a conservative approach with the clean break disconnect, it is possible to perform a purging cycle to ensure a foreign particle-free environment. Using an oxygen sensor, which measures the oxygen concentration, the number of purging cycles can be calculated so that there is only one ppm of oxygen in the system. Due to the resolution limit of 100 ppm of the spectrometer [93], one purging process would be sufficient to get below a concentration of 1 ppm O2.

Finally, it can be concluded that a clean break disconnect would be the best solution for handling LH2, as there are time and cost advantages with similar safety. Nevertheless, the Johnston disconnect with purging is also considered in the thesis because it is fully developed and is the simplest method to implement.

3.2.3 Chill Down of Hose and Reduced Mass Flow

The next step in the refuelling procedure is to chill down the system and the lines. As already described in Section 2.3.1, a section on the aircraft or ground vehicle will heat up and have to be chilled down. The reason for this is that for a continuous, steady and vapour free flow, the line must reach a temperature range that flow boiling, as described in Section 2.1.3, can no longer occur [64]. In addition, the temperature gradients in the material or pipe create undesirable stresses that can lead to damage and fatigue failures [102]. To keep the thermal stress low, only a reduced mass flow can be refuelled in the chill down time, which has a temporal influence on the refuelling duration.

The duration of the chill down and consequently the time of the reduced mass flow can be calculated with the lumped capacitance method. With this transient approach, the temperature in the material does not vary significantly with position. Furthermore, the fluid temperature is assumed to be constant and not a function of time. This approach is correct as the LH2 arrived throughout the refuelling hose in the first few seconds of LH2 transport. A similar fluid temperature of 20 K is established in the hose due to the proximity to the NBP. In other words, the proximity to the wet vapour region is advantageous for using this method, as the pressure and temperature remain constant while the LH2 evaporates. The lumped capacitance method requires a Biot number lower than 0.1 [18].

$$Bi = \frac{h \cdot L_\mathrm{c}}{k_\mathrm{solid}} < 0.1 \tag{3.17}$$

The Biot number is calculated with the heat transfer coefficient h, the characteristic length $L_\mathrm{c} = V/A$ and the thermal conductivity of the solid material k_solid. A Biot number greater than 0.1 indicates more complex transient heat transfer equations and that the spatial temperature uniformity is not given.

Considering the heat transfer coefficients from Section 2.1.3 and stainless steel as the material with thermal conductivity of 20 W/mK, the Biot number is below 0.1 in widespread areas of the Nukiyama curve. In the nucleate boiling area, the Biot number becomes larger than 0.1 because, at this point, the heat transfer coefficient increases significantly. Nevertheless, the nucleate boiling is only in a negligible temperature range, which does not have an enormous influence on the chill down time. Furthermore, this error in the requirements can be tolerated, as the lumped capacitance method is analytically solvable and quickly shows a trend. A detailed consideration would require transient, position-dependent numerical modelling, which is not necessary for the preliminary design.

The differential equation can be applied from the principle of conservation of energy:

$$m \cdot c_p \cdot \frac{\delta T}{\delta t} = \dot{Q} \tag{3.18}$$

$$m \cdot c_p \cdot \frac{\delta T}{\delta t} = q(T) \cdot A = h(T) \cdot (T_\infty - T) \cdot A \tag{3.19}$$

$$h = f\left(h_{\text{boiling}}, h_{\text{convective}}\right) \tag{3.20}$$

The negotiation of the convective heat transfer [67] is not adopted, as the consideration of the heat flux through the Nukiyama curve is more accurate. In addition, all energy balances must be fulfilled in order to obtain realistic results.
Due to the cooling from ambient temperature to the cryogenic temperature of LH2, the specific heat capacity of stainless steel is no longer constant. It must also be treated as a function of temperature. [88]

$$m \cdot c_p(T) \cdot \frac{\delta T}{\delta t} = q(T) \cdot A \tag{3.21}$$

$$\int_{T_0}^{T} \frac{c_p(T)}{q(T)} \,\mathrm{d}T = \int_0^t \frac{A}{V} \cdot \frac{1}{\rho} \,\mathrm{d}t \tag{3.22}$$

$$\frac{A}{V} = \frac{\pi \cdot d_i \cdot l}{\pi/4 \cdot \left({d_o}^2 - {d_i}^2\right) \cdot l} = \frac{4 \cdot d_i}{\left({d_o}^2 - {d_i}^2\right)} \tag{3.23}$$

According to this equation, the chill down time is almost independent of the length of the pipe. Typically for the lumped capacitance method, the derived equation is a function of the characteristic length, which in this case is approximately the wall thickness of the pipe. Conversely, this method does not show all physical effects since, in reality, the chill down time is a function of the pipe length. However, the simplified approach results are in the same order of magnitude as experimental data [136, 23]. The pipe length is only indirectly (iteratively) considered in the calculation, as the surface of the pipe determines the vapour content, see Section 3.2.3. Another possibility of simplified modelling can be found in Rame et al. and Steward et al. [114, 136]. In addition, the equation shows the dependencies of the equation. The term of specific heat capacity and density of the material enters into the time duration. An aluminium alloy would thus have an advantage over stainless steel. Due to the wall thickness, which depends significantly on the tensile strength and Barlow's formula, stainless steel is again advantageous in the combination of all variables.

In the transfer pipe's overall design, which should have vacuum insulation to keep the heat input low, this means that the inner pipe only has the load case against internal pressure. The outer structure can therefore take all other loads and is the load-bearing structure. The inner pipe could thereby have a low wall thickness, which lowers the cooling duration. In the further design, the operating gauge pressure, the same as for conventional Jet A-1 hoses of 600 psi or 42 bar [108], corresponds to a wall thickness of 2.5 mm for a stainless steel pipe.

Figure 3.2 shows the maximum LH2 flow rates to avoid excessive thermal stress due to rapid chill down. This diagram thus gives the reduced mass flow during the chill down phase, which is necessary to calculate forced convection.

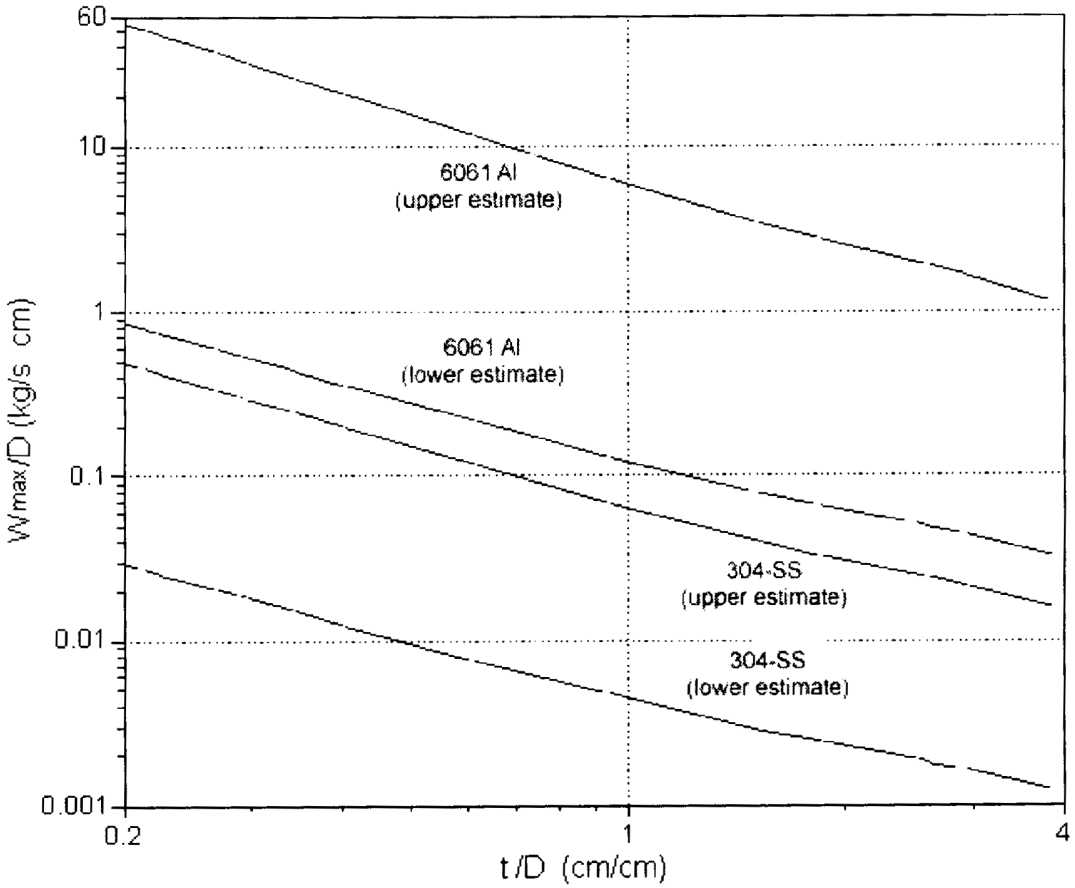

Figure 3.2: Limits for LH2 mass flow to avoid excessive chill down stresses [105]

Minimum flow rates are also theoretically to be observed in order to avoid wave or stratified flows [105, 102]. However, these minimum rates are so low that they have no relevance for the refuelling of an aircraft. A second requirement for the start of refuelling with the regular mass flow are temperature sensors. These sensors must be located on the respective lines and provide feedback on the pipe temperature, which should be below 25 K to avoid transition boiling, see Section 2.1.3. The results of the chill down time and reduced mass flow can be found after the definition of the pipe diameter in Section 3.2.5.

Definition of GH2 Recovery Line

Due to the vaporisation losses, the refuelling process differs fundamentally from conventional Jet A-1. Due to the required recovery line, it is essential to connect two lines to the aircraft, but only one can transfer a deliverable mass flow of LH2. In contrast to the automotive application in Section 2.3.1, a coaxial pipe is not considered because the outer diameter would be too large.

The vaporised H2 must be removed from the aircraft tank during the refuelling process, which requires a dimensioning of the recovery line. By considering the energy balances of the material, heat transfer and LH2, an evaporated fraction of the mass flow can be calculated.

$$\dot{m}_{\mathrm{vap}} = \frac{q(T) \cdot A}{\Delta h_{\mathrm{v}}} \tag{3.24}$$

The maximum vaporised H2 mass flow during the chill down phase is used as the design point for sizing the recovery line's diameter. For safety reasons, the return line's static pressure or pipeline should not fall below 1.2 bar. In Equation 3.25, a Mach number can be calculated by applying the isentropic outflow. The total pressure corresponds in a first approximation to the tank pressure since the assumption is made that the fluid settles at this point. Since this back pressure should be kept as low as possible during the refuelling process, a total pressure of 1.25 bar results in a Mach number of 0.22. Equation 3.27 can thus be used to calculate the recovery line's diameter for a given mass flow that must be removed.

$$\frac{p}{p_0} = \left(1 + \frac{\kappa - 1}{2} \cdot M^2\right)^{\frac{\kappa}{1-\kappa}} \tag{3.25}$$

$$\dot{m}_{\mathrm{vap}} = \rho \cdot v \cdot A \tag{3.26}$$

$$\dot{m}_{\mathrm{vap}} = \frac{M}{\left(1 + \frac{\kappa-1}{2} \cdot M^2\right)^{\frac{\kappa+1}{2\cdot(\kappa-1)}}} \cdot \sqrt{\frac{\kappa}{R \cdot T_0}} \cdot p_0 \cdot A \tag{3.27}$$

Nevertheless, the theoretical consideration must be made about what Mach number and what tank pressure would result from the complete vaporisation of the reduced mass flow. A further calculation task is whether the recovery adapter in the fast fill, without reduced mass flow, could remove possible proportionate vaporised amounts of H2 that occur due to environmental heat impact. A heat flow in the order of 4 W/m occurs through the Vacuum Insulated Pipe (VIP) [43, 42, 54, 75]. In addition, the heat input to the aircraft tank is in the order of 30 W/m^2 [95]. The heat flow that occurs during the stationary refuelling process is therefore negligible and no design point.

Mass and Loss of Vaporised Hydrogen Through Chill Down

The following equation can calculate the vaporised mass of LH2 from the amount of energy for the temperature change of the pipe:

$$m_{\mathrm{vap}} = \frac{m \cdot c_p \cdot (T_\infty - T)}{\Delta h_{\mathrm{v}}} \tag{3.28}$$

The evaporated mass also represents a loss term that must be additionally included in the operating costs. Cold H2 remains in the supply line to keep the loss of LH2 as low as possible and avoid the necessity of cooling the entire line from the ground vehicle to the aircraft tank during each refuelling process [26]. By switching valves, LH2 can be retained in the feed line, whereby this part remains at cryogenic temperature and does not have to be cooled during the following refuelling process. This procedure is possible with both the clean break disconnect and the Johnston disconnect, as purging processes can be carried out through the recovery line. A small expansion tank is attached to the ground vehicle to avoid a disproportionate pressure increase in the line in which LH2 remains due to heat input and vaporisation. This expansion tank represents a kind of heat capacity and extends the time between possible refuelling processes.

3.2.4 Fuelling Mass Flow of Liquid Hydrogen

The time for the refuelling process during aircraft turnaround is essential for many flights and a good utilisation. According to Section 2.5 the turnaround segment of feeding or flowing fuel is the main part in the refuelling process. For a carbon neutral H2 aircraft, the refuelling procedure has to be investigated to derive impacts on aircraft costs. According to the Clean Skies for Tomorrow report [160], the refuelling time could be 2-3 times longer than conventional Jet A-1. This statement is based on the assumption of the same volume flow of 900 l/min [91]. First, this assumption of a volume flow of 900 l/min is low and nonsensical according to an average flow rate from an A320 of 1250 l/min [11] and the maximum flow rate of one hose and single point refuelling of 1800 l/min [118]. Second, the comparison of dimensional values of different fluids with large differences in physical properties is difficult and doubtful.

The simplest comparison from H2 and Jet A-1 refuelling flow rate is to set the energy flow of 2100 MJ/s equal. This is in first contemplation possible because a flight with a comparable aircraft configuration needs the same amount of energy, assuming the same efficiencies. It results in a LH2 mass flow of 20 kg/s or a volume flow of 17,000 l/min, that would be necessary to get the same refuelling time. From this point of view, the refuelling flow time is constant, and there should be no impact on the turnaround. On the other side boundary conditions, like flow velocity and hose dimensions, are not determined by this approach. Considerations like Sefain [127] with just the information of volume flow of 5000 l/min and no consideration of the entire system are therefore only of limited use because the replicability of the limitation is not guaranteed.

In Table 3.1, there is a literature comparison for H2 aircraft refuelling parameters. The mass flow rates tend to be similar to 20 kg/s. In addition, the table gives an overview of the simplified Reynolds number $v \cdot d$ and the velocity in the hose. It is noticeable that the first investigations assume a lower Reynolds number, which leads to a lower flow velocity or a larger hose diameter.

Source	$\dot{m}$ kg/s	$\dot{V}$ l/min	d in	$v \cdot d$ m^2/s	v m/s
Brewer [26]	20	16,950	4.9	2.90	23.39
Boeing [147]	15	12,710	7.0	1.52	8.51
Brewer et al. [25]	13	11,020	8.0	1.15	5.67
ISO/PAS 15594 [72]	20	16,950	5.5	2.57	18.35

Table 3.1: Comparison of aircraft refuelling flow rates for LH2 from literature research

The limitation in velocity of Jet A-1 refuelling system and especially in the deck hose set a boundary in fuelling capacity, see Section 2.5. Edeskuty et al. [48] and OSMA [105] describe the electric charge build-up for LH2 as no problem, because the electrical conductivity is in the range of 10^{-19} S/cm. According to Edeskuty et al. [48] it is just a problem for electric conductivity from 10^{-15} S/cm to 10^{-10} S/cm. As a result, there is no limit to the Reynolds number and velocity for LH2. In comparison with Jet A-1 the Reynolds number of the Space Shuttle loading, see Section 2.3.2 and 2.5, is two magnitudes higher and shows the influence and restrictions to static electricity of Jet A-1.

The space shuttle refuelling is the most significant comparison in this work because it has already worked and proven to be reliable for decades. Therefore, the Reynolds number of $122.3 \cdot 10^5$, as in Section 2.3.2, is set as the limit for the flow regime, expressed in the simplified size in Equation 3.29. This must be observed. A limitation, as with Jet A-1 in the maximum speed, is also introduced for reasons of comparability. This velocity limitation for short lines results from the values in Table 3.1, see Equation 3.30.

$$v \cdot d \leq 2.35\,\mathrm{m^2/s} \tag{3.29}$$

$$v \leq 15.5\,\mathrm{m/s} \quad | \text{ short pipe} \tag{3.30}$$

$$v \leq 8.0\,\mathrm{m/s} \quad | \text{ long pipe} \tag{3.31}$$

Applying both limits results in a refuelling hose with a inner diameter of 6 in for a mass flow of 20 kg/s. In contrast to Jet A-1, this larger diameter is no problem for the handling by the ground staff because the connection would be carried out automatically, see Section 3.2.1.

Figure 3.3 shows a comparison of the refuelled energy. By looking at the amount of energy, the refuelling time is possible under the assumption of the same aircraft performance and efficiency. The gradient at null shows the design point of the LH2 refuelling because there the gradient is the same as with two Jet A-1 hoses. Also, the refuelling flow does not drop exponentially because the design considers the increasing hydrostatic pressure. However, this consideration does not include the necessary procedure before and after the refuelling process but only shows the comparison of the refuelled energy over time. Nevertheless, it can be seen that LH2 has an advantage because the design point was chosen at the maximum of the volume flow of Jet A-1.

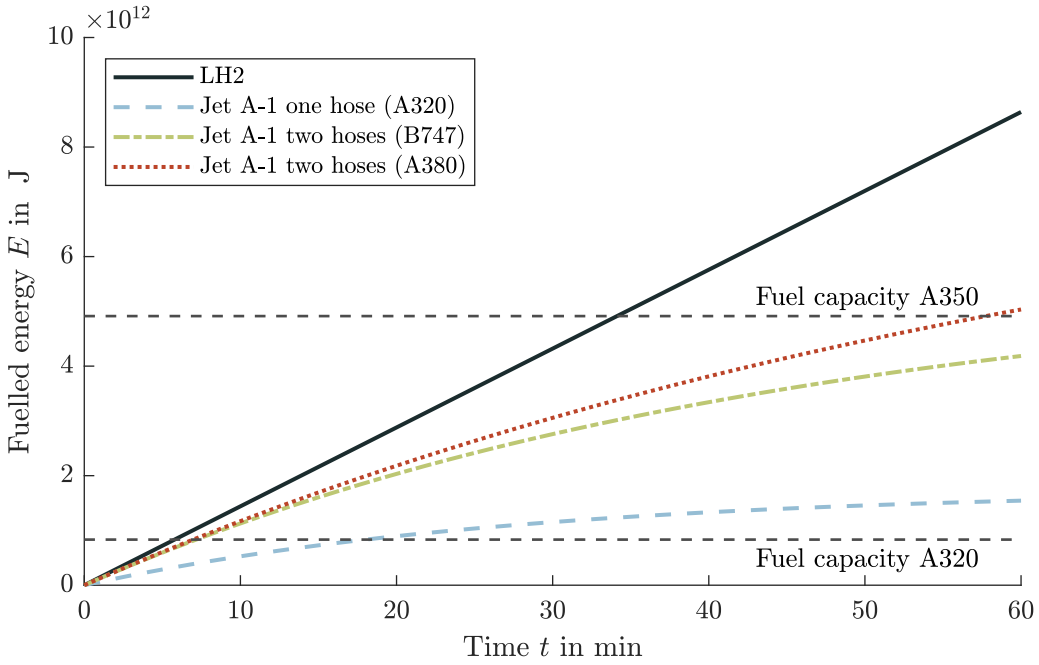

Figure 3.3: Refuelling comparison between Jet A-1 and LH2

Finally, the question about the measurability of the volume flow and the amount of refuelling: Due to the physical properties and evaporation that occurs, for example, during chill down, the volume flow measurement is not trivial. The calculation of the Mach number shows a significantly increased speed with an evaporating part. As a result, not all measuring devices are suitable; they must be able to cope with a two-phase flow or withstand high flow speeds or excessive rotor speed without damage [68]. In addition, most measuring devices work with an indirect measurement of the mass flow through the volume flow and the density. However, this is made more difficult by the two-phase flow since there must be a density. Thus, the mass flow is determined with a direct measurement by a Coriolis mass flow meter [149]. This has no rotating components in the flow area and is therefore not susceptible to two-phase flows and higher speeds.

3.2.5 Results of the Refuelling Procedure

The results from the calculation of the previous sections are to be presented in this part. Due to the individual steps' dependency, it is impossible to consider them separately from each other. It must be designed as a complete system. The mass flow is 20 kg/s at the refuelling, which defines the inner diameter of the feeding line of 6 in by the restrictions. Due to the diameter, the material (stainless steel) and the pipe's wall thickness, a reduced mass flow of 3 kg/s is defined for slow fill according to Figure 3.2. Thus the chill down time of 40 s can be calculated with the lumped capacitance method, independent of the line length. By calculating the heat flow over time, the theoretical maximum vaporisation fraction of the mass flow of 1.4 kg/s is determined. In the design case for the recovery line, this mass flow corresponds to an internal diameter of 5 in at a Mach number of 0.22 and a total pressure in the tank of 1.25 bar_a. If the complete reduced mass flow of 3 kg/s vaporises, a Mach number of 0.5 and total pressure in the tank of 1.35 bar_a will result. This maximum tank pressure is an important design criterion for the following pump or pressure feed system design. After the refuelling system's dimensions between the ground vehicle and aircraft tank have been defined, the time required for purging can be calculated.

The evacuation and pressurisation are carried out via the recovery line with an assumed length of 10 m. This length means that a volume of 0.25 m^3 must be accounted for, which leads to an evacuation time of 13.5 s and a pressurisation time of 13.5 s: In combination for one purging cycle of 30 s. For a Johnston disconnect, the purging cycle has to be done three times. This repetition corresponds to a time of 90 s each before and after refuelling. For the semi-automated docking and de/positioning, a duration of 150 s is considered. At the beginning and the end of the refuelling procedure, this time is equivalent to Jet A-1 refuelling. Table 3.2 shows the rounded values of the individual steps:

Refuelling Step	Time min
Positioning and connecting	2.5
Purging	1.5
Chill down	1.0
Refuelling	$f(m_{\text{fuel}})$
Purging	1.5
Disconnecting and removal	2.5

Table 3.2: Required time intervals for the individual consecutive steps of the refuelling procedure of liquid hydrogen; time durations are independent of the refuelled quantity, refuelling time is a function of the required fuel mass or volume; the individual steps' sum is 9 min for a Johnston disconnect and 6 min for a clean break disconnect

These time intervals of the individual steps are independent of the mass of LH2 to be refuelled. The sum of 9 min must be accounted for each time the refuelling system is connected with a Johnston disconnect. With the clean break disconnect, where purging is omitted, a time of an additional 6 min is required for each refuelling procedure.
Brewer [26] estimates the time required before refuelling at 7 min and after refuelling at 5 min. Connecting for the hydrant pit and the aircraft adapter takes 2 min, purging takes 3 min and cooling down the lines 2 min. After refuelling, 3 min are needed for inerting and 2 min for disconnecting the hoses. In total, this means 13 min.
Compared to the calculated duration for a Johnston coupling, which also prescribes a purging process of 9 min, this is a slight deviation. The duration of the purging is also the most considerable difference. This discrepancy can be explained by the fact that Brewer [26] does not specify the exact number of repetitions for purification (pressurisation and evacuation) but mentions the number of three or four repetitions. The evaluation is to be derived from experimental data. Also, Brewer [26] describes that both lines, the LH2 support line and GH2 return line, must be purged. However, this assumption significantly increases the volume to be purged, which also justifies the longer duration. However, Brewer [25] contradicts this assumption that the feed line must also be cleaned since the feed line should remain filled with H2 to reduce the chill down process time.
Consequently, complete cleaning of the feed line is unnecessary. Only the connection adapter needs to be purged through the recovery line. In a pipeline dispenser case, the hydrant lines cannot be ignored but can be neglected due to the short line lengths.

3.3 Airport Distribution System for Liquid Hydrogen

For implementing the refuelling procedure at the airport, there are two ways of transferring the fuel from the storage facility to the aircraft tank, similar to Jet A-1: Firstly, a refuelling truck picks up the LH2 at the storage tank and then drives along the airport roads to the aircraft parking position. Secondly, a pipeline system transfers LH2 to the aircraft through hydrants at the parking position using a dispenser. Both methods can be designed and dimensioned using the following equations.

The basis for this is the incompressible Bernoulli equation, which determines the supply pressure based on friction losses, height differences and velocity terms. This approach enables the dimensioning of the overpressure or total pressure without the actual flow rate. In other words, it is independent of the mass flow.

$$p_1 = p_2 + \frac{\rho}{2} \cdot v^2 + \rho \cdot g \cdot h + \Delta p_{\text{friction}} + n_{\text{valve}} \cdot \Delta p_{\text{valve}} \tag{3.32}$$

The friction losses of the pipes can be determined with the Moody diagram. The approach with the Darcy friction factor λ and the Colebrook and White equation [104], which calculates a rough hydraulic pipe, is chosen:

$$\Delta p_{\text{friction}} = \lambda \cdot \frac{l}{d} \cdot \frac{\rho}{2} \cdot v^2 \tag{3.33}$$

$$\frac{1}{\sqrt{\lambda}} = -2 \cdot log\left(0.27 \cdot \frac{k}{d} + \frac{2.51}{Re \cdot \sqrt{\lambda}}\right) \tag{3.34}$$

$$\tag{3.35}$$

The friction losses through valves can be calculated with the following equation [142]:

$$\Delta p_{\text{valve}} = \left(\frac{Q}{K_{\text{valve}}}\right)^2 \cdot \frac{\rho}{1000} \cdot 1e5 \tag{3.36}$$

The supply pressure strongly depends on the number of valves, which is different for the two variants in the first estimation. A roughness value of $k = 0.08\,\text{mm}$ [151] is used for the friction in stainless steel pipes, and a flow coefficient of the valves of $K_{\text{valve}} = 300\,\text{m}^3/\text{h}$ [49] is calculated. In a first estimate, the delivery head is 10 m, and the pipeline length is 20 m. The tank pressure should be kept as low as possible and is set to $1.2\,\text{bar}_\text{a}$, for further considerations see Section 3.4.

3.3.1 Refuelling Tank Truck for Interim Phase

The simplest distribution system for fuel is the refuelling of aircraft by tank truck from a hardware and architectural standpoint. However, this concept has not been considered further in the terminal ramp area because of the physical requirements for room there. [147]

The fact that nowadays, the refuelling process with Jet A-1 is carried out with tank trucks at airports anyway shows this statement's discrepancy. The choice of distribution system depends on the airport's daily fuel demand, and therefore no general conclusion can be drawn. A refuelling truck supplying can be a possible variant for a transition phase between Jet A-1 and LH2, where only small amounts of LH2 are needed. The refuelling truck concept enables a conventional airport to refuel with LH2 without significant modifications and investment costs.
However, complete consolidation of LH2 is challenging to implement, as the capacity per refuelling truck is limited. Thus, a large number of trucks would have to be provided, especially for long-range or widebody aircraft. This space requirement near the terminal would not be available during a turnaround and could not be implemented.
Boeing [147] therefore only uses the refuelling truck for remote places such as at maintenance or cargo areas. Besides, the tank truck is intended for unloading LH2 from a decommissioned aircraft in preparation for recovery operations. However, refuelling at airports with low widebody traffic, i.e. short-medium-range aircraft, and use in maintenance areas are not excluded in principle. A refuelling truck concept must nevertheless be available for emergency refuelling.
The advantage of a tank truck on short-medium-range or single-aisle aircraft relates to the aircraft tank's capacity. The volume for the LH2 tank of an A320-like aircraft with 180 passengers will be in the range of 40 to 70 m^3, which is just the possible volume of an LH2 truck, see Section 2.2. Boeing [147] names the capacity of the fuel truck shown in Figure 3.4 as 57 m^3.

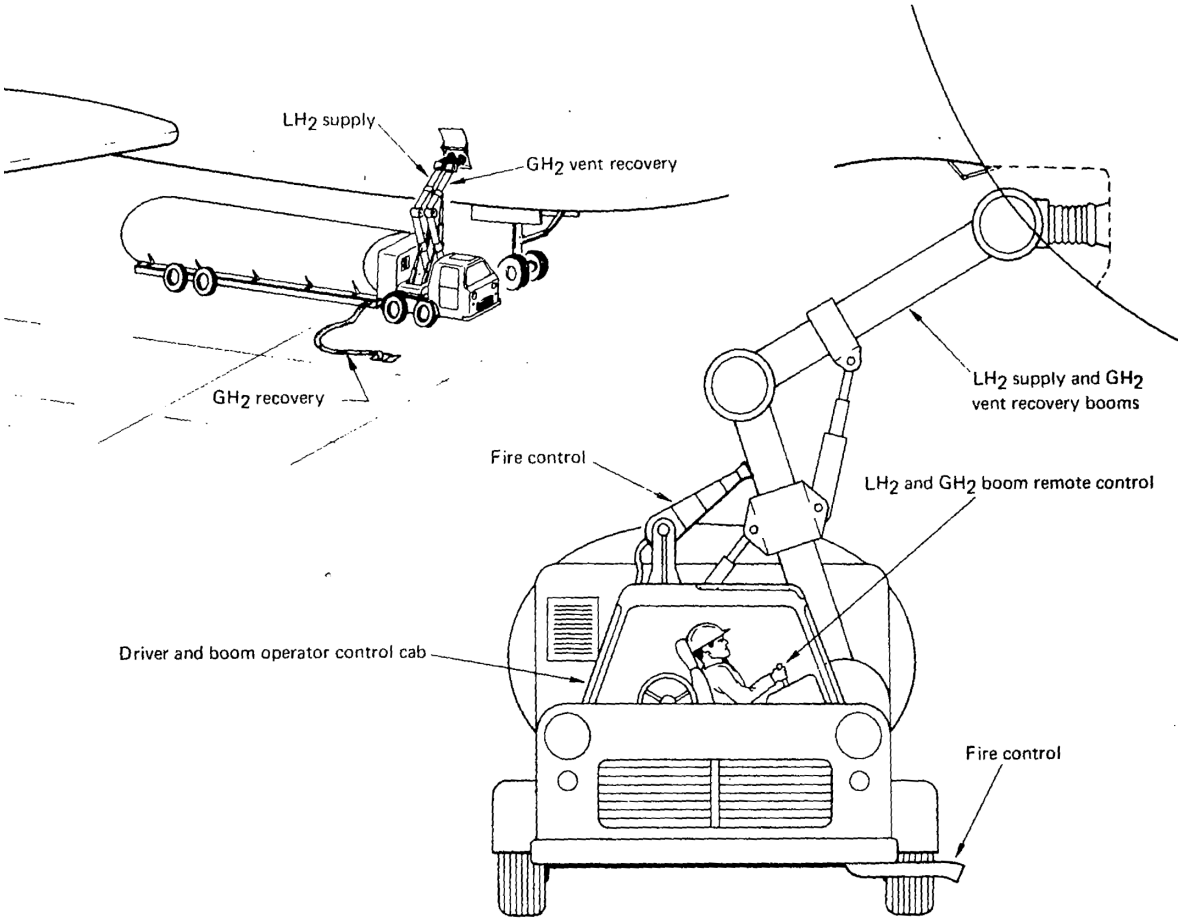

Figure 3.4: LH2 tank truck for refuelling remote areas [147]; capacity of 57 m^3; requires a recovery pipeline to remove GH2

Figure 3.4 shows the concept of a refuelling truck, which is only used in remote locations. In other words, the provision of LH2 at the gate with refuelling trucks is excluded. Another problem with this concept is the need for a recovery pipeline for GH2, as shown in the upper right corner of Figure 3.4. Assuming that the refuelling truck can only be used in remote areas, it is questionable whether a pipeline is available there. The necessity of a recovery line no longer gives the advantage of a mobile vehicle's flexibility.

The following reasons are given by Boeing [147] for not consideration a refuelling truck:

1. Safety and environmental impacts from venting GH2 into the atmosphere
2. Long-term costs for the loss of GH2 during venting
3. Acquisition costs and operating costs for the refuelling trucks
4. Congestion due to additional ground vehicles

Conversely, meaningful use of refuelling trucks is possible if these negative reasons can be revised. The argument of the investment costs and operating costs that would be required for the provision and use of refuelling trucks is excluded by Boeing [147] itself since the costs would have to be ignored for a pipeline system.

Congestion from the additional ground vehicles may be significant in the case of general refuelling with tank trucks. However, this is not an argument if the use is intended in an interim phase or in small quantities.

The effects of the loss of GH2 during the venting process are considered in the following overall system analysis of the refuelling vehicle. In general, a refuelling vehicle carries all the necessary parts to execute the refuelling process in Section 3.2. These essential parts are a vacuum pump, helium gas bottles and necessary valves and fittings to control the volume flow [26]. Boeing [147] has used a recovery line to avoid venting H2 into the environment, in conjunction with the pipeline to collect the vaporised H2 during the refuelling process and send it to a liquefaction plant. Thus, by recycling GH2, the two criticisms of venting H2 into the atmosphere can be refuted.

No pipeline system will be installed for the transition phase and the use of LH2 and Jet A-1 at the airport. The recirculation of GH2 through a pipeline is therefore not possible. In order to avoid H2 losses, another solution must be considered. Loss-free refuelling without venting into the environment is possible with fuel trucks by using an additional storage system. The required system consists of a compressor and a high-pressure tank for the storage of GH2. As there should be no losses due to venting during the entire refuelling process, two additional tanks are required for a helium-air mixture and a helium-GH2 mixture if a purging process is performed. The use of a clean break disconnect eliminates the need for these additional tanks. Figure 3.5 shows a refuelling truck with the necessary structure for zero loss refuelling. To be able to classify the dimensions of the refuelling truck, an aircraft to be refuelled with 180 passengers (similar to the A320) is in the background.

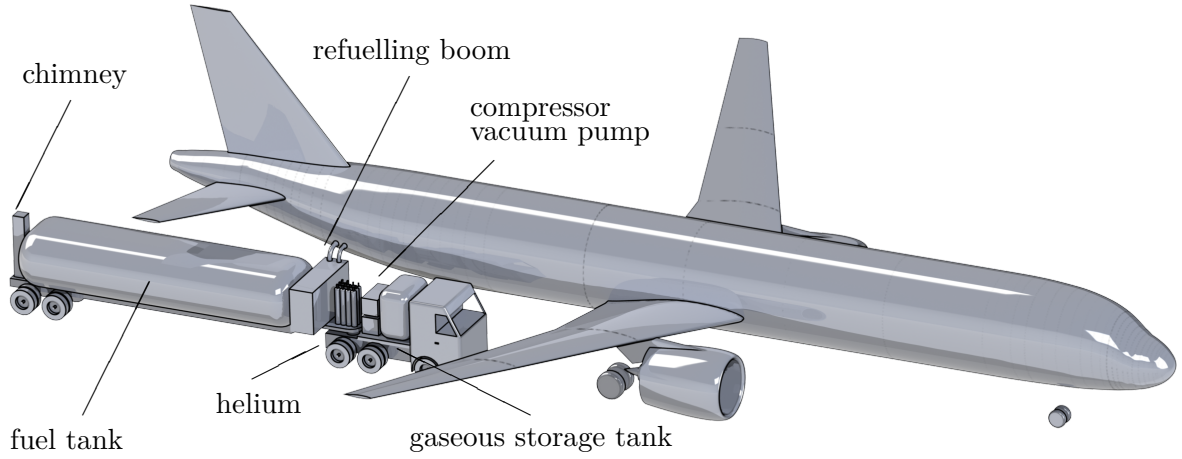

Figure 3.5: Refuelling truck independent from pipeline system; capacity of 70 m^3 LH2; truck including LH2 tank, helium bottles, vacuum pump, compressor, boom, gas tank, chimney

The ground vehicle tank has a volume of 70 m^3 and can hold a mass of 5000 kg LH2. The robot arm and boom that perform the docking manoeuvre are simplified. A compressor and a gaseous tank are now attached in order to be able to collect the losses. For the design of the compressor and gaseous tank, the following assumptions can be made:

The maximum pressure in the tank is 350 bar at a temperature of 288 K, hence thermal equilibrium with the environment, resulting in a density of 24 kg/m^3. The chill down losses are estimated at 13.6 kg in Boeing [147]. In the calculation of Section 3.2.3, each meter of pipe that has to be cooled down from ISA+15 results in a vaporised quantity of H2 of 6.2 kg/m. To dimension the tank sufficiently large and to allow several connections, a mass of 50 kg should be able to be stored in it. These characteristics correspond to a volume of 2 m^3.

The maximum volume flow of a compressor is between 0.3 and 3.0 m^3/s, which in the first assumption corresponds to a mass flow of 0.3 - 3.0 kg/s with a density of GH2 of 1.0 kg/m^3 (T = 30 K, p = 1.2 bar_a). With a maximum mass flow of 3.0 kg/s, the compressor can theoretically compress the entire mass flow delivered with the reduced fill. However, the consideration of the compressor power shows the limits of continuous compression. For the case of an ideal gas and an isothermal compression (22 K) from 1.2 bar_a to 350 bar_a, a power of 515 kW would be required for a mass flow of 1 kg/s. In the case of isentropic compression under real gas conditions, a power of 1900 kW for a mass flow of 1 kg/s follows. In actual conditions, the state's change is between the two approaches, which only represent the minimum and maximum. This immense power requirement shows a compressible gas problem, which is explained further in Section 4.4.

The power requirement thereby limits the flow rate and the compression, if the gasoues tank is full. Nevertheless, compression is possible in the time average, as the reduced mass flow of 3 kg/s is a theoretical consideration. In practice, a 2 m long piece of pipe will be at ambient temperature, which will have to be cooled.

This results in a vaporised quantity of 12.4 kg, similar to the approach of Boeing [147], which must be discharged within a time frame of 60 s. This simplification results in an evaporated mass flow of 0.2 kg/s, which leads to a power of 105 kW in the isothermal case and a power of 380 kW in the isentropic case. Therefore, the intermediate storage of the vaporised H2 through compression in regular operation is possible.
Furthermore, the intermediate tank is emptied every time the fuel truck is loaded, so the pressure is lower (approx. 2 $\mathrm{bar_a}$), and the compressor power also drops. Another measure would be to increase the volume of the intermediate tank to avoid strong compressions and keep the compressor power low. In other words, the compressor's power depends on the current tank pressure and is, therefore, a function of the filling level.

In refuelling by a tank truck, both possible variants, pump feed system and pressure feed system, are to be considered for the delivery. Fundamentally, the variants can be distinguished in that feeding through a pressure feed system is easy to implement and does not require any significant development effort. On the other hand, a pump solution offers the advantage of avoiding high pressures in the tank and consequently unnecessary masses having to be moved.

Pressurised Gas Feed System

The pressurisation system must be fundamentally divided into two subsystems. The difference is derived from the pressure gas used, which either has an inert behaviour (helium) or is the same substance in gaseous form (H2) as the liquid. This distinction must be made to take thermodynamic effects such as condensation, evaporation, diffusion, and temperature differences into account. However, the following calculation methods can be used for both sub-variants to determine the required mass of pressurant gas.

For a relatively short system operating duration or pressurant gas and fuel temperatures are close to each other, hence heat transfers can be neglected [70]. According to Huzel et al. [70], the ideal gas equation can be used for this calculation of the pressurant mass:

$$m_0 = \frac{p \cdot V}{R \cdot T} \tag{3.37}$$

Huzel et al. [70] describe another approach in which the longer system duration and higher temperatures can be represented. In this method, heat transfers from the pressurised gas to the fuel are taken into account, but environmental heat flows are not. Since the refuelling process only takes a few minutes, this consideration and calculation method is not used.

According to Sutton [143] a simplified analysis of a fuel tank's pressurisation can be carried out based on the law of conservation of energy. The assumption of an ideal gas and an adiabatic process are prerequisites for this method. Initial masses of the gas in pipes and the fuel tank are neglected. A slow expansion of the gas can be attributed to an isothermal process in which the pressurant, ullage and fuel are approximately the same. The actual process varies between an adiabatic and isothermal process depending on the application:

$$m_0 = \frac{p_{\mathrm{tank}} \cdot V_{\mathrm{tank}}}{R_0 \cdot T_0} \left(\frac{\kappa}{1 - p_{\mathrm{tank}}/p_0} \right) \tag{3.38}$$

A third possibility for calculating the mass for the pressurant is by estimating the final ullage gas temperature ($T_2 = 140\,\mathrm{K}$) by using a diagram [87]. In this case, the real gas effects are taken into account by the compressibility factors. However, this calculation method is only permissible for a pressurising of the same substance (GH2 to LH2), as the diagram only considers this case:

$$m_{\mathrm{ullage}} = \frac{p_1 \cdot V_{\mathrm{ullage}}}{Z_1 \cdot R \cdot T_1} \tag{3.39}$$

$$m_{\mathrm{gas}} = \frac{p_1 \cdot V_{\mathrm{tank}}}{Z_2 \cdot R \cdot T_2} \tag{3.40}$$

$$m_0 = m_{\mathrm{gas}} - m_{\mathrm{ullage}} \tag{3.41}$$

The three possibilities yield the following gas masses, which are required for the pressurisation and consequently the delivery and refuelling of the LH2. The pressurant mass depends on the transferred volume of LH2. The gas masses are relevant for the aircraft design and the refuelling process in that the required quantities can be regarded as losses and, therefore, influence the fuel costs.

Finally, the required volume of the additional gaseous buffer tank is calculated with the ideal gas equation. A consideration with the compressibility factor and real gas effects is also possible.

$$V_0 = \frac{m_0 \cdot R \cdot T_0}{p_0} \tag{3.42}$$

Therefore, the pressurising gas requires a tank with a volume of $1\,\mathrm{m}^3$ at a pressure of 700 bar for a LH2 tank volume of $70\,\mathrm{m}^3$. The pressurant gas volume is almost independent of the gas used (helium or GH2). This pressurant must also be refilled during the loading process with LH2 of the truck. For the refuelling of the GH2 or helium, the automotive industry's technology and standards [120, 121] can be used.

Another possibility to pressurise the fuel truck tank with GH2 is using a heat exchanger or, more precisely, a vaporiser, which eliminates the need for an additional gas storage tank on the truck. The vaporiser's performance is defined by the enthalpy of vaporisation and the volume flow required to maintain the pressure. Derived from Huzel et al. [70], the power can be calculated as follows:

$$\dot{m}_{\mathrm{gas}} = \dot{m}_{\mathrm{LH2}} \cdot \frac{\frac{p_{\mathrm{g}}}{R \cdot T_{\mathrm{g}}}}{\rho_{\mathrm{l}}} \tag{3.43}$$

$$P = \dot{m}_{\mathrm{LH2}} \cdot \Delta h_{\mathrm{v}} \cdot \frac{\rho_{\mathrm{g}}}{\rho_{\mathrm{l}}} \tag{3.44}$$

For the delivery of LH2 at 20 kg/s, a power of 510 kW is required at the heat exchanger without efficiency losses. This energy flow can be provided either by waste heat and environmental impact or by an electrical power supply. Moreover, a combination of the two energy sources is possible. On the other hand, providing 510 kW of power is quite demanding, especially when considering multiple refuellings occurring simultaneously. Therefore, the use of a heat exchanger for pressurisation of a pressure feed system is excluded.

The pressurised gas is not vented to the environment at the end of the refuelling process but is released to a recycling plant or liquefaction plant during the tank truck's following loading process. There is no differentiation from the source of the pressure, i.e. heat exchanger or pressure storage tank. Due to the possibility of intermediate storage, the processes have no direct loss, which further renders BOEING's [147] argument of significant losses invalid.
Furthermore, the fuel truck has a synergy through the combination of pressurisation for delivery and compression of the recirculated gas. The recirculated and compressed GH2 can be used as a pressurant for the fuel truck tank. This synergy makes the fuel truck self-sufficient to a certain extent.

Pump Feed System

For the delivery of LH2, as described in Section 2.1.2, an overpressure to the vapour pressure line must be present in order to be able to operate the pump without cavitation. Since no similarity parameters can be derived from the pump literature data of BREWER and BOEING [25, 147] and hence no pump can be re-dimensioned, the following comparison case is considered: The pump design is based on the similarity parameters of the SSME Low Pressure Fuel Turbo Pump (LPFTP) [116]. This results in a specific speed of $n_s = 37.5$ and a suction specific speed of $n_{ss} = 351.5$. In the calculation of these parameters, the conservative approach is chosen that $\mathrm{NPSH_c} = \mathrm{NPSH_a}$. With this approach, a geometrically similar pump can now be designed with a different volume flow without the risk of cavitation, see Section 2.1.2.

With the defined mass flow of 20 kg/s and compliance with the pump parameters, an NPSH value of 37.2 m and a rotational speed of 10,000 $\mathrm{min^{-1}}$ can be calculated. A supply pressure of 5 $\mathrm{bar_a}$ must be established as in the pressure feed system to compensate for friction and height differences. For the refuelling truck, this indicates that the tank pressure must be 0.26 $\mathrm{bar_g}$ over the saturation line in order to pump a cavitation-free, and therefore vapour-free, subcooled liquid. Considering the efficiency of the LPFTP of the SSME of 0.73 [116], the pump requires a power of 148 kW. The power calculation by the incompressible Bernoulli equation and an isentropic compression does not differ due to the low pressure increase.

By pumping and consequently withdrawing LH2, the tank's pressure would drop, and cavitation would occur on the pump's impeller. As already described in Section 2.1.2, pressurisation must also be applied to pump feed systems. The difference is the pressure level in the tank, which is much lower with pump delivery. As a result, a significantly smaller amount of pressurant is needed. Moreover, the pump case differs by a factor of $p_{\mathrm{pressurised}}/p_{\mathrm{pump}} = 5/1.26$ and only heating power of 128 kW is required to maintain the pressure. A gas volume of only 0.3 $\mathrm{m^3}$ would have to be provided for the intermediate storage tank's pressurant. In contrast to the pressure feed system, the required energy flow is realisable and feasible in a pump system. This difference means that there is no need for an intermediate storage tank in the pump feed system.

3.3.2 Dispenser Truck and Pipeline Supply for Large Quantities

The second way to provide fuel for aircraft refuelling is by using a pipeline system. In principle, a pump at the storage tank pumps the fuel through underground pipes to the terminal or apron. However, the transfer of LH2 in the pipeline through a pressure feed system at the storage tank can be excluded immediately. The losses are primarily due to the pressure cycle of pressurisation and depressurisation [25]. The motivation for this is the maintaining of a subcooled liquid.

The fuel is then transferred to the aircraft at the parking position through a hydrant and a ground vehicle, called dispenser. The dispenser in this process serves as a pressure reduction device, filter system, and monitoring unit, similiar to Jet A-1. However, it does not act as a power source to pump the fuel. Therefore, the pipeline's pressure delivers the fuel, and the dispenser only serves as a bridging device.

By calculating the pressure losses of Equations 3.32 to 3.36, the static pressure of 6.5 $\mathrm{bar_a}$ must be present at the hydrant to enable refuelling with a dispenser. The higher pressure, compared to a fuel truck of 5 $\mathrm{bar_a}$ results from an additional pipe section which is added from the hydrant to the dispenser, and additional valves are considered. ISO/PAS 15594 [72] specifies a pressure of 7 $\mathrm{bar_a}$ at the hydrant. In the following work, the pressure at the hydrant of 7 $\mathrm{bar_a}$ is adopted, as the deviation is slight and hence better comparability is achieved.

For the calculation of the pumping capacity and the pressure provided at the storage tank, a 2000 m long pipeline is assumed. For reasons of redundancy, several pipelines must be introduced. Thereby, in the following consideration, one supply pipeline is designed for a mass flow of 40 kg/s, which allows two aircraft to be refuelled simultaneously. The pipe dimension results from compliance with the derived conditions of Equations 3.29 and 3.31 to a diameter of 12 in. The pump must provide a pressure of 10 $\mathrm{bar_a}$ at the start of the pipeline to compensate for friction losses to meet the hydrant's boundary conditions (7 $\mathrm{bar_a}$).

Like the fuel truck pump design, the similarity parameters of the SSME's LPFTP are used to calculate the required NPSH value. This determination results in a speed of 11,700 $\mathrm{min^{-1}}$ and an NPSH value of 73 m, which corresponds to positive pressure to the saturated line of 0.5 bar. The required power of 660 kW for a mass flow of 40 kg/s is calculated considering an efficiency of 0.73. Brewer [25] assumes a differential pressure to the saturated liquid of 0.345 bar. The consideration of an NPSH value from Brewer [25] shows the necessity of the cavitation free pump and a subcooled liquid's advantages. A detailed consideration of the effects on the phase state of H2 is explained in Section 4.2.

The ground vehicle's design can vary depending on the application and will be examined in this section. The minimum requirements for the vehicle are the same as for a fuel truck. In the case of a purging operation, a vacuum pump and helium gas bottles must be carried on the vehicle. An expansion tank to achieve that the supply hose of LH2 remains cold must also be attached to the dispenser, see Section 3.2.3. The fundamental difference with a fuel truck is handling the gases that must be vented from the aircraft. Moreover, to the supply line of LH2, additional pipes are installed through the pipeline system, which lead the GH2 back to the storage tank and, in the best case, to a recycling plant or liquefaction plant. By designing the pipeline system with a supply line and a recovery line, all losses can be collected, and no amount has to be vented.

The pressure in the recovery line is kept at the minimum safety-relevant pressure of 1.2 $\mathrm{bar_a}$ to prevent oxygen from entering. Implementing a constant pressure in the recovery line can be implemented by a pump at the outlet. Moreover, a distinction is made in the different gas mixtures that can arise during refuelling. Therefore, a line for pure GH2 is required, which receives the vaporised H2. A line for a helium-GH2 mixture and a line for a helium-air mixture will also be provided through the purging process, such as additional fuel truck tanks. In principle, this number can be further increased as the number of substances (nitrogen) increases. However, a mixture of H2 and air or oxygen should be avoided, even if the H2 content is mathematically lower than the LEL.

The main tasks of a dispenser truck are, like Jet A-1, to reduce the pressure from the pipeline and establish the connection between hydrant and aircraft. The implementation of a dispenser can be seen in Figure 3.6 from Boeing [147]. A remotely controlled boom is coupled to the aircraft to make the connection with vacuum-insulated pipes. As already described in Section 3.2.1, this semi-automatic system offers the advantage that the system is motorised and, therefore, the mass of the pipes is not crucial.

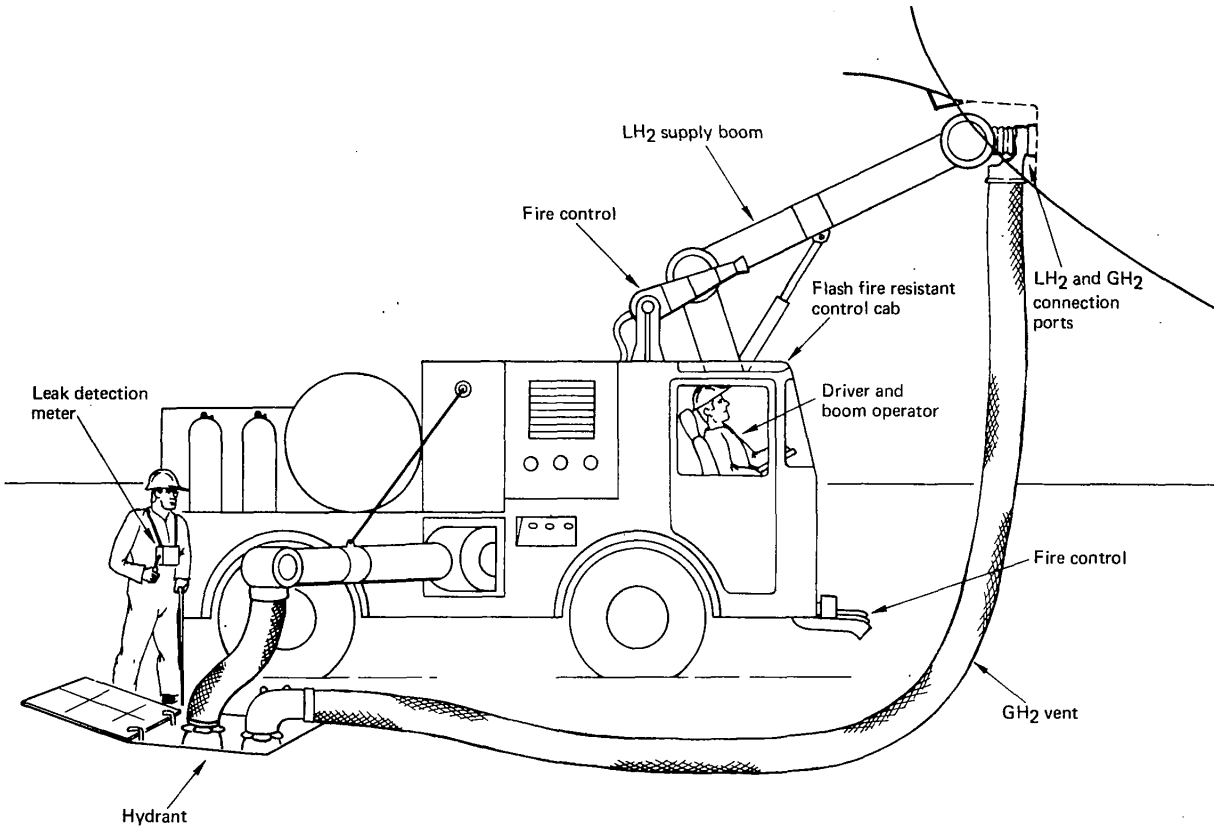

Figure 3.6: Dispenser boom truck for hydrant refuelling of LH2 [147]

Most noticeable about this concept is the separation between the LH2 supply line and the GH2 vent line. This separation allows the dispenser to be disconnected from the aircraft after refuelling and leave the area while the recovery line remains connected. In principle, the separation between the lines is a practical approach that would require fewer dispensers for the airport and increase utilisation. Nevertheless, this system requires a second vehicle to connect and disconnect the recovery lines [147]. This expense neutralises the operational advantages, as it requires even more space in the aircraft's parking position.
Furthermore, in an impeccable turnaround, the time while the refuelling vehicle is not connected is short anyway. This contemplation makes the separable return line superfluous, as the loss is slight. Boeing [147] sees an advantage in the high flexibility of a dispenser.

Brewer's [25, 26] dispenser is similar in design to Boeing's but differs in the boom's length and movement, see Figure 3.7. The aircraft connection is located at the tail cone of the fuselage in the aircraft design. Conversely, an aircraft configuration is also considered in which the tank is positioned at the aircraft's tail. Brewer [25] uses a cherry picker type boom to reach it due to the higher position of the connection.

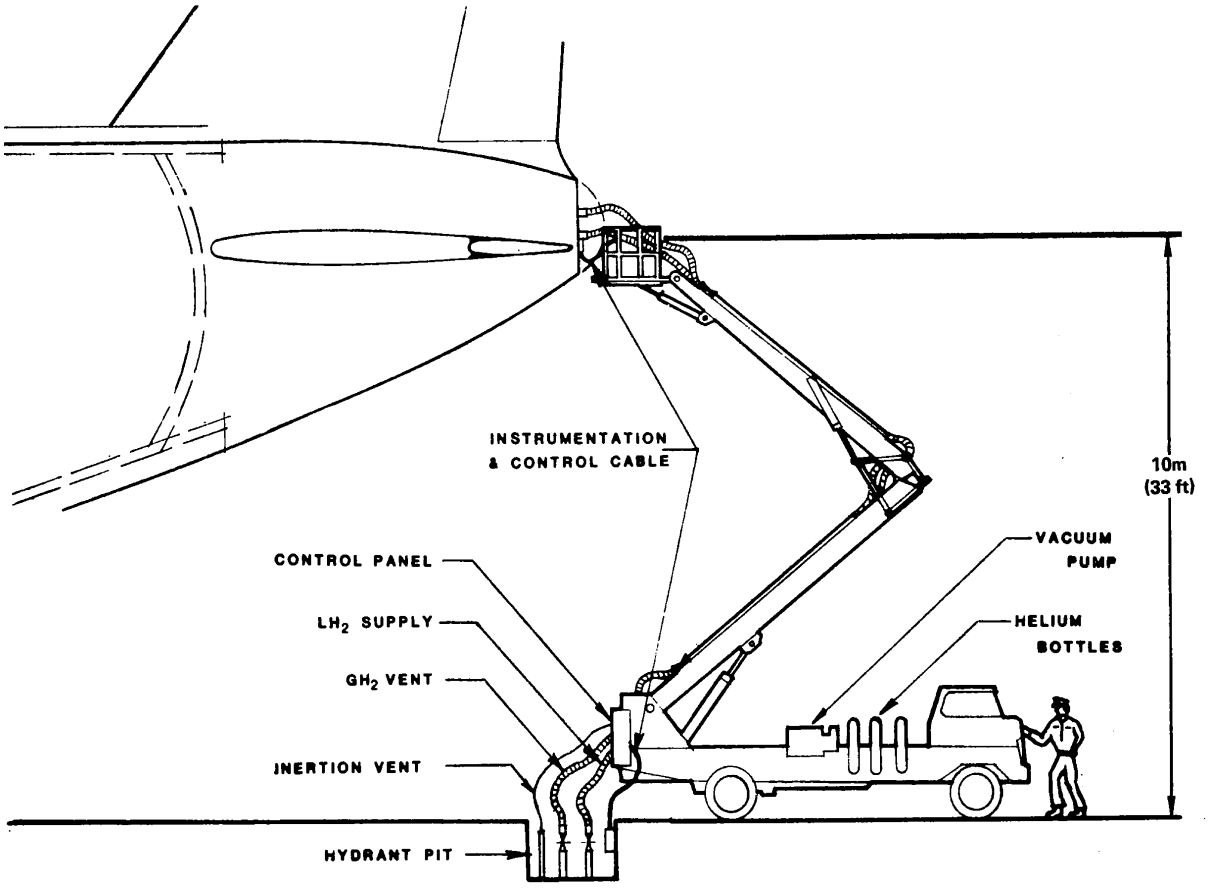

Figure 3.7: LH2 hydrant fuelling vehicle [25]

Furthermore, a distinction is also made between the gas mixtures produced during the refuelling process. This allocation means a return line for GH2 and a line for the inert gas [25].

During aircraft positioning, the tail cone must directly be located under the hydrant for this concept of the dispenser. This direct dependency of the refuelling connection and the hydrant poses a problem for the airport infrastructure. Due to the tank position's open variable in the aircraft design with LH2 as fuel, there is no targeted solution for the tank position. The length of the line between the hydrant and the refuelling vehicle will be limited to a few meters for handling reasons. This constraint means that a hydrant connection at the aircraft's nose cannot be used for refuelling a tank in the tail, as the required line would be too long. Conversely, due to the tank position variance, several hydrants must be installed at one parking position.

From the obtained results and the combination with the safety-relevant aspects, an ideal dispenser can be derived. Figure 3.8 shows a dispenser that is dimensioned for the refuelling of LH2. It should be emphasised that any aircraft size can be refuelled, as the mass flow is designed for vehicle level and therefore independent of the number of hoses. The dispenser has a semi-automated docking system that the operator can remotely control. The boom design assumes a maximum height of the aircraft adapter of 10 m, similar to Figure 3.7. The dispenser carries a pressure regulation unit, a monitoring system and the purging system. The purging system with the vacuum pump and helium cylinders is omitted in the scenario of a clean break disconnect. However, the prerequisite of several recovery lines, which discharge the different gas mixtures, must be given at the airport to avoid an explosive atmosphere.

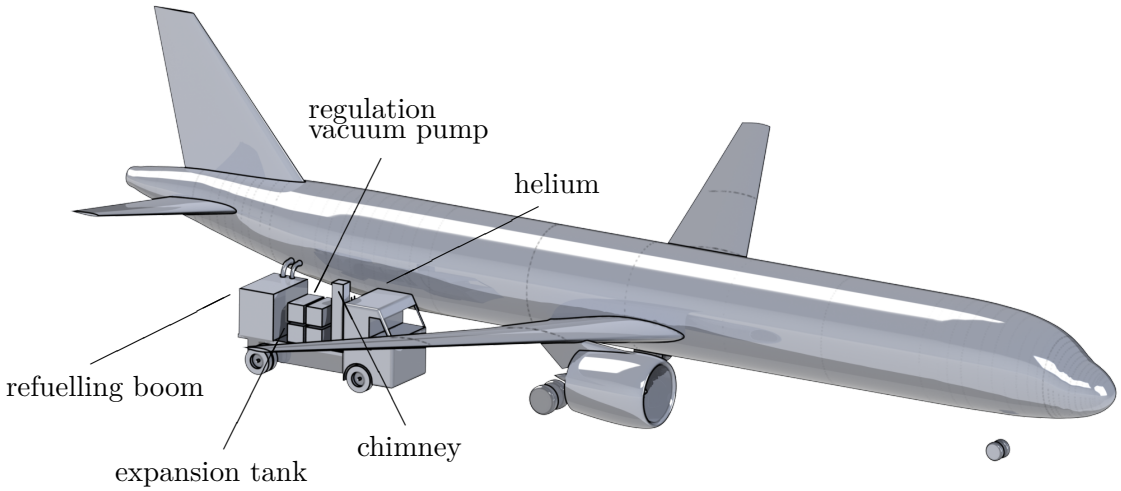

Figure 3.8: Hydrant dispenser for LH2; dispenser carries all necessary parts for a refuelling process including helium bottles, vacuum pump, pressure regulation, expansion tank, boom, chimney; size comparison to a 180-passenger aircraft (similar to A320)

From this, it can be concluded that two possible dispenser variants must be provided, depending on whether the aircraft manufacturer prescribes a purging process and the disconnect variant or not. Figure 3.8 also shows a chimney that can vent H2 in an emergency case. The possibilities of safe venting are explained in Section 4.6.

Another possibility for bridging the pipeline to the aircraft is the terminal boom fuelling concept in Figure 3.9 from Boeing [147]. A boom is located at the terminal building, controlled by an operator and guided to the forward fuel tank position using electronic sighting control. The boom contains the LH2 supply and GH2 vent lines. The docking manoeuvre is performed with a semi-automatic system, as described in Section 3.2.1.
As shown in Figure 3.9, the boom concept can only connect to the right front part of the fuselage. This means that close connections to other tank arrangements are not feasible. This concept reduces the normal congestion caused by ground equipment in the ramp area and eliminates the possibility of damage to the refuelling connection system by ground vehicles [147].

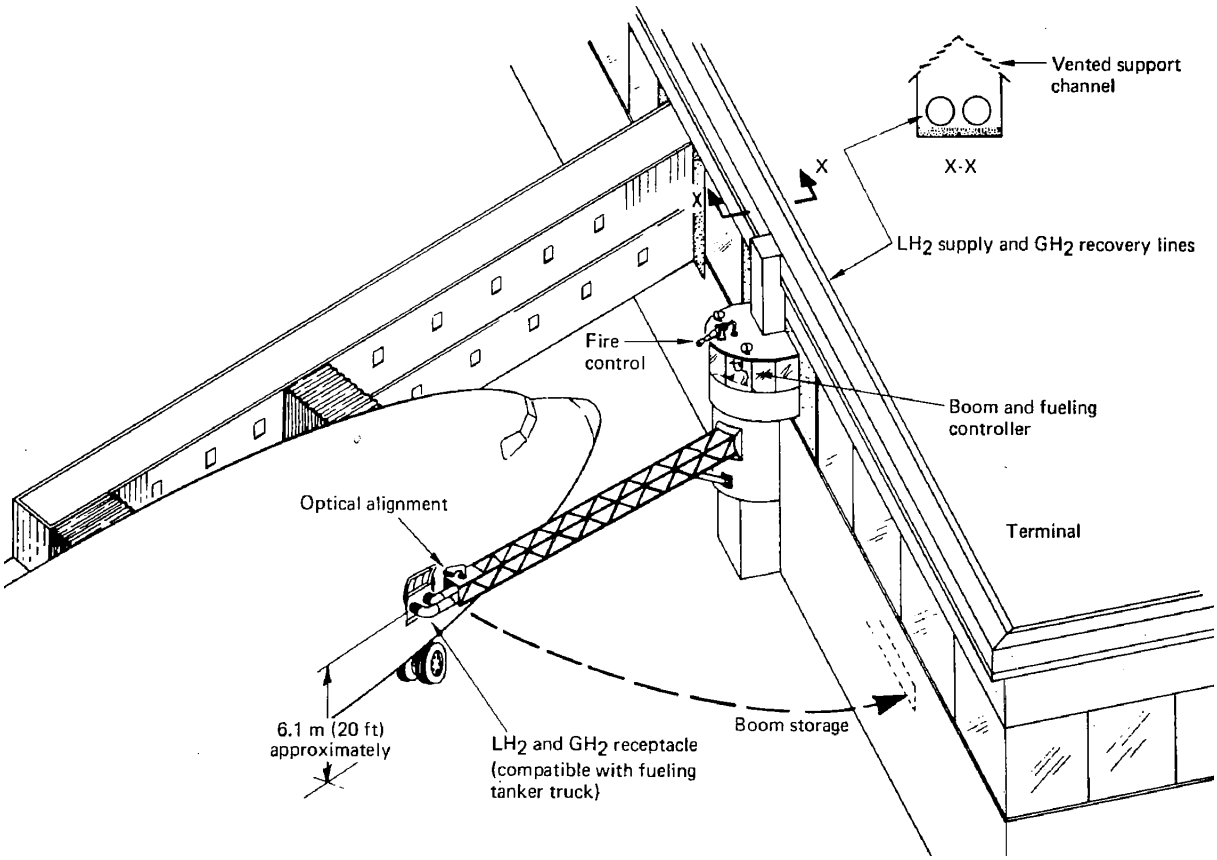

Figure 3.9: Terminal boom fuelling concept [147]; low manoeuvrability and flexibility due to the installation at the terminal gate

In principle, this system offers the advantage that one less ground vehicle is needed in the parking position. However, this advantage also entails the disadvantage of less flexibility. Due to the boom's design characteristics, refuelling is only possible on the right, front side. However, this position is only optimal if the LH2 tank is located directly behind the cockpit so that the pipes in the aircraft are short. Feeding a refuelling line through the entire aircraft to fill the tank in the tail would result in considerable losses if the line is not permanently cooled.
Moreover, this system provides precise positioning of the aircraft so that the boom can reach the aircraft adapter. Furthermore, positioning in three-dimensional space is a problem because all aircraft size variants should be fuelled but have different heights. The flexibility of the boom fuelling concept is not available and is therefore excluded as a possible fuelling scenario.

The distribution of LH2 at the airport can be implemented using two methods based on the findings. Therefore, the choice of the fuel service operator depends primarily on the amount of LH2 distributed annually. The trade-off between high investment costs for a pipeline dispenser system and the possibility of refuelling large quantities or a fuel truck system with low investment costs where the refuelling of long-range aircraft is a problem due to the limitation of the fuel truck tank volume. Because the dispenser is independent of the amount of LH2 required, it is more suitable for large capacities than a refuelling truck. However, due to the higher investment costs associated with implementing a pipeline system, the fuel truck will be more cost-effective for small quantities. In summary, the implementation of fuel distribution at the airport is possible. Nevertheless, a pipeline or tank truck system's profitability also arises with conventional refuelling with Jet A-1 and requires further investigation.

For completeness, the tank must be completely emptied and then purged for longer out of service periods. This procedure takes between 4 and 6 h [26]. The fuel is returned to the storage tank. For the aircraft's preparation after a maintenance operation, the tank must first be purged and then slowly chilled down. This procedure takes between 6 and 18 h [25]. The long durations are due to the thermal stress that arises when chilling from ambient temperatures to the cryogenic temperatures of LH2. The thermal stress, especially with many thermal cycles, poses a question. In addition, Brewer [26] states that for short out of service periods of less than seven days, the aircraft tank is constantly kept cool by leaving a residual amount of LH2 in the tank.

3.4 Airport Storage and Distribution Requirements

The airport infrastructure must guarantee the sufficient supply and provision of LH2 for the aircraft. Since the amount of fuel refuelled per day is highly dependent on the size and utilisation of the airport, the storage tanks' capacity will not be taken into account. A list of the required quantities of LH2 can be found in Brewer [25] and Boeing [147] for the airports in San Francisco International (SFO) and Chicago-O'Hare International (ORD).

The thermodynamic properties, such as temperature, pressure, and phase state in the airport's storage tank, are more critical for the refuelling process and thus also for the turnaround of the aircraft. These state variables determine the further process and handling of H2 until it enters the aircraft tank. Besides, safety-relevant aspects must be taken into account to ensure safe storage or interim storage.

When designing the storage tank, the minimum pressure of the system of 1.2 $\mathrm{bar_a}$ is given by compliance with explosion protection. This gauge pressure of a 0.2 $\mathrm{bar_g}$ prevents ambient air and oxygen from entering the tank due to the primary explosion protection. However, Brewer [25] (1.034 $\mathrm{bar_a}$) and Boeing [147] (1.103 $\mathrm{bar_a}$) set the minimum and nominal storage tank pressures, respectively, below these safety regulations in order to keep the temperature of LH2 as low as possible. By storing at a pressure slightly above ambient, less energy is required in the following handling to refuel LH2 into the aircraft. However, this method compromises airport safety. Therefore it is not applied.
The maximum pressure of the storage tank is only limited by the critical pressure of 12.9 $\mathrm{bar_a}$ since a supercritical gas would form above this point. The mass of the tank is therefore not relevant because it is not necessary to transport the tank.

The temperature of the H2 in the tank, which together with the pressure also determines the phase state, is relevant for aircraft design because the density and thus the tank volume depends on it. In storage tanks, which can be described as long-term tanks with the storage of several hours and days, the content is in thermodynamic equilibrium. The temperature of the liquid and gas phases are equal, as shown in Figure 2.3. This relation also determines the density. Increasing the (minimum) pressure increases the temperature and decreases the density, which has a negative effect on the overall design, see Section 4.1.

The pressure must be increased for feeding, as described in Section 3.4, to compensate for pressure losses and height differences and create a flow. This pressure build-up can be achieved by a pump or a pressurisation system. However, there is a significant difference in the behaviour in the storage tank between the different designs.

The main disadvantage of a pressure feed system are the losses that occur due to the alternating pressurisation and depressurisation in the storage tank [25]. However, this procedure must be executed because otherwise, the fluid temperature increases due to the environmental heat transfer and the heat impact caused by the gas phase. Due to the increased pressure and the thus subcooled fluid, the heat input would only occur sensitively and not directly in latent vaporisation. However, this temperature increase should not occur, wherefore the pressure is dropped back to the minimum pressure after the refuelling process. This flash evaporation manifests itself as a system loss of LH2.
Brewer [25] determined a three times higher loss of a pressure feed system than a pump system. However, the pump system's disadvantage is the increased complexity and thus the reduced reliability and flexibility. The implementation concept can explain this behaviour: Different volume flows in a pressure feed system can be controlled via overpressure and require a vaporiser. In this case, the control of a pump system has to be performed via the pump's rotational speed, whose efficiency and behaviour, however, strongly depend on it. In addition, bearing damage and wear are possible due to the high rotational speeds.
Nevertheless, Brewer [25] chooses a pump system because LH2's lower losses are sufficiently more attractive. The losses lead to higher fuel prices, which harm aircraft profitability. A pump system's negative aspects at the storage tank can be considered harmless due to regular maintenance and redundancy. The following thesis considers a pump system at the storage tank for the delivery of LH2 through the arguments. The distribution system, from the storage tank to the aircraft tank, is explained in Section 3.4.

For the delivery of LH2, as described in Section 2.1.2, an overpressure to the vapour pressure line must be present in order to be able to operate the pump without cavitation. Brewer [25] specifies a value of $0.345\,\mathrm{bar_g}$, which corresponds to an NPSH value of 50 m. Thus, the stored liquid in the saturated state (thermodynamic equilibrium) must first be pressurised. This pressurisation can be achieved by helium or by a vaporiser. Due to the higher pressure to the saturated line, a subcooled fluid is present. This subcooling allows the pump to deliver the LH2 as a single-phase fluid, which has the advantage of minimising flash-off [25].
As a result of the non-thermodynamic equilibrium, the liquid heats up and is returned to its saturated state by flash evaporation after the refuelling process. Therefore, pump delivery has a similar effect to a pressure feed system, where losses occur due to boiling out. However, since the pressure difference between pure storage and pumping is much smaller than with the pressure feed system, it is more economical.
Brewer [25] and Boeing [147] define the maximum volume flow by simultaneously refuelling four aircraft. This approach is also chosen to ensure a sufficient fuel supply and corresponds to the pump's system design for a mass flow of 288,000 kg/h and a volume flow of $4000\,\mathrm{m^3/h}$. The similarity parameters introduced result in an NPSH value of 73 m, which corresponds to an overpressure to the saturated line of $0.5\,\mathrm{bar_g}$. This value now determines the pressurisation level in the storage tank to enable pumping.

In the further consideration between the pressure increase of the pump and the flow entering the tank, the properties of a real compressible fluid, as defined in Section 2.1.1, are essential. The rise in pressure by the pump can be described by an isentropic change of state, in which part of the energy employed results in a temperature rise. Downstream of the pump, an isenthalpic change of state, without energy input from external sources, can be considered to determine the properties of LH2. The isenthalpic flow approach can be applied in a vacuum insulated pipe since the temperature change due to the heat input of a typical vacuum insulated pipe of $3.5\,\mathrm{W/m}$ [43] in a 2000 m long pipe only translates into a temperature change of 0.05 K.

The heat input into the pipeline system is low due to vacuum insulated pipes, but it leads to a heating of LH2. However, the supply of subcooled LH2 is necessary to minimise losses and prevent the liquid's flashing. The system always remains chilled by circulating the fuel in the pipeline system, which means that no heating occurs during the non-delivery period. A delay due to cooling processes is eliminated. Immediate availability of subcooled LH2 at each hydrant station results.

The circulating liquid that is returned to the storage tank can be re-cooled in two ways. The first way is to pump the liquid into an additional tank with a pressure of 1.2 $\mathrm{bar_a}$, which causes the liquid to boil back (flash evaporation) and thus reach a saturated state. The LH2 can then be transferred back to the storage tank. The GH2 produced by evaporation and, in the end, by cooling must be liquefied in a recycling plant for loss-free consideration.

The other way to keep the liquid in the circulating system constantly cool is to insert a heat exchanger in the pipeline system or after the pump from the storage tank, which cools a continuous mass flow. By this method, no additional vaporised H2 is produced, which means that liquefaction is no longer needed at this point. The Coefficient of Performance (COP) can determine the cooling capacity of the heat exchanger [15]:

$$\mathrm{COP} = \frac{\dot{Q}_{\mathrm{heat}}}{P_{\mathrm{el}}} \tag{3.45}$$

$$P_{\mathrm{el}} = \frac{\dot{Q}}{\mathrm{COP}} = \frac{\dot{m} \cdot \Delta h}{\mathrm{COP}} \tag{3.46}$$

The COP describes the ratio of extracted heat flow and applied electrical power and is a characteristic of the cooling system's efficiency. In the ideal case of an ideal Carnot process, the COP is 0.056. However, the values vary depending on the cooling system (densification system) from 0.004 for a cryocooler to 0.032 for a thermodynamic venting system and Claude cycle. [15] A COP of 0.032 is therefore assumed for further considerations.

The pressure losses due to valves and friction in the pipe express a temperature increase in an isenthalpic flow. These changes significantly affect the state of the phase of LH2, as the frictional energy is converted into internal energy. As described in the previous section, maintaining a single-phase flow is vital to avoid a flashoff. The combination of pressure and temperature is crucial in this regard. Therefore, when flowing into the tank, there must be at least a saturated liquid with a vapour content of $x = 0$. Otherwise, a two-phase flow will establish, leading to a significant increase in velocity due to the phase change. Considering the isenthalpic change of state, this leads to a partial vaporisation of the liquid phase, which has a significantly lower density (factor 27 at 2 bar). This two-phase flow has the same negative properties as the pump cavitation in Section 2.1.2.

This condition must therefore be prevented under any circumstances. In principle, there are two ways to prevent this phenomenon by maintaining the subcooled liquid. One is to increase the pressure in the system, and the other is to decrease the temperature. The pressure increase is limited by the maximum pressure or burst pressure of the aircraft tank and cannot be increased significantly. The maximum pressure varies between 1.45 and 2.75 $\mathrm{bar_a}$ in previous investigations [26, 95].

However, reaching the saturated liquid at maximum tank pressure entails disadvantages due to reduced density and increased tank volume (see Section 4.1). Also, the pump would require a higher power to provide the pressure increase. Therefore, subcooling LH2 is the more suitable choice for better aircraft performance. Thus, the tank's pressure can be kept low during the refuelling process, preferably at the safety-relevant minimum pressure of 1.2 $\mathrm{bar_a}$.

Figure 3.10 shows the isenthalpic flow or state change just described due to the pressure loss of a pipeline system. Due to the conversion of energies, the temperature at the inlet to the tank rises to 20 K. Alternatively, in other words, LH2 must be cooled to 19 K after the pump. Thus, there is still a subcooled fluid at the tank inlet conditions, which has the significant advantage that the entire mass flow delivered by the pump also flows into the tank as a single-phase fluid, and no losses occur due to vaporisation.

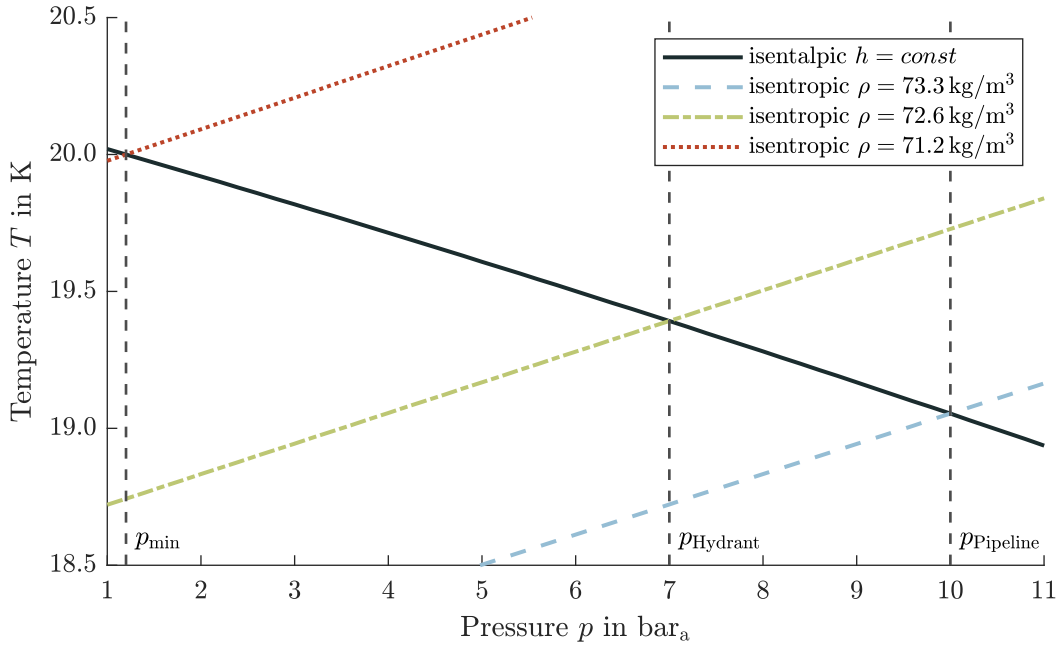

Figure 3.10: Effects of temperature and density of a real compressible fluid on pressure losses due to friction; showing an isenthalpic change of state from the storage tank pump to the aircraft tank

A detailed breakdown of the energy and power required to implement this method is determined in the following section. Table 3.3 shows the previous steps, based on Figure 3.10, from the storage tank to the inflow into the pipeline system. Isentropic compression and isobaric cooling are assumed as changes of state for the calculation. The pumping capacity has already been calculated in Section 3.3.2. For the refrigerator, an electrical power of 13.38 MW for a mass flow of 20 kg/s follows for the cooling of LH2 that it enters the tank at a temperature of 20 K under a pressure of 1.2 $\mathrm{bar_a}$. This cooling capacity corresponds to an additional energy input of 666 kJ/kg LH2. Considering the energy input of 210 MJ/kg for the production of LH2, this additional energy input of 0.32 % is reasonable because, on the one hand, it ensures a single-phase liquid and, on the other hand, because a densification process takes place.

Location	Pressure p $\mathrm{bar_a}$	Temperature T K
Storage Tank	0.12	20.9
Pump	10.0	21.3
Refrigerator	10.0	19.0

Table 3.3: Pressure and temperature conditions from storage tank to refrigerator

Subcooling to 15 K instead of 19 K would mean an energy input of 0.79 % compared to the 210 MJ/kg. Thus, LH2 would arrive at the tank inlet with a temperature of 16.3 K and a density of 74.89 $\mathrm{kg/m^3}$. A detailed explanation of the advantages of densification can be found in Section 4.1. However, further subcooling of LH2 is no longer possible under the single-phase region's condition since a fraction of H2 then freezes, and SLH2 is formed. The use of SLH2 is not considered further, however, because other problems then become more relevant.

Effects of Two-Phase Flow on Refuelling

In the previous considerations of the refuelling process and the flow through pipes, a single-phase flow's essential requirement is always fulfilled. However, if the tank pressure is too low and/or the fluid's temperature is too high (according to vapour pressure curve), a two-phase flow is formed. Two-phase flow is characterised by a vapour content of $x > 0$. In an isenthalpic flow, the vapour content must increase to keep the energy of the flow constant. In other words, this behaviour means that part of the LH2 vaporises to fulfil the isenthalpic change of state. The energy required for the vaporisation process is dissipated by the liquid phase, resulting in a lower temperature. A liquefaction or densification system ultimately uses this process to cool, which can be applied through a negative Joule-Thomson coefficient. Boeing [147] specifies a flash vaporiser as a way to cool warm LH2 in the deck hose. In the intentional or unintentional application of a two-phase flow, the disadvantage is the decreasing actual LH2 mass flow.
However, it should be mentioned that the continuity equation is still fulfilled, but the vapour phase takes over a fraction of the mass flow. Due to the density change, the velocity would increase enormously, which would, however, lead to an infringement of the introduced limitation in the velocity and simplified Reynolds number. Conversely, Equations 3.29 and 3.31 must also be observed in the case of a two-phase flow, which leads to a reduced inlet mass flow. Thus, the liquid phase's mass flow decreases disproportionately and leads to a considerably longer refuelling process. By (iteratively) solving the following equation, this phenomenon can be calculated:

$$h = h_{\mathrm{tank,l}} \cdot (1 - x) + h_{\mathrm{tank,v}} \cdot x = const. \tag{3.47}$$

$$\rho_{\mathrm{b}} = \left(\frac{x}{\rho_{\mathrm{v}}} + \frac{1 - x}{\rho_{\mathrm{l}}} \right)^{-1} \tag{3.48}$$

$$v_{\mathrm{avg}} = \frac{\dot{m}}{\rho_{\mathrm{b}} \cdot A} \tag{3.49}$$

When calculating the actual mass flow rate, considering the defined limitations, a 50 % reduction in the LH2 mass flow rate of 10 kg/s results even with low vapour fractions of $x = 0.022$. Therefore, the refuelling time increases in inverse proportion to the reduced mass flow, which would revise the statement that refuelling is not on the critical path and has no effect on the turnaround. A significant increase in operating costs would follow.

In addition, there is the question of what happens to the vaporised H2 that is fed into the tank. This GH2 must be recovered, as otherwise, the pressure in the aircraft tank would rise, which would lead to the undesired temperature increase of the fluid and density reduction, as described above. Relating these results back to the aircraft design, the volume of the aircraft tank is determined from these tank conditions, which has a considerable influence on the mass and hence the performance of the aircraft, see Section 4.1.
However, a high mass flow of vaporised H2 to be removed would be reflected in the recovery line's dimensions. High velocities should also be avoided because phenomena such as resonances and pressure shocks should be prevented to limit the flow-related loads on the components.

3.5 Comparison and Impacts of LH2 to Conventional Jet A-1 Turnarounds

By analysing and designing the refuelling procedure and its feasibility, the following comparison is made to a conventional refuelling procedure with Jet A-1. Figure 3.11 shows the comparison of the time required for the refuelling process of LH2 and Jet A-1. The refuelled volume is shown as refuelled energy in order to make the transported quantities comparable. In a theoretical consideration, the same fuelled energy of LH2 and Jet A-1 means the same aircraft range.

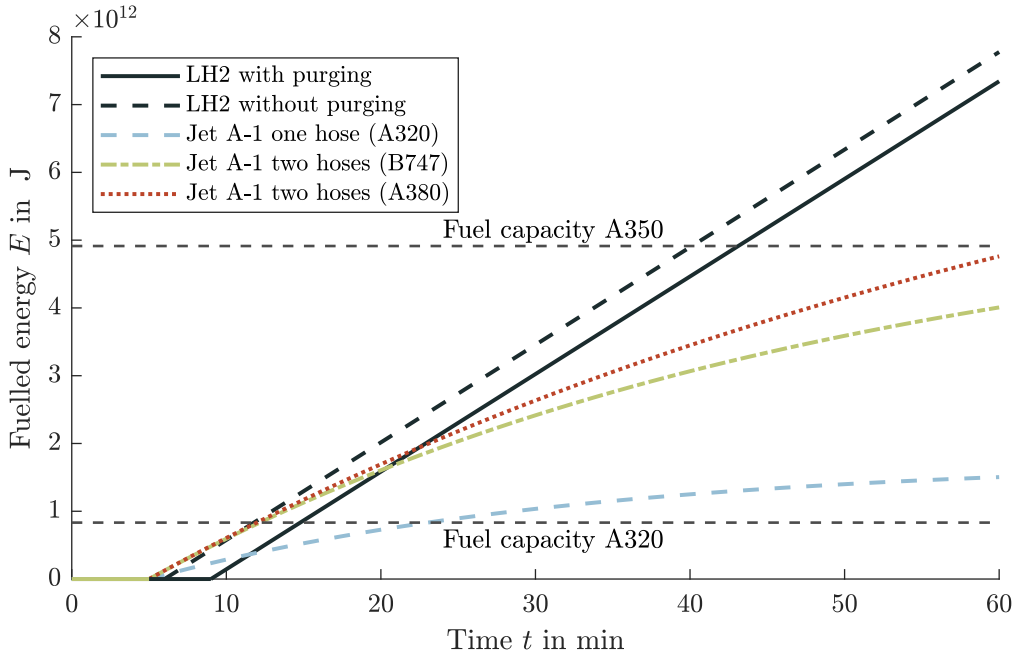

Figure 3.11: Refuelling comparison between Jet A-1 and LH2; considering time influences before (purging, chill down) and after (purging) the refuelling process

The diagram shows the entire refuelling process's duration because the necessary processes before and after the actual refuelling are included by shifting the curves to the right. It can be seen that the processes in which no mass flow is delivered take more time with LH2. Therefore, the time required by Jet A-1 is shorter for small quantities. This effect is due to the additional time required for cooling down the lines and any purging that may be required. Due to the H2 refuelling system's design compared to the maximum volume flow of Jet A-1, the gradient on the x-axis is almost the same. Assuming that LH2 is fed into the upper part of the aircraft tank, the volume flow is not reduced compared to Jet A-1.

Due to the different procedures of LH2 and Jet A-1, the intersection of the same refuelling energy results after 11.5 min with one Jet A-1 hose and 20.5 min with two hoses. To classify these results with purging, the refuelled mass of Jet A-1 with one hose after 11.5 min corresponds to 8425 kg and with two hoses after 20.5 min to a mass of 39,180 kg. For comparability, the horizontal dashed lines are drawn as maximum tank capacity for an A320 and A350 in Figure 3.11.

It is thereby evident that in a refuelling process with the maximum fillable volume, LH2 has a time advantage. With smaller volumes and hence shorter ranges, on the other hand, the refuelling times are similar. To better analyse this behaviour, three scenarios are presented in the following section through a Gantt chart. The conservative approach is chosen that the purging process must occur to the full extent. For the use of a clean break disconnect, the time duration of 3 min can be deducted from the results. The different scenarios handle different refuelling masses and an aircraft configuration with tank pods on the wings.

Figure 3.13 shows the Gantt chart for an A320-like aircraft refuelling at the maximum tank volume. Here, the previous hypothesis applies that the aircraft have the same efficiency and performance and can fly the same distance with identical amounts of energy. As a result, the mass of LH2 can be determined by the ratio of the calorific values. It follows that the H2 mass is lower by a factor of 2.8. A time advantage of 3 min is shown with the Gantt diagram in Figure 3.12 when refuelling Jet A-1 the equivalent energy amount.

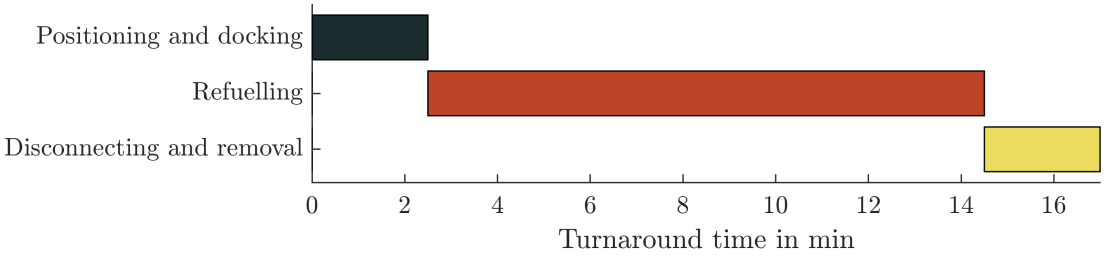

Figure 3.12: Gantt chart for Jet A-1 refuelling of 15,000 kg with one deck hose; initial volume flow of 1800 l/min

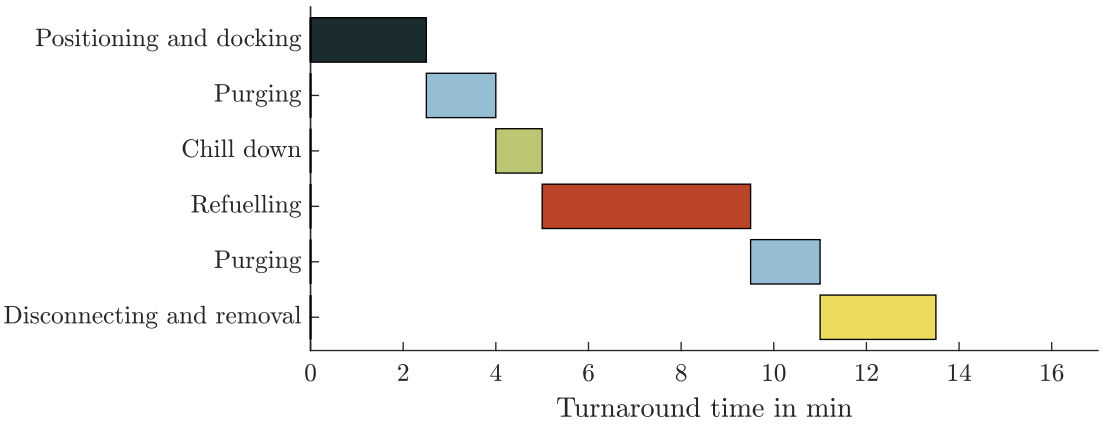

Figure 3.13: Gantt chart for LH2 refuelling of 5350 kg

In contrast, scenario 2 compares a refuelling volume for a 500 NM mission. Figure 3.14 shows the Gantt diagram for this purpose. Due to the small volume, the advantage of LH2 is no longer present, but the refuelling time is in the same order of magnitude. Based on the findings from Section 2.4, the advantage in refuelling time is of no benefit, since in most cases, refuelling is not on the critical path of the turnaround. In other words, an extension of the refuelling time by a few minutes would not lead to any noticeable effects of the turnaround process.

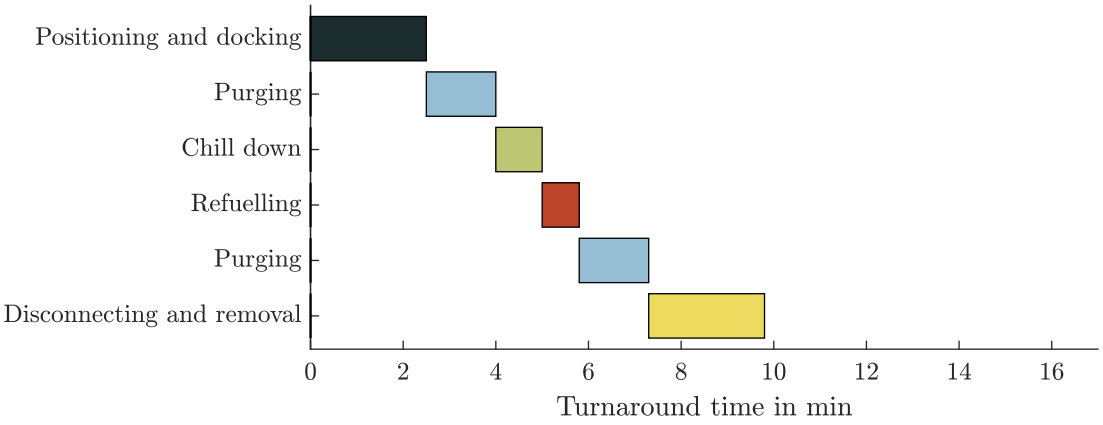

Figure 3.14: Gantt chart for LH2 refuelling for a 500 NM mission, excluding reserves; fuelled mass of LH2 1000 kg; corresponding refuelling time for 500 NM mission of Jet A-1 is 7 min

The previous consideration of the refuelling time is independent of the aircraft configuration and the position of the LH2 tank in the aircraft. In scenario 3, the comparison of the refuelling time for a 1500 NM mission of an aircraft with the tanks mounted at the wings will be investigated. A comparable aircraft configuration can be found in Silberhorn et al. [129]. The comparison will be between the possibility of parallel refuelling with one pod connected to feed the other pod and the possibility of sequential refuelling. Figure 3.15 shows the Gantt chart for parallel refuelling in this comparison situation.

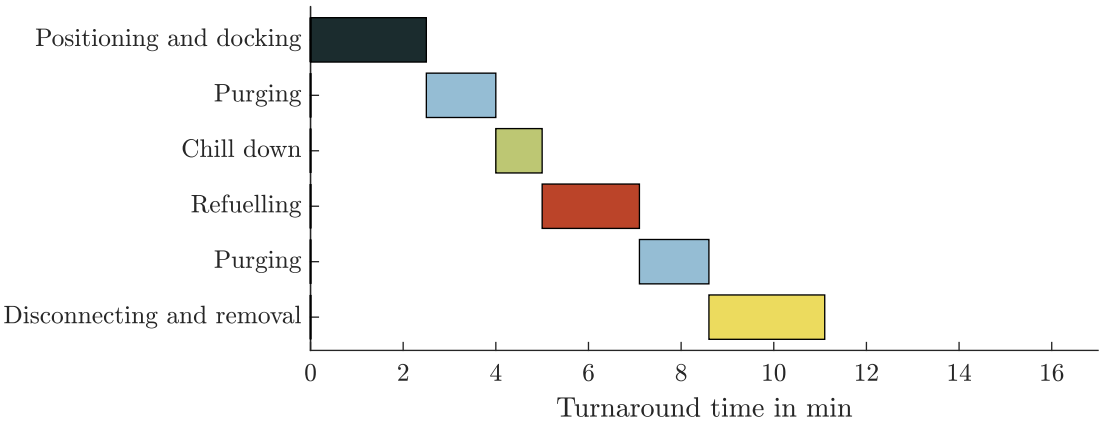

Figure 3.15: Gantt chart for parallel LH2 refuelling for a 1500 NM mission, excluding reserves; fuelled mass of LH2 2500 kg; corresponding refuelling time for 1500 NM mission of Jet A-1 is 10 min

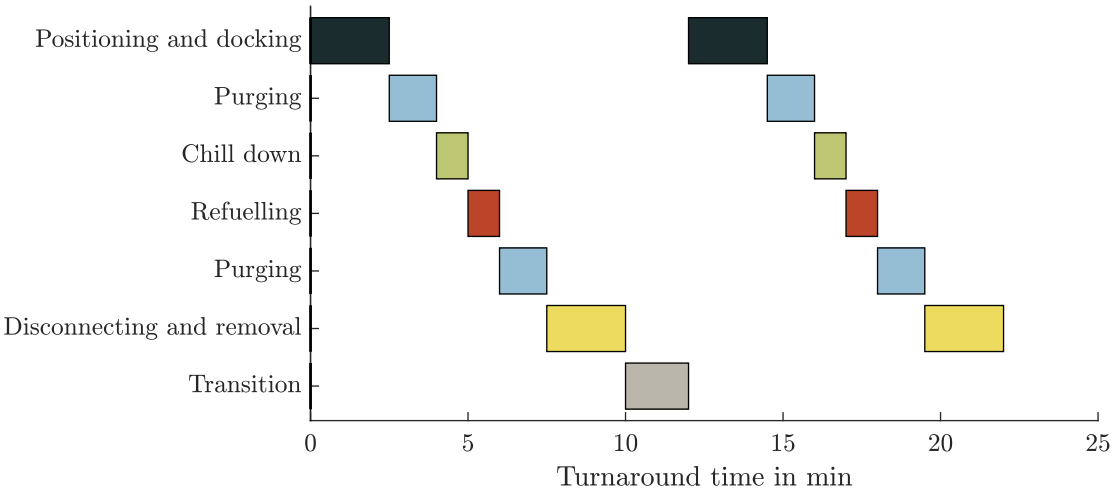

Figure 3.16: Gantt chart for sequential LH2 refuelling two podded tanks; refuelling for a 1500 NM mission, excluding reserves; fuelled mass of LH2 is 2500 kg

In sequential refuelling, where the pods are filled consecutively, the refuelling process takes 11 min longer than in the parallel case, see Figure 3.16. This difference is because each sub-process in the refuelling has to be performed twice, and the vehicle has to drive around the aircraft once. The refuelling process for a 1500 NM mission on Jet A-1 would take 10 min with one hose. Considering the special aircraft configuration, the refuelling process in sequential operation takes 12 min longer than Jet A-1. The parallel process, on the other hand, takes 1 min longer than Jet A-1. However, in the parallel refuelling process, the cooling time is independent of the pipe's length between the pods. This assumption is only valid if this connecting pipe is short or kept at cryogenic temperatures permanently. However, the case of a required cooling in the refuelling process cannot be appropriately considered, as the chill down time's analytical solution is independent of the pipe length, see Section 3.2.3.

Cash Operating Costs of Liquid Hydrogen Fuelled-Aircraft

An extension of the refuelling time due to a particular LH2 aircraft configuration can therefore occur. However, as described in Section 2.4, the effects on the turnaround will only be weak. As a result, a change in the refuelling time has only a minor effect on the aircraft's utilisation. Conversely, the profitability of the aircraft and thereby the market existence hardly changes. In Figure 3.17, this finding is illustrated by the COCs. It becomes clear that for longer turnaround times, there is no linear correlation on the COCs. In connection with the flight range, it can be seen that the influence of the turnaround time on the costs decreases with increasing flight range. This behaviour is due to the application of the stochastic values from Figure 2.20. A longer turnaround time does not affect the utilisation or costs for longer flight distances since the aircraft can compensate for the delay during the flight. For short-haul flights, this compensation is only possible to a limited extent, as the turnaround time accounts for a much larger percentage of the available time.

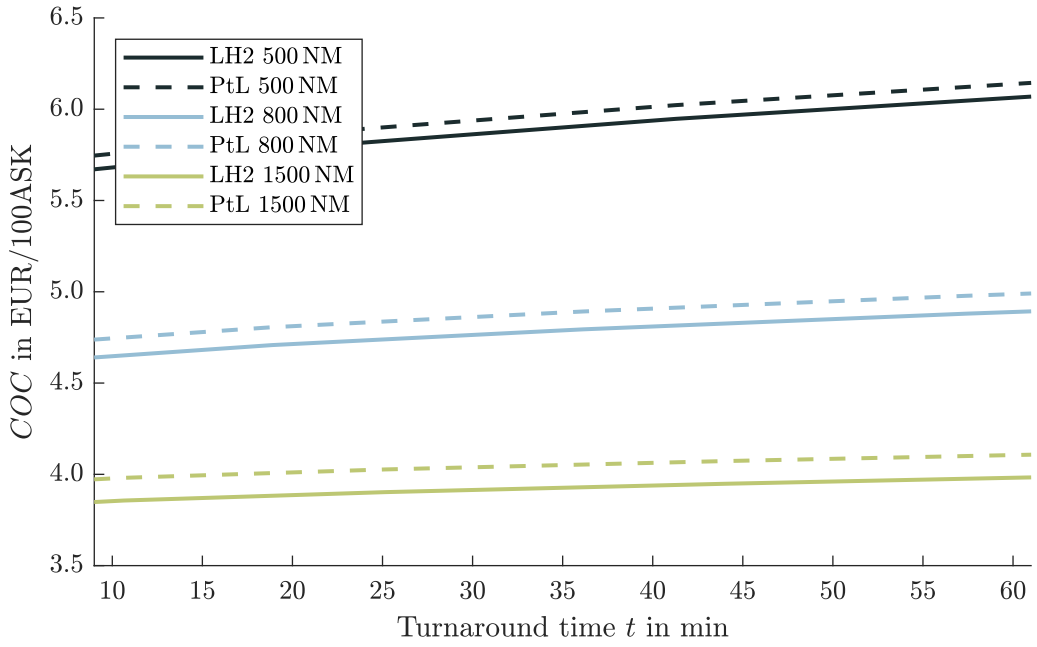

Figure 3.17: COCs for a 180-passenger aircraft versus the turnaround time; additional dependence on the flight distance and by differentiating the energy carrier from LH2 or sustainable aviation fuel

To classify the calculated COC values, the costs for a comparable aircraft with sustainable aviation fuel produced renewably by PtL are plotted in Figure 3.17. The curves of the different energy sources behave in the same way, but there is an offset between them. This is because PtL requires more energy for production, and thus the fuel price is higher. The price for LH2 in this diagram is assumed to be 29.15 EUR/GJ and for PtL 35.6 EUR/GJ [130]. Thus, the 22 % price difference between the fuels is only reflected in the COCs in a weakened form.
Due to the low fuel price, LH2 has an advantage when considering the COCs. However, considering the DOCs, in which capital costs are also taken into account, would lead to PtL causing the lower costs. This is because the development costs for an LH2-powered aircraft would increase significantly compared to PtL.

3.6 Losses and Cost Adaption Due to Refuelling With Liquid Hydrogen

The losses that occur during the refuelling process should be minimised. However, these losses cannot be avoided and impact the fuel costs of LH2, as additional quantities are fed that cannot be used for the flight mission. There is a differentiation of losses between the refuelling variants and the refuelling process, which are broken down and analysed below to determine the fuel price's impact. However, the price increase is based purely on the additional energy consumption and helium or hydrogen consumption. Capital expenditures (CAPEX) and operational expenditures (OPEX) are not considered, as they are strongly dependent on utilisation and quantity delivered.

The fuel price is based on an analysis of the energy required to produce the fuel by Silberhorn et al. [130]. This investigation results in a LH2 price of 29.15 EUR/GJ. This analysis makes it possible to compare different energy sources regardless of density or calorific value. The conversion of the energy price results in a mass-related price of 3.5 EUR/kg LH2. Including other literature sources, this results in a price range for possible fuel costs of LH2 of 1.0 to 5.7 EUR/kg [130, 91, 36]. A detailed investigation for the LH2 price is not made due to the different production assumptions, such as the location, the process and the energy price.
As a result, losses of LH2 caused by chilling and vaporisation can be added proportionally to a refuelling operation on the fuel price. In addition to these direct losses of LH2, there are also the costs that have to be incurred to transfer the fuel. These influences include the power consumption of pumps or the gas's cost in a pressure feed system. When a purging process is executed, the cost of the inert gas must also be considered.
To include the electricity price in the costs independently of location, the electricity price is based on the fuel price and the energy required to produce LH2 in an environmentally friendly process. As defined in Section 2.1, renewable LH2 requires specific production energy of 210 MJ/kg LH2. With the fuel price of 3.5 EUR/kg LH2, the electrical energy price results in 0.0167 EUR/MJ or 0.06 EUR/kWh. Therefore, this electricity price is the origin of the further calculation of the costs that arise from the consumption of electrical energy to be able to refuel LH2. The helium required for the refuelling process is assumed to have 22 EUR/kg in the following cost calculation [150].

The following list shows the fixed costs that are accrued per refuelling procedure and are independent of the vehicle type:

- 0.3 kg of helium is required for pressurisation as part of the purging process per refuelling, resulting in costs of 6.6 EUR
- The evacuation of the pipes as the second part of the purging process requires a vacuum pump with a power of 10 kW. There is a cost of 0.0135 EUR per refuelling
- The chilling down of the pipes is estimated to produce an evaporated quantity of 12.4 kg of H2, which results in a cost per refuelling of 43.4 EUR (without recycling)

The independent, fixed costs per refuelling cause a price increase of 0.29 % a refuelling quantity of 5000 kg LH2. In contrast, the price increases by only 0.08 % when the vaporised H2 is recycled in a liquefaction plant.
The additional operational costs for the distribution system, which are also independent of the vehicle type, i.e. independent of pipeline or fuel truck, consist mainly of the pump and the pressure system and keeping the tank pressure constant:

- The pump at the storage tank requires energy of 16.3 kJ/kg for feeding. This performance results in costs of 1 EUR for pumping 5000 kg LH2
- A vaporiser with an electrical power of 140 kW is needed to maintain the pressure for a mass flow of 20 kg/s. This consumption results in additional costs of 0.6 EUR for a delivery of 5000 kg LH2
- The vaporised LH2 for pressurisation amounts to 29.1 kg LH2 for a delivery of 5000 kg. These losses, therefore, result in additional costs of 101.5 EUR (without recycling)
- Considering the cooling of LH2 in the refrigerator, which is necessary to produce LH2 as a single-phase fluid, there is a cost increase in the fuel price of 0.32 %

These variable costs for feeding from the storage tank increase the fuel price by 0.59 % without recycling the vaporised H2. With recycling through a liquefaction plant, a price increase is associated with the liquefaction energy of 0.09 %.

The dependent refuelling costs depend on the refuelling method and therefore differ according to the refuelling vehicle.
For a pipeline system with a dispenser as a refuelling vehicle, there are no further costs for refuelling LH2. The dispenser causes no losses and requires negligible electrical power.

There is a wide variation in additional costs for the refuelling truck due to the large number of possible systems that can be used. In principle, all trucks with a compressor and a high-pressure tank to store losses have an electrical cost of 3.78 EUR for refuelling of 5000 kg of LH2. In the following section, the possibility of using a pump on the fuel truck to deliver LH2 is considered first:

- The pump in the refuelling truck has a power of 148 kW, which means a cost of 0.62 EUR for a delivery of 5000 kg. This value is lower than the pump on the storage tank because less pressure head is needed
- Three possible methods are conceivable for maintaining the required pressure in the vehicle tank so that the pump can operate without cavitation:
    1. The pressurisation of the tank with helium causes additional costs of 540 EUR in the conservative case and 324 EUR in the optimistic case. The different variants depend on the calculation method; see Section 3.3.1
    2. Taking into account a vaporiser, additional costs of 86 EUR will arise without reuse. With the recycling of the vaporised H2, costs of 13 EUR arise.
    3. Pressurising with GH2 from pressurised bottles costs an additional 24.5 EUR to 52 EUR depending on the calculation method, see Section 3.3.1

Therefore, the fuel costs for refuelling with a tank truck and a pump increase between 0.09 % and 3.09 %.

The second way to feed fuel into the aircraft is through a pressure feed system. This system also differs in the choice of pressurant:

1. Tank pressurisation with helium costs between 1285 EUR and 2180 EUR
2. With the pressurisation with GH2 from bottles, costs of 101.5 EUR to 206.5 EUR arise

The pressure feed system thus results in a price increase of LH2 between 0.11 % and 12.45 %.

Following only the maximum and minimum increase in fuel costs are represented as follows. The minimum increase includes no purging and the lowest cost for each method. The maximum increase, on the other hand, includes a purging operation. Table 3.4 shows the methods with the maximum and minimum price increases.

Fuelling method	Subsystem	Minimum increase %	Maximum increase %
Pipeline dispenser system		0.45	1.20
Refuelling truck	Pump feed	0.54	4.92
	Pressurised feed	0.56	13.62

Table 3.4: Price increase of LH2 depending on refuelling method; split into minimum and maximum fuel price increase related to the purchase price of 3.5 EUR/kg LH2

In conclusion, the pipeline dispenser system has the lowest operational costs, neglecting the investment costs. A refuelling truck solution is therefore also reasonable if the losses are recovered by intermediate tank storage. Otherwise, the high losses are not sustainable. From these results, for the airport infrastructure can be concluded that in a transition phase, fuel trucks are a reasonable choice because the operating cost is not significantly higher, and the investment cost is considerably less. Conversely, if there is a large daily demand, a pipeline system will be cheaper. This variety creates a trade-off between low capital cost and higher operating cost for a fuel truck system and high capital cost and low operation cost for a pipeline dispenser system. However, this break-even point will not be investigated further.

Nevertheless, it must be mentioned that the purging operation accounts for only 0.04 % of the increase. The helium price has the highest uncertainty because helium is only available in a limited amount. Thus, the recycling of helium is significantly important to establish LH2 as a fuel.

4 Impact of Liquid Hydrogen on Aircraft Design

The scientific findings from the refuelling process and the thermodynamic aspects can be transferred to the overall aircraft design. In the following chapter, these effects will be further investigated and analysed. The calculation of the required tank volume based on different assumptions will be discussed. Subsequently, consequences for using pumps are explained, which selection influences the tank and fuel system. Simplified losses during a flight mission can be derived from these conditions. Thus, the distinction between vaporised and vented hydrogen becomes relevant. The difference between a gaseous and a liquid hydrogen feed is worked out to determine the required performance for feeding the engine. This distinction takes into account the use of available and expendable energies. For a possible operational scenario for H2 aircraft, where the return flight is to occur without refuelling, the convertible range is calculated over the ground time. This scenario does not include ground support at the intermediate airport. In the last section, the prevention of venting by ground support and the vented hydrogen's safe handling is elaborated.

4.1 Liquid Hydrogen Tank Volume

The tank volume calculation is an essential task for the aircraft design, which serves to verify the available mass to fly a mission. In contrast to Jet A-1, where the tank is accommodated in the wing without significant effort, this implementation can only be realised with considerable losses in LH2. This difficulty is because the tank cannot be vented to ambient pressure during a flight, resulting in a noticeable pressure difference at cruising altitude. Due to the increased pressure difference, the wall thickness and the tank's weight depend on the ratio of the volume to the surface area. This ratio is lowest for a sphere, making a long thin cylinder, as it could be installed in the wing, too heavy. Consequently, the aircraft tank should be spherical or in the shape of a cylinder with a low length to diameter ratio. Due to these regularities, a different type of aircraft configuration is created that allows LH2 to be used as fuel.

The tank volume can be determined by summing up the following volume requirements. The usable tank volume can be calculated from the block fuel mass and the density of LH2. The block fuel mass corresponds to the required fuel mass at the design point of the aircraft. The other necessary volumes included in the tank volume are called allowances by Brewer [26]. These allowances include the volume for the ullage, boiloff, trapped and unusable fuel, internal equipment, and the tank's contraction due to the coefficient of thermal expansion. In the space application, these individual volumes are grouped into subcategories. However, these are the same variables that have to be taken into account for the volume calculation. The following formula can be derived after Huzel et al. [70] and Brewer [26]:

$$V_{\text{tank}} = V_{\text{LH2}} + V_{\text{trapped}} + V_{\text{losses}} + V_{\text{ullage}} \tag{4.1}$$

$$V_{\text{tank}} = m_{\text{LH2}} \cdot \frac{(1 + \text{allowance})}{\rho_{\text{LH2}}} \tag{4.2}$$

Depending on the source, the allowances vary between 3 and 10% [143, 26, 70]. Therefore, the density of LH2 is the decisive parameter for the tank volume. By understanding the thermodynamic properties, three calculation methods for the tank volume in the aircraft can be derived.

The first method calculates the tank's volume with the density on the saturated line, see Figure 4.1, with the maximum tank or venting pressure. This approach is the most conservative method to determine the tank volume because the density of LH2 is the lowest at this point. However, it must be mentioned that a higher tank pressure does not imply a lower density of LH2. Conversely, a higher tank pressure does not automatically mean a larger tank volume, but rather that only a conservative approach has been chosen.

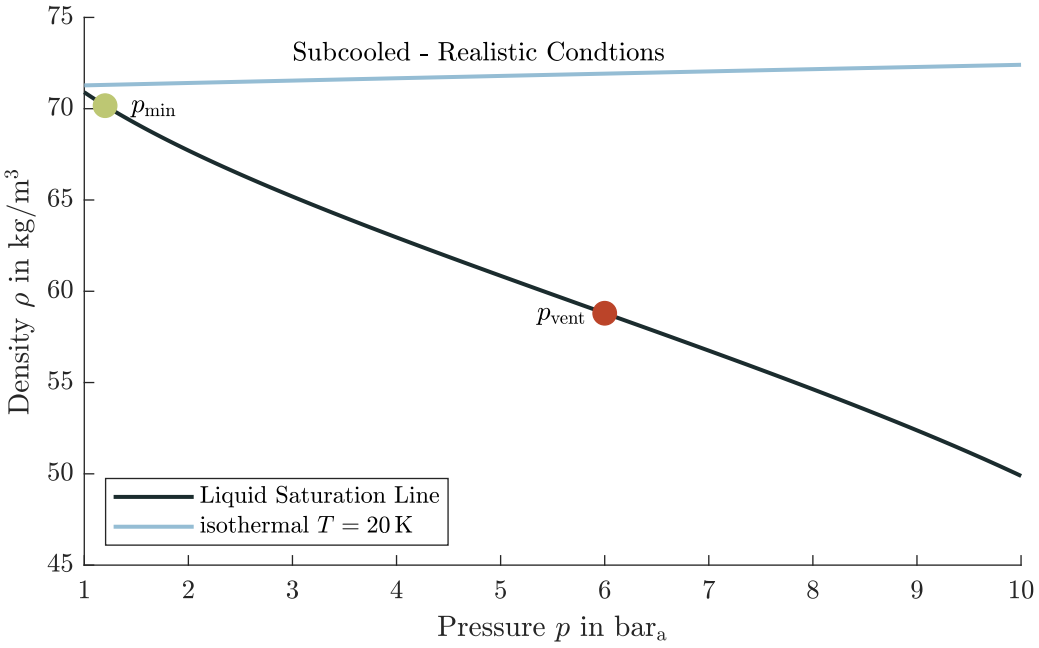

Figure 4.1: Density of LH2 over pressure for short term storage; difference between saturated and subcooled conditions

In the second optimistic method, the density is determined based on the minimum tank pressure and the saturated state, see Figure 4.1. In space travel, except SpaceX, this calculation method is used. This approach with the density as a function of the minimum pressure as a saturated liquid can be explained using the loading procedure, see Section 2.3.2. After the tank is almost filled, the pressure is reduced to the minimum pressure, resulting in a saturated liquid in thermodynamic equilibrium through vaporisation. However, this flash vaporisation takes time, which must be included in the time before liftoff, see Figure 2.14. According to Ring [115], the order of magnitude of the time needed to reach equilibrium is 10 to 15 min, but it is a function of the refuelling system and the vehicle's venting system. In contrast to this short duration, Stroman et al. [140] states more than four hours until thermodynamic equilibrium is reached.

This behaviour shows the reason why the first method is a conservative approach to determine the tank volume. Usually, the liquid should not warm up because it has adverse effects on the pump. The approach of Verstraete [152] and Winnefeld et al. [158] to select the density at equilibrium at maximum tank pressure, therefore, proves to be impractical. The statement that a higher tank pressure will also lead to a larger volume is only correct in the theoretical approach if equilibrium would be reached at maximum tank pressure. This chapter shows that this condition must be prevented and therefore has no relevance in the aircraft design.

In the third variant for determining the density, a realistic approach is chosen. Here, the density is determined from the actual tank and refuelling conditions. Conversely, this means that a subcooled liquid also belongs in this variant. Due to the subcooling, LH2 is not in equilibrium and is therefore not in a saturated state. As a result, as described in Section 2.1.1, the density becomes a function of pressure and temperature, and LH2 must be treated as a real compressible fluid. The statement that the fluid is always on the saturated line is therefore not valid.
The advantage of densification (subcooling of the fluid) is to increase the density. SpaceX uses this advantage in Falcon 9 by refuelling with subcooled liquid oxygen. This effort reduces the tank volume, which has a similar snowball effect on the mass calculation [157, 15]. Furthermore, the refuelling procedure changes. The launch of the rocket follows immediately after the completion of the refuelling. As a result, there is no replenish and topping procedure as for the Space Shuttle. Instead, the rocket is launched after reaching the desired fill level called Load and Go. In other words, the time between the end of the refuelling process and the rocket launch must be kept as short as possible to prevent the liquid from heating up. The liquid does not vaporise immediately due to heat input, as is the Space Shuttle case, since the sensitive heat must be provided first. Furthermore, the fluid's subcooling offers advantages for pump cavitation because the temperature at the pump inlet is reduced. Therefore, the vapour pressure also decreases, which means an increase in the NPSH value [157, 101].

In conclusion, it can be summarised that the choice of density for calculating the tank volume can be determined with three methods. The first two methods differ mainly in their dependence on the pressure in the tank. The third method refers to the actual tank and refuelling conditions, where the additional variable of temperature is also taken into account. Hence, in aircraft design, one method can be chosen for the design depending on fidelity and uncertainties. Table 4.1 shows values for the density of LH2 for the three methods. In method two, which is used as a reference value, LH2 has a density of $70.15\,\mathrm{kg/m^3}$. This results in an $9.59\,\%$ reduction in density than method one with a pressure of $3.5\,\mathrm{bar}$. Compared with method three and the realistic refuelling conditions, an increase in density of $1.45\,\%$ or $4.55\,\%$ results depending on subcooled level.

However, the different methods for determining the density of LH2 require conditions to be implemented in the aircraft design. When designing an aircraft using the Breguet range equation, the actual tank conditions are not relevant, and methods one and two can determine the tank volume. Due to this fidelity analysis at Level 0, the uncertainties are significant, making a conservative estimate of the tank volume more reasonable. For example, method two can be used in the design mission, and method one can be used in the recalculation task for shorter ranges to derive sensitivities.

Method	Pressure p $\mathrm{bar_a}$	Temperature T K	Density ρ $\mathrm{kg/m^3}$	Deviation %
1	3.5	25.28 (saturated)	64.01	−9.59
2	1.2	20.86 (saturated)	70.15	0
3	1.2	20.00 (subcooled)	71.17	1.45
	1.2	18.00 (subcooled)	73.34	4.55
	1.2	16.30 (subcooled)	74.89	6.76

Table 4.1: Density and density variation of the different determination methods for density and tank volume; extensive consequences for the overall aircraft design as 15 % differences can occur

In contrast, Method 3 with realistic tank conditions requires an accurate non-equilibrium thermodynamics model. For an aircraft mission calculation in which the flight envelope is calculated, the tank model must determine the thermodynamic state variables as a function of several variables. Hence, a distinction between subcooled and saturated liquid is possible. Due to the non-equilibrium thermodynamics, the model must also represent a stratification of the fluid in combination with a heated gas phase in the ullage. A corresponding thermodynamic model can be found in Daigle et al. [40], Osipov et al. [107], Vietze [154] or Ring [115].

4.2 Realistic Tank Conditions

The calculation of a flight envelope with realistic tank conditions requires a thermodynamic non-equilibrium model, as described in the previous chapter. This modelling shows the tank pressure and temperature history over the flight time, which the simplified analysis in Section 4.3 cannot resolve. This analysis allows a distinction to be made between vaporised and vented H2.
The investigation in Section 4.4 describes the necessity of feeding a single-phase fluid to the high-pressure pump. The avoidance of a two-phase flow can be ensured, as described in Section 2.1.2, by the installed pump's characteristic in combination with the pressure conditions at the pump inlet. A fundamental distinction must be made between the two types of pumps. The first option is a pump with a defined $\mathrm{NPSH_c}$ value, for which an excess pressure to the saturated line must be present to pump mass flow without cavitation. The second option is a pump that requires a Zero-NSPH value. In other words, the liquid in the tank can be at equilibrium and thereby on the saturated line.

However, the two pump variants have extreme effects on the tank system, as the $\mathrm{NPSH_c}$ pump requires a subcooled liquid in every flight condition. Figure 4.2 shows this behaviour through a condition flight box. The horizontal distance between the saturated line and the condition box shows the $\mathrm{NPSH_c}$ value of the pump. By re-dimensioning the LPFTP of the SSME, a NPSH value of 26 m must be present or expressed by the overpressure to the saturated line of 0.18 bar.

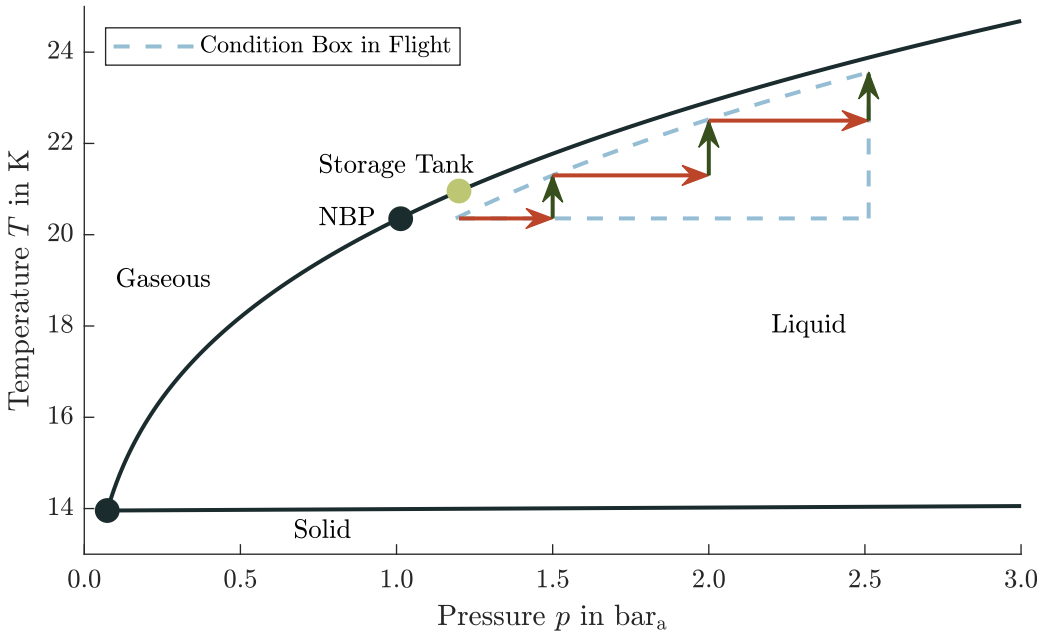

Figure 4.2: Realistic thermodynamic tank conditions adapted from Mustafi et al. [97]; simplified process for maintaining the subcooling level through isothermal pressurisation and isobaric heating for low-pressure pump inlet requirements

Due to the heating of the tank contents by the heat input (isobaric), the tank condition moves closer and closer to the limitation. This process can happen after initial pressurisation (isothermal). However, this limit must not be exceeded. Otherwise, damage and pump failure could occur, as described in Section 2.1.2. This condition can only be prevented if the tank is pressurised again. This re-pressurisation establishes a subcooled liquid again, and the $\mathrm{NPSH_a}$ is greater than the $\mathrm{NPSH_c}$. However, due to the pressure increase, where a heated gas is introduced into the ullage, the liquid in the tank can heat up further again, which would lead to further pressurisation. This process can also be expressed in terms of energy levels. Due to the pressurisation, the total energy in the tank increases, which over time is converted into the fluid's internal energy and, as a result, heats up. Hence, this effect is continuously amplified, which leads to considerable problems in the tank design. The maximum pressure in the tank must therefore be significantly increased. To be able to provide a sufficient distance to the saturated line at the end of the flight. However, when the maximum pressure is increased, the tank becomes heavier, leading to the aircraft's performance losses.

In contrast to an $\mathrm{NPSH_c}$ pump's other required systems, a Zero-NSPH pump does not require the pressurisation system. Due to the characteristics of this pump, see Section 2.1.2, it can feed a saturated liquid. The main advantage of using this pump is that it is unnecessary to know the tank conditions exactly. Furthermore, no non-equilibrium thermodynamics model would be needed. This is mainly because the fluid always wants to be in the equilibrium state. After all, it has the lowest energy level. This advantage is used by Brewer [26] and Airbus [10]. This application eliminates all the problems associated with the use of an $\mathrm{NPSH_c}$ pump. Using a Zero-NSPH pump is consequently a progressive technology variant that makes LH2 aircraft much more economical and easier to implement in aircraft design. Problematically, a Zero-NSPH pump still has to be developed according to Airbus [10].

For the feasibility of LH2 aircraft, this problem could become a show stopper in selecting the pump. The required subsystems for an $NPSH_c$ pump, the mass estimation of which has not yet been carried out, combined with the mutually amplifying process of pressurisation and the resulting maximum tank pressure increase, have not been sufficiently researched. Disregarding the different pump technologies in principle would be grossly negligent and risky.

Therefore, using an NSPHc or a Zero-NSPH pump is more of a consideration in the overall aircraft design and a decision for a Technology Readiness Level (TRL). The use of Zero-NSPH pumps has already been tested in space research, and their functionality has been proven [138]. Physically, however, a two-phase flow must be present at the pump inlet due to the acceleration, which is converted into a single-phase flow (subcooled/ compressed liquid) by the impeller's pressure increase. However, this process describes precisely the characteristics of cavitation, in which vapour bubbles implode and lead to considerable damage, see Section 2.1.2. The space application of Zero-NSPH pumps only requires a few minutes' service life, whereas an aircraft should function perfectly for 400-600 flight hours until A-Check without maintenance. Consequently, a transfer of research results from space flight to aviation is questionable, as the operating time increases significantly.

Suppose that Zero-NSPH pumps from space applications, characterised by high rotational speeds and a low mass, are not feasible. In that case, it may be possible to fall back on heavy, slowly rotating pumps that do not tend to cavitate. This creates a trade-off between the respective system masses and thus the resulting aircraft performance expressed in profitability.

4.3 Simplified Influences on Tank Pressure During a Flight Mission

The thermodynamic modelling of the tank interior requires, as described in Section 2.3.2, a method where non-equilibrium thermodynamics can be taken into account. The liquid fraction in the tank should be understood with stratification to be able to consider hydrostatic effects. Also significant in the modelling is the property of the mass flow taken to feed the engines. The pressurisation system, be it helium, GH2 or an vaporiser, also influences the contents' behaviour in terms of pressure and temperature in the gaseous or liquid fraction.

However, this complex behaviour with multiple variables is fundamental for a reliable system and aircraft design with H2. Nevertheless, simplifications can approximate an estimate of the losses that occur and the energy requirements during a flight mission. During the flight, the tank pressure varies due to heat input and fuel extraction. For the prediction of the pressure change, Lin et al. [85] assume a homogeneous model, which assumes thermodynamic equilibrium in the tank:

$$\frac{dp}{dt} = \frac{1}{V} \cdot \left[\rho \left(\frac{\delta u}{\delta p} \right)_{\rho} \right]^{-1} \cdot \left[\dot{Q} - \dot{m} \cdot \Delta h_{\mathrm{v}} \cdot \left(x + \frac{\rho_{\mathrm{g}}}{\rho_{\mathrm{l}} - \rho_{\mathrm{g}}} \right) \right] \tag{4.3}$$

This formulation results from the application of the first law of thermodynamics and the continuity equation. Winnefeld et al. [158] introduce this approximation for aircraft applications, and Millis et al. [95] use a similar approach for modelling the tank pressure. By assuming thermodynamic equilibrium, the tank content is on the saturated line, which means that the extracted mass flow in Equation 4.3 depends on the vapour content and the vaporisation enthalpy.

Lin et al. [85] describe that the experimental data, however, deviate from the model equation by a factor of 2. This deviation can be explained in that the tank content is not in thermodynamic equilibrium, and thus there is a temperature difference between the ullage and the fluid. In other words, the fluid is subcooled, and the temperature of the gas in the ullage is above the saturated vapour line of the corresponding pressure.

Since this complex thermodynamic behaviour cannot be transferred to just one equation, a further simplification is made to determine the losses or heat inputs for constant tank pressure. By assuming that the tank pressure remains constant during the flight mission, the pressure term's time derivative is omitted $\frac{dp}{dt} = 0$.

This simplification also revises the statement that a factor of 2 must be introduced to represent the pressure change with time. Besides, the derivation of the internal energy is omitted. Thus, for a given mass flow, which serves to supply the engine, the required heat input can be calculated to keep the tank pressure constant. The mass flow is taken from the flight envelope. The following equation results from this:

$$\dot{Q} = \dot{m} \cdot \Delta h_\mathrm{v} \cdot \left(x + \frac{\rho_\mathrm{g}}{\rho_\mathrm{l} - \rho_\mathrm{g}} \right) \tag{4.4}$$

Since the previous equation model assumes the extraction of a saturated liquid and the enthalpy difference also corresponds to the enthalpy of vaporisation, more general modelling is introduced. In this model, the enthalpy difference corresponds to the enthalpy of GH2 that is not on the saturated vapour line subtracting the enthalpy of a subcooled liquid. The density term on the right-hand side, depending on pressure and temperature, also corresponds to the enthalpy values' properties and not of the saturated vapour line and saturated liquid line. This definition allows the temperature in the ullage to be varied, which is close to the behaviour of non-equilibrium thermodynamics. Equation 4.5 results from this modelling:

$$\dot{Q} = \dot{m} \cdot (h_\mathrm{g} - h_\mathrm{l}) \cdot \left(\frac{\rho_\mathrm{g}}{\rho_\mathrm{l} - \rho_\mathrm{g}} \right) \tag{4.5}$$

This equation can also be derived from an isochoric change of state in which a liquid phase is withdrawn from the tank, and a quantity of the liquid phase is vaporised and returned in gaseous form. The isobaric behaviour can also be expressed by a constant volume where a gaseous fraction replaces the liquid fraction. Figure 4.3 shows the amount of heat required for a constant pressure of $1.38\,\mathrm{bar_a}$ over the flight time. Here, the heat quantities differ by the returned gas temperature, reflecting the value of the enthalpy difference and the density ratio term since all variables are a function of pressure and temperature.

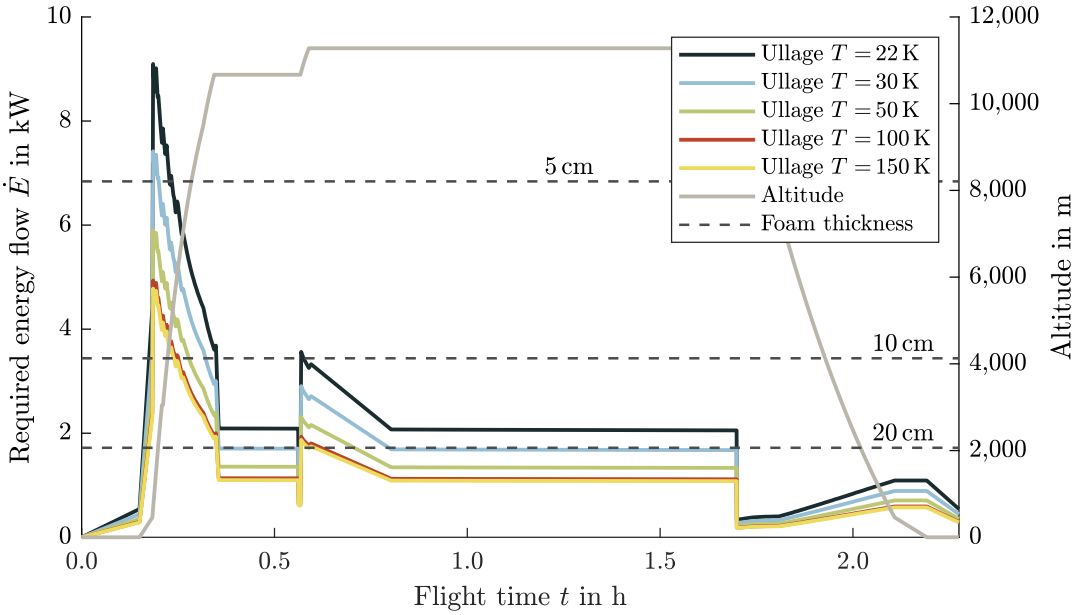

Figure 4.3: Required energy input to aircraft tank for constant tank pressure with the variation of ullage gas temperature; flight envelope for a 180-passenger aircraft over an 800 NM mission

The dependence of the heat input on the extracted mass flow or the flight phase can be seen. It should be particularly emphasised that the heat flow only has to be introduced into the tank's system boundary and is thus independent of the type of energy flow. It can be concluded from this that the heat input can either enter the tank from outside due to environmental influences or be introduced by electrical work (e.g., heat exchanger). Conversely, this energy input must take place in order to keep the tank pressure constant. The integration of the heat flow over the flight time results in the required energy of a mission. This energy, which has to be introduced into the system boundary, can be converted into a mass of LH2 by the enthalpy difference, which has to be refuelled additionally but cannot be used. Consequently, this unusable mass or volume must be included in the calculation for the tank volume. In this context, the loss of LH2 means that this mass remains in the tank and is not vented but cannot be used.
Conversely, the required heat flow can be traced back to a heat transition coefficient or insulation thickness. Hence, depending on the flight envelope, an optimal insulation thickness would result as a function of the mass flow. For example, the optimal thickness varies from 5 cm during take-off with the maximum mass flow to 20 cm of insulation foam during cruise flight. The horizontal dashed lines in Figure 4.3 are drawn as examples of insulation thickness. The environmental heat flow into the tank would consequently reduce the electrical work required to keep the tank pressure constant. In other words, the integration between the required energy flow and the heat flow through the insulation gives the required additional energy.
The loss mass of LH2 is shown in Figure 4.4 over the returned gas temperature of H2. In addition, the other variable of the flight distance is shown in this diagram, which shows a more significant loss at longer flight distances. It is also apparent that a lower gas temperature means a larger loss mass. This behaviour can be explained using the ideal gas equation: A higher temperature at constant pressure and volume means a lower mass. The behaviour of the heat flow in Figure 4.3, on the other hand, shows that a lower temperature requires a higher heat flow to keep the pressure constant. This coherence can be explained by the enthalpy difference and density term, which has a non-proportional behaviour of the temperature.

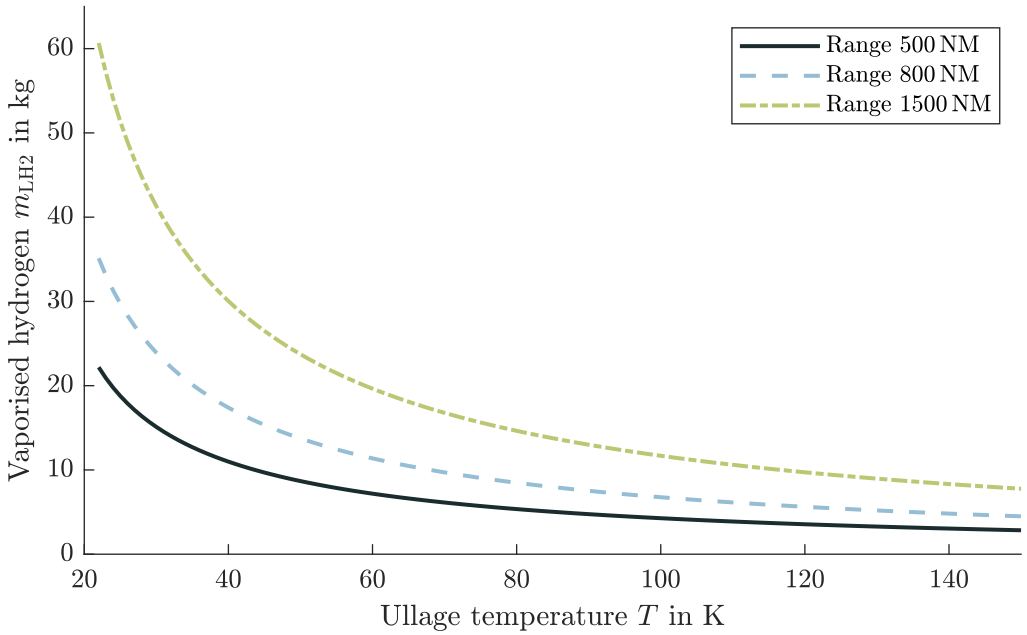

Figure 4.4: Vaporised LH2 quantity for a constant tank pressure over the flight mission; dependence on the gas temperature in the ullage and the flight range

In summary, these findings are relevant due to the simplified approach in that they represent the possible limits of losses through simple modelling. In reality, the ullage temperature will be in the temperature range shown in Figure 4.3 and 4.4. In this modelling and approach, however, it must be added that no interaction at the phase boundary layer has been considered. This omission is relevant because the temperature difference and the non-equilibrium thermodynamics cause an interaction between the ullage and the liquid phase.
Condensation and vaporisation are not considered by the simplifications and would have a significant influence at higher gas temperatures. As a result, the loss mass would increase again at higher temperatures, unlike shown in Figure 4.4. Conversely, there is an optimum gas temperature for which a minimum amount of loss occurs. As already mentioned, a thermodynamic model must be used for the actual behaviour that takes all effects into account.

4.4 Feeding Hydrogen From the Tank to the Power Source

The transport of H2 from the aircraft tank to the power source can, in principle, be accomplished in two ways. The power generation can be directly combustion in an engine or catalysis with the oxidiser oxygen to produce electrical energy. The two types of use differ primarily in the pressure level, which is 2-5 bar in the case of fuel cells [25] and around 50 bar for the combustion in jet engines [26]. In both variants, however, GH2 is fed in, which means that the stored LH2 must first be vaporised and accordingly requires a specific temperature to keep system efficiency high. A temperature of 260 K is present in a combustion engine when injected into the combustion chamber [26]. Therefore, the question now arises how the transport from the tank to the consumer can be designed to realise the energy supplier's boundary conditions.

In principle, feeding in a liquid or gaseous phase is possible in both cases. To enable a comparison of both variants, an isentropic pressure increase by the pump and an isobaric heat input for the heat exchanger by enthalpy differences can be considered in a simplified way. The starting point for both considerations is liquid storage in the aircraft tank in the subcooled region with a temperature of 20 K and pressure of 1.5 $\mathrm{bar_a}$.
Two system designs are conceivable to meet the inlet conditions of the fuel cell. One is to directly take the gaseous phase in the ullage from the tank and deliver it. With this variant, a vaporiser is needed in the tank to keep the pressure up and constant. Therefore it is possible in principle to use a pressure feed system, in which the tank pressure is increased until the pressure difference can take over the transferring. This option will not be considered in the thesis because it implies a heavy tank.
The second option for a fuel cell is when the pump feeds a liquid phase, which a heat exchanger then vaporises. Using the isentropic enthalpy difference, the pump's specific energy or electrical power can be calculated to reach a pressure level of 5 $\mathrm{bar_a}$. Subsequently, the differential temperature to the inlet conditions must be compensated by a heat exchanger.
However, comparing the two options for feeding a fuel cell is only possible to a limited extent. With a higher tank pressure and gaseous delivery, the pressure can build up through the self-pressurisation of hydrogen, which in this respect does not require any electrical power. In contrast, pump feeding requires electrical power but is characterised by a lighter tank. This circumstance means that the comparison for feeding a fuel cell can only be applied to the overall system design, including power, efficiency and mass.

For the combustion of H2 in an engine that generates thrust directly, two delivery options are conceivable, similar to those for a fuel cell. In both variants, a low-pressure pump installed near the tank delivers LH2. The pressure head by the low-pressure pump only has to compensate for the pressure losses due to friction reaching the engine. Close to the engine, the combustion variant differs in two possible subsystems. First, a high-pressure pump can compress the LH2 to the desired pressure level, which is then vaporised in a heat exchanger and heated to the desired inlet temperature. The advantage of this arrangement is the adept use of the waste heat from the engine jet, which is available and can be used. In the second option, the order of the system components is reversed. First, the LH2 can be vaporised and then compressed to be injected into the combustion chamber. The advantage of this arrangement is the free positioning of the heat exchanger and high-pressure pump. Both components can thus also be placed close to the tank, which means that transport to the consumer takes place in gaseous form instead of liquid form.

Table 4.2 and 4.3 illustrate the respective electrical energies and heat quantities for both variants with isentropic compression and isobaric heat input by enthalpy differences. It should be emphasised here that the total amount of energy is the same for both variants, verifying the calculation method. However, the main difference lies in the type of energy required to meet the engine's boundary conditions. For gaseous transport, the amount of heat required decreases significantly compared to liquid transport. In contrast, the electrical energy for compression in the pump increases to the desired pressure level.

Process	p_1	T_1	p_2	T_2	Δh	P	$\dot{Q}$
	$\mathrm{bar_a}$	K	$\mathrm{bar_a}$	K	kJ/kg	$\mathrm{kW_{el}}$	$\mathrm{kW_{heat}}$
isentropic	1.2	20.00	5.0	20.17	4.91	0.98	-
isentropic	5.0	20.17	50.0	22.06	61.58	35.19	-
isobaric	50.0	22.06	50.0	260.00	3806.87	-	761.37

Table 4.2: Arrangement: liquid low-pressure pump, liquid high-pressure pump, heat exchanger/vaporiser; isentropic and isobaric change of state for the consideration of the required power, divided into electrical power and heat input

Nevertheless, in consideration of the overall aircraft design, there is a massive difference in the feasible delivery of the energy type. In the liquid transport of LH2, only a fraction of electrical energy of the total energy is required compared to the gaseous one. Most of the energy required is thermal energy, which is already available in the hot exhaust gas stream and has been unused ever since. The generation of electrical energy in the aircraft is complex and costly and reduces the engine's efficiency.

Process	p_1	T_1	p_2	T_2	Δh	P	$\dot{Q}$
	$\mathrm{bar_a}$	K	$\mathrm{bar_a}$	K	kJ/kg	$\mathrm{kW_{el}}$	$\mathrm{kW_{heat}}$
isentropic	1.2	20.00	5.0	20.17	4.91	0.98	-
isobaric	5.0	20.17	5.0	143.19	1989.05	-	397.81
isentropic	5.0	143.19	50.0	260.00	1879.40	375.88	-

Table 4.3: Arrangement: liquid low-pressure pump, heat exchanger/vaporiser, gaseous high-pressure pump; isentropic and isobaric change of state for the consideration of the required power, divided into electrical power and heat input

The sums of the required energies from Table 4.2 and 4.3 are equal. On the one hand, this realisation shows that the variable is a state variable since the result is independent of the process path. On the other hand, that both methods are theoretically feasible because the thermodynamic boundary conditions are met.

Hence, GH2 transport finally does not make sense since such electrical energy quantities are not available. The existing synergies are not used by utilising the heat in the exhaust gas jet. All in all, for the combustion of H2, a transport of LH2 by a low-pressure pump, high-pressure pump and subsequent heat exchanger is preferable. For fuel cells operating at a lower pressure level, both variants, gaseous and liquid transport, are possible.

4.5 Operation Scenario for Return Flight Without Refuelling

Due to the cryogenic temperatures of LH2, there is always a heat input into the aircraft tank because of the temperature difference to the environment. The amount of heat flow depends on the quality of the insulation. Two possible insulation variants are conceivable for aircraft design: vacuum insulation combined with multilayer insulation or microspheres and foam insulation. Besides, the structure of the tank wall in an integral or non-integral tank must be differentiated. More detailed investigations can be found in Brewer [27]. Therefore, the insulation quality also determines the time until H2 has to be vented, which is referred to as dormancy time. The effects of typical foam insulation with a heat input of $30\,\mathrm{W/m^2}$ on a possible aircraft operation for a return flight without refuelling is investigated in the following. For comparison purposes, a H2-powered and a conventional Jet A-1 aircraft with 180 passengers and a design range of 1500 NM are considered. Table 4.4 summarises the Top Level Aircraft Requirements (TLAR) and Table 4.5 the resulting characteristic aircraft properties.

Parameter	Value
Design range	1500 NM
Cruise Mach number	0.78
Take-off field length	1900 m
Landing field length	1600 m
ICAO Aerodrome Reference	Code C
PAX (Single Class Design)	180
Mass per PAX	95 kg
Alternate distance	200 NM
Loiter time	30 min
Contingency	3 %

Table 4.4: Top Level Aircraft Requirements for the comparison of different energy sources

Parameter	Jet A-1-Aircraft	LH2-Aircraft	Unit
MTOM	65,133	68,057	kg
OEM	39,959	47,716	kg
MZFM	57,969	65,716	kg
MLM	59,481	66,216	kg
Thrust to weight (MTOM)	0.290	0.308	–
Wing loading (MTOM)	600	563	$\mathrm{kg/m^2}$
Max. fuel mass	15,054	3266	kg
L/D	17.5	16.7	–
SFC	0.0481	0.0174	kg/h/N
SEC	2.079	2.087	MJ/h/N
Design block energy	272.7	301.3	GJ

Table 4.5: General data of the aircraft

It becomes evident that the LH2 aircraft has an extended fuselage due to the LH2 tanks, and the glide ratio is consequently lower than that of the Jet A-1 aircraft. Nevertheless, the Specific Energy Consumption (SEC) of the engines is approximately the same, making a comparison possible due to the same technology assumptions.

To evaluate the possible scenario of an outgoing flight followed by a return flight without refuelling, the influence of the ground stay time at the landing airport is examined. Figure 4.5 shows the result of this analysis. The abscissa shows the ground stay time, reflecting the time difference between reaching the parking position and the push back for the return flight. The ordinate shows the single operation range, flown in each case for the outgoing and return flight. The horizontal lines are the ranges that can be performed with a Jet A-1 aircraft. The single operation range is independent of the time spent on the ground since no Jet A-1 vaporises. The upper and lower horizontal lines are differentiated by a case distinction in the boundary conditions, titled Scenario 1 and 2.

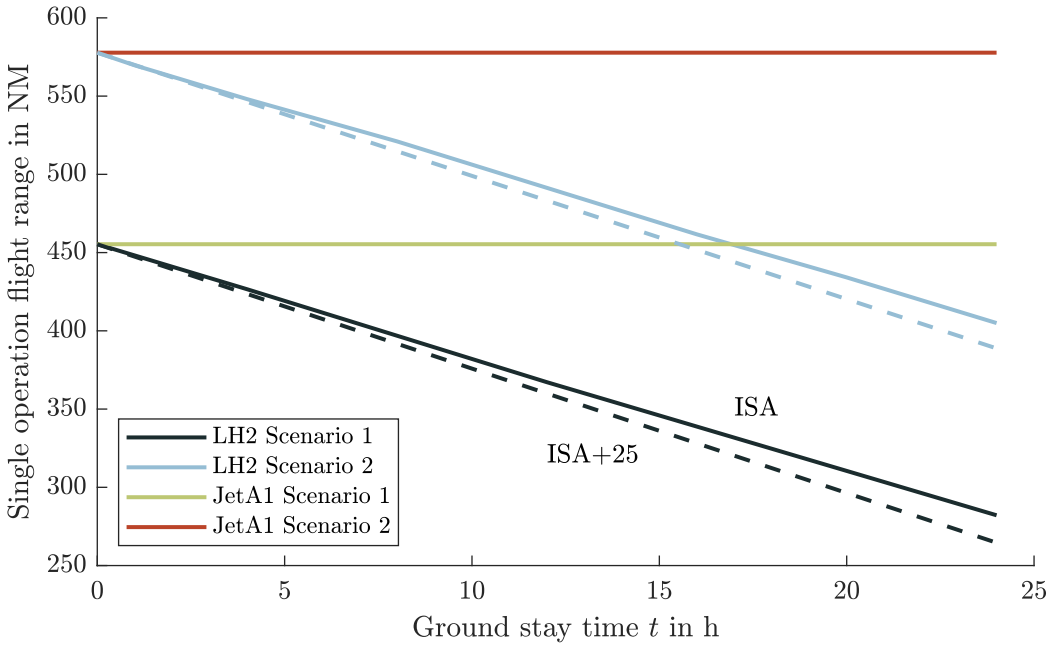

Figure 4.5: Single operation flight range over the ground stay time; ground time defines environmental heat impact and losses of LH2; return flight without refuelling to enable high flexibility

In scenario 1, an alternate of 200 NM is accounted for on the outgoing and return flight. This means that it is possible to switch to an alternate airport on the outbound flight and return to the original airport without refuelling. Furthermore, this scenario provides for an alternate on the return flight.
In contrast, scenario 2 does not provide for an alternate on the outgoing flight. This operation is possible because the aircraft tank is fuller than required for the one-way flight anyway. Hence, in a non-feasible landing, the aircraft could simply fly back to the airport of origin.
The difference between Scenario 1 and 2 is that in Scenario 1, even if the flight is to an alternate airport, the flight home is still possible, and an alternate airport can be approached again at the destination. In scenario 2, on the other hand, another alternate airport is no longer possible.

For the LH2 aircraft, the range decreases with increasing ground time. This behaviour is due to the environmental heat impact, which leads to vaporisation and thereby to a loss of LH2. In this approach, the tank pressure is vented to 1.2 bar after reaching the parking position, resulting in a saturated liquid. The penetrating heat flow is directly transferred into a latent heat by this procedure, which leads to a direct vaporisation and no sensitive heating. As a result, the H2 remains cool according to the saturated temperature with a pressure of 1.2 bar. For the return flight, the tank must be pressurised to compensate for the pressure drop due to the required mass flow in take-off.

To consider the influence of the ambient temperature at the airport, the single operation range is plotted for the International Standard Atmosphere (ISA) with 15 °C and a temperature of ISA+25 with 40 °C. This indicates that the ambient temperature has only a minor influence on the range and that this means a 7 % shorter flight distance after a ground time of 24 hours. The small influence is due to the proportionality of the temperature difference between ambient temperature and LH2 temperature on the heat flow. The increase in temperature difference is only 9 %, which reflects the shorter flight distance.

In conclusion, this flight operation is feasible with LH2 as fuel. In the case of a night flight ban, which would mean a ground time of 6 hours, a 10 % shorter range would be the result compared to Jet A-1. This slight loss in flight distance offers the advantage of extended flexibility, as only the take-off airport has to provide refuelling of LH2.

4.6 Vaporisation Prevention and Handling

The loss of LH2 harms performance and utilisation in the aircraft design. This behaviour is mainly because the tank's proportions must be oversized to take the losses or unused portions into account. In Section 4.5, these losses are quantified by a reduction of the range. Therefore, a methodical approach can be applied, which in the primary case provides for the avoidance of venting and a direct loss, and in the second case for the safe handling of H2, which must be vented.

Prevention of LH2 Losses

Using a refrigerator makes it possible to avoid heating and vaporisation due to the environmental heat impact. However, the cryocooler only cools the liquid marginally and is not to be confused with liquefaction. Therefore, the cryocooler can remove the penetrating heat flow out of the tank's system boundary again. For aircraft design, two quantities are substantial, the ratio between electrical power and heat flow defined as the specific power (reciprocal of COP) and the mass related to the electrical power or heat flow.

A single-stage cryocooler operating at a temperature of 20 K has a specific power of 450 W_{el}/W_{heat} and a weight to power ratio of 0.0419 kg/W_{el} [37]. In contrast, Milles et al. [95] gives a specific power of 34.4 W_{el}/W_{heat} and a weight to power ratio of 0.0539 kg/W_{el}. Furthermore, Deserranno et al. [44] used a cryocooler with a specific power of 61 W_{el}/W_{heat} and a weight to power ratio of 0.0621 kg/W_{el}. This variance in variables shows the different levels of efficiency of the systems. A factor of more than ten also indicates different technologies that are applied.

Hence a trade-off between efficiency and mass has to be made, to be able to classify this substantial discrepancy and the specific key numbers from Milles et al. [95], Deserranno et al. [44] and Colozza et al. [37]. The resulting values for typical foam insulation of $30\,W_{heat}/m^2$ and a tank volume of $70\,m^3$, which together correspond to a heat input of $2600\,W_{heat}$, are tabulated in Table 4.6.

Source	Mass kg	P kW_{el}
Colozza et al. [37]	49,023	1170
Millis et al. [95]	4820	89
Deserranno et al. [44]	9675	159

Table 4.6: Comparison of different cryocoolers in terms of mass and power required for an environmental heat impact of 2600 W

The significant variance in the results reflects the uncertainties in the technology and the development. In contrast, the efficient variant only requires an electrical power of 89 kW, which could be provided during a mission. Nevertheless, the mass increases significantly to 4820 kg due to the efficiency gain. Thus, installing in the aircraft is only possible through considerable weight losses, which can also be used by better tank insulation.
The required electrical power and mass take on large values for all cryocoolers. In comparison, with vacuum insulation, the heat flow into the tank could decrease significantly, which would allow the use of the cryocoolers again. Nevertheless, the vacuum insulation makes the tank heavier, which results in an optimum between heavy tank insulation, cryocooler and required dormancy time.
Another possibility is to have the refrigerator on board of the aircraft but only through the terminal's power supply. This way, the electrical power would not have to be taken from the engines during flight, reducing their efficiency. However, carrying this extra mass is questionable, as performance is degraded. To nevertheless take advantage of a cryocooler when stationary and thus eliminate the losses of LH2, a portable cooling unit can be used. This additional ground vehicle is connected to the aircraft to generate a cycle of LH2 and thus cool it. This system has no sensitive mass limitation and can be designed with high efficiency to keep power requirements low.

There are two additional possibilities to prevent the problem of H2 venting. Consideration of the vaporisation rate and the resulting pressure build-up can be included in the tank pressure design. Thereby, the dormancy time can be extended so that only H2 vaporises during a flight mission but does not have to be vented. However, this procedure poses a problem of snowball effect in the mass calculation of the aircraft design. Finally, a compromise must be found between maximum tank pressure and required dormancy time, as well as the loss due to venting.
A further possibility to vaporise only small amounts is the refuelling of subcooled LH2. As already examined in Section 2.1.1, the subcooling first causes sensitive heating of the fluid before vaporisation occurs. This energy conversion results in a time advantage until the heat flow has heated the subcooled fluid to a saturated state:

$$Q_{tank} = Q_{liquid} \tag{4.6}$$

$$\dot{q}_{tank} \cdot S_{tank} \cdot t = m \cdot (h_{saturated} - h_{subcooled}) \tag{4.7}$$

This simple calculation ($m_{\mathrm{LH2}} = 4500\,\mathrm{kg}$, $\dot{q}_{\mathrm{tank}} = 30\,\mathrm{W/m^2}$, $S_{\mathrm{tank}} = 87\,\mathrm{m^2}$) over the enthalpy difference results in a time interval of 4.7 h until LH2 subcooled by $\Delta T = 1\,\mathrm{K}$, at constant pressure, reaches the saturated state. The period can be scaled approximately linearly with larger subcooling. However, with this estimation, the simple calculation is based on the assumption of constant pressure in the tank. In reality, this condition is only fulfilled if the tank is constantly vented. Due to the venting, GH2 escapes from the tank, which must be evaluated as a loss. On the other hand, vaporised hydrogen cannot be used for combustion, making this estimate more realistic. This calculated time cannot be used as dormancy time because of the venting, but it offers a first indication of the enormous advantage of subcooled LH2.

The prevention of H2 venting can be delayed by the variants shown but not avoided without considerable effort. The temperature difference always creates a heat flow, which can be compensated for by using a cryocooler in case of a vacuum insulation, which leads to more flexibility in the operation of an LH2 aircraft. However, the use of a cryocooler is disproportionate when considering energy consumption.

Safe Handling of Vented Hydrogen

The venting of H2 into the environment is only possible under consideration of the safety regulations from Section 3.1. The primary explosion protection with the avoidance of a hazardous explosive atmosphere is in focus and observed. In this section, the venting of H2 is to be considered independently of the cause to verify possible variants. The options for the safe venting of H2 differ fundamentally in whether the vented H2 can still be used or is released into the atmosphere without being used.

The release of H2 without use can be done in three different ways. In the first variant, H2 is released into the environment without further treatment. For reasons of explosion protection, it must be ensured that H2 and ambient air are mixed at the transition point so that the volume fraction of H2 remains below 10 % of the LEL (0.4 %). This procedure can be implemented, for example, with a chimney on the tailplane or the ground vehicle. In the second variant, the H2 can be mixed with air in a venturi tube and then catalysed to heat in a passive catalytic converter [46]. This process originates from the automotive industry [80], see Section 2.3.1. Furthermore, in the third variant, the H2 can be burnt through a nozzle. It is ensured that no explosive atmosphere can develop in all variants because the H2 has reacted and therefore is below the LEL.

Reuse of vaporised LH2 that has to be vented can be implemented by an Auxiliary Power Unit (APU). In this case, the H2 is not vented to the environment but used to generate electrical power. The type of APU is independent, but a fuel cell is a suitable option. However, classical combustion is also possible. If necessary, the fuel cell can also be implemented as a ground unit. By the recovery line of the refuelling vehicle, the GH2 is fed.

5 Conclusion

The refuelling process was in focus as a potentially critical factor of LH2-powered aircraft, which could significantly reduce economic efficiency. An extended turnaround caused by safety issues or a longer refuelling time would reduce utilisation and increase the cost of operating an aircraft. Short-range aircraft, where the ground time has a much greater impact on utilising the aircraft, are therefore in focus and have been investigated in more detail.
For a conventional aircraft with Jet A-1, the turnaround has been investigated in terms of the time influence of the individual ground handling services. By analysing the critical path, which defines the longest time sequence of processes, the influence of refuelling was analysed. The findings of this investigation show that by parallelising the refuelling and de/boarding of passengers, the refuelling process does not lie on the critical path and has no influence on the turnaround time. Only under the condition of a half service with a low-cost airline does it become apparent that refuelling could become critical with very short turnaround times of less than 18 min.
To be able to compare the refuelling operations of Jet A-1 and LH2, the delivery of Jet A-1 has been examined for limitations. The velocity in the fuel line is limited by the static charge and the ignition hazard by a build-up of electrostatic energy. These restrictions relate to a simplified Reynolds number and velocity, limiting the volume flow and consequently the mass flow. These relationships result in an optimal hose diameter. The refuelling personnel must manually lift the deck hose to the underwing adapter, which creates a limitation in the mass. Therefore, an increase in the hose diameter is not possible. This results in two hoses which have to be connected to the aircraft instead of one for a faster refuelling process. For long-range aircraft, a second refuelling vehicle is also involved.
The safety-relevant aspects were first examined in order to be able to assess the refuelling process with LH2. The avoidance of a dangerous explosive atmosphere results as the primary measure to ensure safety. This precaution must be implemented due to the low ignition energy of 0.017 mJ since preventing a spark with this low energy is not feasible. To prevent an explosive atmosphere in the fuel system, it must have an overpressure to the environment of at least $0.2\,\mathrm{bar_g}$. The system must be designed to be technically sealed in the long term, which prevents H2 from escaping. For these reasons, parallel refuelling of LH2 with passengers on board is also possible, as with Jet A-1.
In contrast to Jet A-1, the refuelling process of LH2 requires additional process steps in order to perform the refuelling. However, the positioning and removal of the refuelling vehicle are the same as with Jet A-1. Since a human influence limits Jet A-1 because the mass of the hose must not increase, for LH2, a semi-automated system is introduced that takes over the docking manoeuvre. This type of system is already being studied and used in the automotive industry. The boom can be controlled remotely, or an autonomous system takes over the control. The next step is the connection with the aircraft, which can be realised with two different disconnect types. These disconnects differ in need for purging with an inert gas. When using a Johnston disconnect, a purging process is required to prevent oxygen from entering the system due to safety considerations. The purging process is carried out by evacuating the hose with a vacuum pump and then pressurising the hose and the connection with helium. Helium should always be used when the fluid temperature is below 80 K. All other substances, such as nitrogen, freeze at 20 K and can only be used with a process change.

The second option is to use a clean break disconnect, where no spillage occurs, and no ambient air enters. This eliminates the need for purging, which has a time advantage. Afterwards, a section of the line that has reached ambient temperature must be chilled down again. The chill down process's temporal influence was determined with the help of the heat transfer of the Nukuyiama curve. The heat capacity of the pipe is converted into heating of LH2. This conversion finally leads to evaporation and must be regarded as a loss. To keep the thermal load caused by the resulting temperature gradients in the tube at an acceptable level, only a reduced mass flow of 3 kg/s is used for refuelling during the chill down process. A recovery line is needed to discharge GH2 again in order to keep the tank pressure constant.
The actual refuelling process of LH2 is carried out with a mass flow rate of 20 kg/s. To be able to draw a comparison with Jet A-1, the respective mass flows correspond to the same energy flow of approximately 2100 MJ/s. However, this first possibility for determining the mass flow does not consider the dimensions of the refuelling hose. To be able to relate the flow regime and thus the dimensions of the hose to the mass flow, a comparison was made with the Space Shuttle refuelling process. The comparison of dimensionless parameters is essential, as they are independent of the actual size and material properties. Therefore, a comparison of Jet A-1 and LH2 in dimensional quantities is also not meaningful. The space shuttle comparison thus results in comparable limitations as for Jet A-1. However, the Reynolds number is not limited due to no electrostatic charges and is thus two orders of magnitude larger. This results in limitations in the simplified Reynolds number of $v \cdot d = 2.35$ and the velocity for short tube sections of 15.5 m/s and longer sections of 8.0 m/s. The inner diameter of the refuelling hose is 6 in, and the inner diameter of the recovery line is 5 in.
After refuelling the required amount, a purging process must be carried out again, depending on the disconnect. The line can then be disconnected, and the refuelling process ends. In summary, the previous and following processes (without refuelling) require 9 min for a Johnston disconnect and 6 min for a clean break disconnect. The time breakdown is divided into positioning and connecting (2.5 min), purging (1.5 min), chill down (1 min), refuelling (depending on volume), purging (1.5 min) and disconnecting and removing (2.5 min).

During the refuelling process, it is necessary to consider an isenthalpic flow to avoid two-phase flows. A too low tank pressure combined with a too warm temperature of LH2 creates a vapour fraction, which reduces the actual liquid mass flow and increases the refuelling time. This problem can be avoided in two ways, subcooling the liquid or increasing the tank pressure. However, increasing the tank pressure is limited due to the tank design, so subcooling LH2 to 19 K after the storage tank was favoured. The subcooling causes a non-equilibrium, as the vapour pressure curve is a function of temperature.

The implementation of the fuelling process at the airport was worked out with two possible infrastructures. The principle of not causing direct losses by venting H2 and helium has been followed. For low quantities of LH2 per year, which could apply for a transitional phase, a refuelling truck is a solution that entails low investment costs. The refuelling truck is a simple system with a low probability of failure. With additional systems on the truck, such as a compressor and an additional gas storage tank where vaporised H2 and helium can be collected and recycled. The refuelling truck has a volume of 70 m^3 LH2, with which a short-range LH2 aircraft can be fully refuelled. Due to the limitation of the volume of a refuelling truck, a pipeline system is more advisable for long-range refuelling aircraft. A dispenser can also refuel long-range aircraft regardless of the volume and is the second option. The boom of the dispenser and refuelling truck can be constructed like a deicing vehicle, which is already semi-automated.

The different refuelling methods and their implementation result in a fuel price increase of 0.45 % to 13.62 %. The price increase differs according to the refuelling process, i.e. with purging or without, the ground vehicle used, as well as the feeding method and the use of a recycling process. As a summary, it can be said that refuelling with LH2 is possible, and the refuelling time is in the same order of magnitude as Jet A-1. For small refuelling quantities for short ranges (500 NM), there is an advantage for Jet A-1 because additional procedures are needed with LH2. On the other hand, there is an advantage for LH2 for larger refuelling quantities, especially for short-medium-range aircraft, because, unlike Jet A-1, two feeding hoses are not required for refuelling.

Based on the findings of the refuelling process and the thermodynamic properties of LH2, three calculation methods have been derived to determine the tank volume of the aircraft. The methods differ in the density used, which determines the volume for a given mass. This results in a conservative method (1), in which a saturated liquid at the maximum pressure of the tank determines the density. The second optimistic method determines the density of a saturated liquid at the minimum pressure (2) of the tank. This methodology is used in space programmes such as the Space Shuttle. The third method, which uses actual tank conditions to determine density, is also the most accurate. A subcooled liquid, which entails densification and increased dormancy time, can be interpreted as the practical method (3). In this method, the conditions apply when flowing into the tank and are thus essentially dependent on the refuelling and the previous handling of LH2. SpaceX uses this method for the Falcon 9 with liquid oxygen. Method 1 and Method 2 do not require detailed considerations to be applicable for aircraft design. However, for the meaningful use of Method 3, non-equilibrium thermodynamic tank modelling must be used to obtain the correct conclusions.

The delivery of LH2 from the tank to the engine requires a low-pressure pump, a high-pressure pump and a heat exchanger to inject LH2 into the combustion chamber at the proper boundary conditions. With this fuel architecture, only a small amount of electrical power is required for the pumps. The waste heat from the propulsion unit can be used for vaporisation. However, gaseous delivery from the tank to the engine is not practical, as the compressibility of GH2 requires much more electrical power than liquid feeding. The waste heat from the exhaust gas jet is not fully utilised. However, for the operation of fuel cells, gaseous delivery is also possible because the pressure level is much lower.

For pumping, there are two ways to achieve a single-phase flow. Thus, the Net Positive Suction Head (NPSH) value of the pump sets the boundary conditions in the tank for the pressure level in combination with the liquid temperature. For a cavitation-free pump, a positive NPSH value must be present at the pump inlet as used in rocket engines. The positive NPSH value corresponds to an overpressure to the vapour pressure curve, which is dependent on the temperature and can be referred to as the level of subcooling. Refuelling with subcooled LH2 is helpful due to the increase in density, the dormancy time and the lower pressure level because the vapour pressure decreases. Therefore, the pressure in the tank must be above the saturation pressure during the entire flight duration, whereby the tank system and the pressurisation system, respectively, are dimensioned. The pressurisation system can be a vaporiser or an inert gas, as used in aeronautics. For the aircraft design, an additional mass must be taken into account and an increase in the maximum tank pressure to maintain the necessary condition at the end of the flight. This effect is problematic because the liquid temperature rises due to the environmental heat impact and the pressurisation and thus amplifies each other.

The second option is to use Zero-NSPH pumps, which can pump a saturated liquid. However, the problem with this application is that cavitation and two-phase flow occur in the pump inlet. The long-term consequences, such as cavitation erosion and damage to the pump, could occur, especially with many flight cycles in aviation. In addition, pressure oscillations and unsteady flows can occur, which influence a constant engine thrust. Nevertheless, the use of Zero-NSPH pumps has a far-reaching impact on aircraft design, as no pressurisation system is required. Therefore, answering this question is essential which should be done in future work.

In order to prevent H2 from being vented, a refrigerator can be used in principle. This avoids evaporation and consequently a pressure increase in the tank. However, implementing a cryocooler in an aircraft is only possible to a limited extent since the energy requirement and the mass of this system are considered too high. Only with very strong insulation, the installation in the aircraft is conceivable. However, it is possible to use an external mobile cooling device to prevent evaporation on ground.
Nevertheless, if the tank pressure rises to the maximum and venting can no longer be prevented, the H2 must be removed, taking into account the safety-relevant aspects. The H2 can be reused by a fuel cell to generate electrical power. If this is not possible, the H2 can be catalysed by a catalyst to avoid an explosive atmosphere. Other options for safe venting include combustion or mixing with air in a venturi below the explosion limits.

A possible application of an LH2 aircraft, in which the return flight is carried out without refuelling and no ground vehicles are available for cooling, has been worked out. In this case, the range of the aircraft decreases linearly with the ground time. In the case of a ban on night flights and a ground time of 6 h, this results in a 10 % reduction in range for an aircraft with 180 passengers and foam insulation of the tank.

In conclusion, it can be said that the refuelling procedure with LH2 is feasible. The refuelling procedure complies with the applicable safety standards and hence has no impact on the turnaround. A time comparison with Jet A-1 shows that refuelling with LH2 in most cases takes less time, as other boundary conditions apply to the refuelling rate. The turnaround at the airport can be performed by a fuel truck or a pipeline dispenser system without generating direct losses. Understanding the thermodynamic properties leads to three calculation methods of the tank volume, the choice of the pumping system and the influence of an environmental heat impact.

For the transition phase, in which Jet A-1 and LH2 aircraft are used, combining a Hybrid Hydrogen aircraft is also conceivable. In this outlook, the advantages of both fuels are used to design an environmentally friendly aircraft that flies the mission with LH2 as fuel and keeps the available space in the wing for Jet A-1 to carry out the reserve mission. This allows the LH2 tank to be smaller and the mass of Jet A-1 in the wing reduces the wing root bending moment, which reduces the structural mass of the wing. This combination enhances aircraft performance and lowers costs. However, an engine has to be developed that can use both fuels without significant loss of efficiency.

References

[1] RICHTLINIE 1999/92/EG DES EUROPÄISCHEN PARLAMENTS UND DES RATES vom 16. Dezember 1999 über Mindestvorschriften zur Verbesserung des Gesundheitsschutzes und der Sicherheit der Arbeitnehmer, die durch explosionsfähige Atmosphären gefährdet werden können (Fünfzehnte Einzelrichtlinie im Sinne von Artikel 16 Absatz 1 der Richtlinie 89/391/EWG).

[2] RICHTLINIE 2009/104/EG DES EUROPÄISCHEN PARLAMENTS UND DES RATES vom 16. September 2009 über Mindestvorschriften für Sicherheit und Gesundheitsschutz bei Benutzung von Arbeitsmitteln durch Arbeitnehmer bei der Arbeit (Zweite Einzelrichtlinie im Sinne des Artikels 16 Absatz 1 der Richtlinie 89/391/EWG).

[3] RICHTLINIE 2014/34/EU DES EUROPÄISCHEN PARLAMENTS UND DES RATES vom 26. Februar 2014 zur Harmonisierung der Rechtsvorschriften der Mitgliedstaaten für Geräte und Schutzsysteme zur bestimmungsgemäßen Verwendung in explosionsgefährdeten Bereichen (Neufassung).

[4] Technische Regeln für Betriebssicherheit/ Gefahrstoffe TRBS 2151 Teil 1/ TRGS 721 Gefährliche explosionsfähige Atmosphäre - Beurteilung der Explosionsgefährdung, 2006.

[5] Verordnung zum Schutz vor Gefahrstoffen (Gefahrstoffverordnung - GefStoffV), 2010.

[6] Technische Regeln für Betriebssicherheit/ Gefahrstoffe TRBS 2152 Teil 2/ TRGS 722 Vermeidung oder Einschränkung gefährlicher explosionsfähiger Atmosphäre, 2012.

[7] Verordnung über Sicherheit und Gesundheitsschutz bei der Verwendung von Arbeitsmitteln (Betriebssicherheitsverordnung - BetrSichV), 2015.

[8] Technische Regeln für Betriebssicherheit/ Gefahrstoffe TRBS 3151/ TRGS 751 Vermeidung von Brand-, Explosions- und Druckgefährdungen an Tankstellen und Gasfüllanlagen zur Befüllung von Landfahrzeugen, 2020.

[9] Technische Regeln für Gefahrstoffe TRGS 720 Gefährliche explosionsfähige Gemische - Allgemeines, 2020.

[10] Airbus Deutschland GmbH. Liquid Hydrogen Fuelled Aircraft – System Analysis. Technical report, Cryoplane, 2013.

[11] Airbus S.A.S. A320 Aircraft Characteristics - Airport and Maintenance Planning, Apr. 2020.

[12] American Petroleum Institure. Protection Against Ignitions Arising Out of Static, Lightning, and Stray Currents. API RP 2003 6TH ED, 1998.

[13] G. Arnold and J. Wolf. Liquid Hydrogen for Automotive Application Next Generation Fuel for FC and ICE Vehicles. *TEION KOGAKU (Journal of Cryogenics and Superconductivity Society of Japan)*, 40(6):221–230, 2005.

[14] H. D. Baehr and S. Kabelac. *Thermodynamik: Grundlagen und technische Anwendungen*. Springer Vieweg, Berlin, Heidelberg, 16 edition, 2016.

[15] J. H. Baik and A. T-Raissi. R&d processes for increasing density of cryogenic propellants at fsec. *Cryogenics*, 44(6):451 – 458, 2004. 2003 Space Cryogenics Workshop.

[16] A. Bain. Nasa space program experience in hydrogen transportation and handling. *International Journal of Hydrogen Energy*, 1(2):173 – 188, 1976.

[17] A. Bain. *Sourcebook for Hydrogen Applications*. TISEC, 1998.

[18] R. F. Barron and G. F. Nellis. *Cryogenic Heat Transfer*. CRC Press, second edition, 2016.

[19] T. L. Bergman and A. S. Lavine. *Fundamentals of heat and mass transfer*. John Wiley & Sons, Inc., 2017.

[20] BMW Group. BMW Hydrogen 7, 2006.

[21] T. D. Bostock and R. G. Scurlock. *Low-Loss Storage and Handling of Cryogenic Liquids: the Application of Cryogenic Fluid Dynamics*. International Cryogenics Monograph Series. Springer, Cham, second edition, 2019.

[22] H. Brechna, W. A. Tuttle, R. G. Stewart, J. E. Jensen, U. S. A. E. Commission., and B. N. Laboratory. *Brookhaven National Laboratory selected cryogenic data notebook*. Brookhaven National Laboratory, [New York], 1980.

[23] J. A. Brennan, E. G. Brentari, R. V. Smith, and W. G. Steward. Cooldown of cryogenic transfer lines. *NASA Contractor Report 81338*, 1966.

[24] E. G. Brentari, P. J. Giarratano, and R. V. Smith. Boiling Heat Transfer for Oxygen, Nitrogen, Hydrogen, and Helium. *National Bureau of Standards Technical Note 316*, 1965.

[25] G. D. Brewer. LH2 Airport Requirments Study. *NASA Contractor Report 2700*, 1976.

[26] G. D. Brewer. *Hydrogen Aircraft Technology*. CRC Press, 1991.

[27] G. D. Brewer, R. E. Morris, R. H. Lange, and J. W. Moore. Volume 2 Final Report: Study of the application of hydrogen fuel to long-range subsonic transport aircraft. *NASA Contractor Report 132559*, 1975.

[28] G. D. Brewer, R. E. Morris, D. G. W., E. F. Versaw, G. R. Cunnington jr., J. C. Riple, C. F. Baerst, and G. Garmong. Study of Fuel System for LH2-Fueled Subsonic Transport Aircraft. NASA Contractor Report 145369, 1978. Volume 1.

[29] G. D. Brewer, R. E. Morris, D. G. W., E. F. Versaw, G. R. Cunnington jr., J. C. Riple, C. F. Baerst, and G. Garmong. Study of Fuel System for LH2-Fueled Subsonic Transport Aircraft. NASA Contractor Report 145369, 1978. Volume 2.

[30] British Cryogenics Council. *Cryogenics Safety Manual: A guide to good practice*. Butterworth-Heinemann, 1991.

[31] Bundesanstalt für Arbeitsschutz und Arbeitsmedizin (BAuA). Gefährdungsbeurteilung bei physischer Belastung - die neuen Leitmerkmalmethoden (LMM), 2019.

[32] A. Burgunder, A. Martinez, and S. Tamhankar. Current Status of Hydrogen Liquefaction Costs. *DOE Hydrogen and Fuel Cells Program Record*, 2019.

[33] G. Caine, L. Schafer, and D. Burgeson. Pumping of Liquid Hydrogen. In D. K. Timmerhaus, editor, *Advances in Cryogenic Engineering*, volume 4, 1958.

[34] U. Cardella, L. Decker, and H. Klein. Roadmap to economically viable hydrogen liquefaction. *International Journal of Hydrogen Energy*, 42(19):13329–13338, 2017. Special Issue on The 21st World Hydrogen Energy Conference (WHEC 2016), 13-16 June 2016, Zaragoza, Spain.

[35] Y. A. Cengel and A. J. Ghajar. *Heat and mass transfer: fundamentals and application*. McGraw-Hill Education, 2020.

[36] L. Collins. A wake-up call on green hydrogen: the amount of wind and solar needed is immense. https://www.rechargenews.com/transition/a-wake-up-call-on-green-hydrogen-the-amount-of-wind-and-solar-needed-is-immense/2-1-776481. Accessed: 16.03.2021.

[37] A. Colozza and L. Kohout. Hydrogen Storage for Aircraft Applications Overview. *NASA Contractor Report 2002-211867*, 2002.

[38] Coordinating Research Council. *Handbook of Aviation Fuel Properties*. CRC Report No. 530, 1983.

[39] N. Corner. Was ist Siedekrise – Kritischer Wärmestrom - Definition. https://www.thermal-engineering.org/de/was-ist-siedekrise-kritischer-warmestrom-definition/. Accessed: 29.11.2020.

[40] M. J. Daigle, V. N. Smelyanskiy, J. Boschee, and M. Foygel. Temperature Stratification in a Cryogenic Fuel Tank. *Journal of Thermophysics and Heat Transfer*, 27(1):116–126, 2013.

[41] Daimler AG. Kooperation mit Linde bei Flüssigwasserstoff-Betankungstechnologie. https://www.daimler.com/investoren/berichte-news/finanznachrichten/20201210-betankung-fluessigwasserstoff-lkw.html. Accessed: 14.01.2021.

[42] Demaco Holland B.V. Product Sheet: Vacuum Insulated Flexible, 2021.

[43] Demaco Holland B.V. Product Sheet: Vacuum Insulated Piping, 2021.

[44] D. Deserranno, M. Zagarola, X. Li, and S. Mustafi. Optimization of a Brayton cryocooler for ZBO liquid hydrogen storage in space. *Cryogenics*, 64:172–181, 2014.

[45] J. F. DiStefano and G. H. Caine. Cavitation Characteristics of Tank-Mounted Cryogenuc Pumps and their predicted Performance unter reduced Gravity. In D. K. Timmerhaus, editor, *Advances in Cryogenic Engineering*, volume 7, 1961.

[46] P. Drinovac. *Experimentelle Untersuchungen zu katalytischen Wasserstoffrekombinatoren für Leichtwasserreaktoren*. PhD thesis, Rheinisch-Westfälischen Technischen Hochschule Aachen, 2006.

[47] Eaton Aerospace Group. Carter® underwing refueling nozzle model 60427, 2013.

[48] F. J. Edeskuty and W. F. Stewart. *Safety in the Handling of Cryogenic Fluid*. Springer Science, 1996.

[49] Erhard GmbH & Co. KG. Regelventile, 2011.

[50] EU-OPS 1. Commission regulation no 859/2008, 2008.

[51] J. Evler, E. Asadi, H. Preis, and H. Fricke. Stochastic Control of Turnarounds at HUB-Airports. *Eighth SESAR Innovation Days, 3rd – 7th December 2018*, 2008.

[52] M. M. Fazah. STS Propellant Densification Feasibilty Study Data Book. *NASA Technical Memorandum 108467*, 1994.

[53] T. Fernholz. The "super chill" reason SpaceX keeps aborting launches. https://qz.com/627430/the-super-chill-reason-spacex-keeps-aborting-launches/. Accessed: 11.01.2021.

[54] J. Fesmire and S. Augustnynowicz. Thermal Performance of Cryogenic Piping Multilayer Insulation in Actual Field Installations. *Cryogenics 2002*, 2002.

[55] Festo AG & Co. KG. BionicSoftArm. https://www.festo.com/group/en/cms/13527.htm. Accessed: 13.12.2020.

[56] J. Feyrer, J. Jepsen, and T. Schulz. Wasserstoff und dessen Gefahren: Ein Leitfaden für Feuerwehren. *Arbeitsgemeinschaft der Leiter der Berufsfeuerwehren*, 2008.

[57] T. Flynn. *Cryogenic Engineering, Revised and Expanded*. CRC Press, second edition, 2004.

[58] J. Foust. NASA approves "load-and-go" fueling for SpaceX commercial crew launches. https://spacenews.com/nasa-approves-load-and-go-fueling-for-spacex-commercial-crew-launches/. Accessed: 11.01.2021.

[59] H. Fricke and M. Schultz. Improving Aircraft Turn Around Reliability. *ICRAT 3rd International Conference on Research and Air Transportation*, 2009.

[60] P. Gerstl. Solutions for the LH2 Supply Chain. *International Hydrogen Forum 2019*, 2019.

[61] P. J. Giarratano and R. V. Smith. Comparative study of forced convection boiling heat transfer correlations for cryogenic fluids. *Cryogenic Engineering Conference*, 1965.

[62] V. Grewe, K. Dahlmann, J. Flink, C. Frömming, R. Ghosh, K. Gierens, R. Heller, J. Hendricks, P. Jöckel, S. Kaufmann, K. Kölker, F. Linke, T. Luchkova, B. Lührs, J. Van Manen, S. Matthes, A. Minikin, M. Niklaß, M. Plohr, M. Righi, S. Rosanka, A. Schmitt, U. Schumann, I. Terekhov, S. Unterstrasser, M. Vázquez-Navarro, C. Voigt, K. Wicke, H. Yamashita, A. Zahn, and H. Ziereis. Mitigating the climate impact from aviation: Achievements and results of the dlr wecare project. *Aerospace*, 4(3), 2017.

[63] J. F. Gülich. *Kreiselpumpen: Handbuch für Entwicklung, Anlagenplanung und Betrieb*. SpringerLink. Bücher. Springer Vieweg, Berlin, Heidelberg, 4., aktual. u. erw. aufl. 2013 edition, 2013.

[64] J. Hartwig, H. Hu, J. Styborski, and J. Chung. Comparison of cryogenic flow boiling in liquid nitrogen and liquid hydrogen chilldown experiments. *International Journal of Heat and Mass Transfer*, 88:662 – 673, 2015.

[65] R. C. Hendricks, R. W. Graham, Y. Y. Hsu, and R. Friedman. Experimental heat transfer and pressure drop of liquid hydrogen flowing through a heated tube. *NASA Technical Note D-765*, 1961.

[66] W. Hettinger, F. Michel, P. Ott, and F. Theissen. Refueling equipment for liquid hydrogen vehicles. *International Journal of Hydrogen Energy*, 23(10):943 – 947, 1998.

[67] M. Hirscher. *Handbook of Hydrogen Storage*. John Wiley & Sons, 2010.

[68] J. Hord. Selected topics on hydrogen fuel. *National Bureau of Standards NBSIR 75-803*, 1975.

[69] T. Horstmeier and F. de Haan. Influence of ground handling on turn round time of new large aircraft. *Aircraft Engineering and Aerospace Technology*, 73(3):266–271, Jan. 2001.

[70] D. K. Huzel and D. H. Huang. *Design of Liquid Propellant Rocket Engines*. NASA SP-125, 1971.

[71] D. K. Huzel, D. H. Huang, and H. Arbit. *Modern Engineering for Design of Liquid-Propellant Rocket Engines*. AIAA, Washington, DC, 1992.

[72] ISO/PAS 15594. Airport hydrogen fuelling facility operations, 2004.

[73] S. Jallais. Pre-normative REsearch for Safe use of Liquid HYdrogen (PRESLHY). *Fuel Cells and Hydrogen Joint Undertaking*, 2018.

[74] M. Janić. Greening commercial air transportation by using liquid hydrogen (LH2) as a fuel. *International Journal of Hydrogen Energy*, 39(29):16426–16441, 2014.

[75] L. Jones, C. Wuschke, and T. Fahidy. Model of a cryogenic liquid-hydrogen pipeline for an airport ground distribution system. *International Journal of Hydrogen Energy*, 8(8):623 – 630, 1983.

[76] K. Jousten. *Handbuch Vakuumtechnik*. Springer Reference Technik. Springer Vieweg, Wiesbaden, 12 edition, 2018.

[77] A. Kazda and R. E. Caves. *Airport Design and Operation*. Emerald, third edition edition, 2015.

[78] KGW ISOTHERM. Kaltgas - Low temperature cooling systemfor cooling applications from max. +100°C (212°F) up to -180°C (-292°F), 2019.

[79] M. Kida, Y. Kikuchci, O. Takahashi, and I. Michiyoshi. Pool-boiling heat transfer in liquid nitrogen. *Journal of Nuclear Science and Technology*, 18(7):501–513, 1981.

[80] M. Klell, H. Eichlseder, and A. Trattner. *Wasserstoff in der Fahrzeugtechnik: Erzeugung, Speicherung, Anwendung*. ATZ/MTZ-Fachbuch. Springer Vieweg, Wiesbaden, 4. aufl. 2018 edition, 2018.

[81] J. W. Leachman, R. T. Jacobsen, E. W. Lemmon, and S. G. Penoncello. *Thermodynamic Properties of Cryogenic Fluids*. International Cryogenics Monograph Series. Springer, Cham, 2nd ed. 2017 edition, 2017. On.

[82] P. Lein. *Brandschutztechnische Anlagen betreiben und instandhalten*. Springer Vieweg, Wiesbaden, 2019.

[83] E. W. Lemmon, , I. H. Bell, M. L. Huber, and M. O. McLinden. NIST Standard Reference Database 23: Reference Fluid Thermodynamic and Transport Properties-REFPROP, Version 10.0, National Institute of Standards and Technology, 2018.

[84] J. Lienhard and L. Witte. An historical review of the hydrodynamic theory of boiling. *Reviews in Chemical Engineering*, 3(3-4):187 – 280, 1985.

[85] C. S. Lin, N. T. Van Dresar, and M. M. Hasan. Pressure control analysis of cryogenic storage systems. *Journal of Propulsion and Power*, 20(3):480–485, 2004.

[86] Linde AG. Linde Kupplung und Betankungssystem: Leistung und Meßergebnisse, 2003.

[87] Lockheed-Georgia Company. Main Propellant Tank Pressurization System Study and Test Program - Design Handbook. Final Report ER-5296, 1961. Volume 3.

[88] E. D. Marquardt, J. P. Le, and R. Radebaugh. Cryogenic Material Properties Database. *11th International Cryocooler Conference*, 2000.

[89] Marshall Space Flight Center Laboratories. Technical Information Summary AS-501 Apollo Saturn V Flight Vehicle, 1969.

[90] R. D. McCarty, J. Hord, and R. H. M. Selected properties of hydrogen. *National Bureau of Standards Monograph 168*, 1981.

[91] McKinsey & Company for the Clean Sky 2 JU and FuelCells and Hydrogen 2 JU. Hydrogen-powered aviation: A fact-based study of hydrogen technology, economics, and climate impact by 2050, 2020.

[92] E. Messerschmid and S. Fasoulas. *Raumfahrtsysteme*. Springer Vieweg, 2017.

[93] Mettler-Toledo GmbH. GPro 500 TDL - Kompaktes Spektrometermit vielseitigen Prozessadaptionen, 2020.

[94] F. Michel. Hydrogen vehicles and infrastructure in view of european licensing. *European Integrated Hydrogen Project - Phase II*, 2004.

[95] M. G. Millis, R. T. Tornabene, J. M. Jurns, M. D. Guynn, T. M. Tomsik, and T. J. V. Overbe. Hydrogen Fuel System Design Trades for High-Altitude Long-Endurance Remotely-Operated Aircraft. *NASA Technical Memorandum 2009-215521*, 2009.

[96] M. Mirza. Economic Impact of Airplane Turn-Times. *Boeing Aero Magazine*, 2008.

[97] S. Mustafi, E. Canavan, W. Johnson, B. Kutter, and J. Shull. Subcooling cryogenic propellants for long duration space exploration. *AIAA SPACE 2009 Conference & Exposition*, 2009.

[98] NASA Lewis Research Center. Hydrogen safety manuel. *NASA Technical Memorandum X-52454*, 1968.

[99] National Fire Protection Association. Standard for Aircraft Fuel Servicing. *NFPA 407*, 2001.

[100] National Fire Protection Association. Standard for the Storage, Use, and Handling of Compressed Gases and Cryogenic Fluids in Portable and Stationary Containers, Cylinders, and Tanks. *NFPA 55*, 2005.

[101] K. Nguyen, T. E. Knowles, W. D. Greene, and T. M. Tomsik. Propellant densification for launch vehicles: Simulation and testing. *38th AIAA/ASME/SAE/ASEE Joint Propulsion Conference & Exhibit*, 2002.

[102] J. K. Novak. Cooldown flow rate limits imposed by thermal stresses in liquid hydrogen or nitrogen pipelines. In K. D. Timmerhaus, editor, *Advances in Cryogenic Engineering, Volume 15*. Springer, 1969.

[103] Occupational Safety and Health Administration. Safety Standard for Explosives, Propellants, and Pyrotechnics. *NASA-STD-8719.12*, 2018.

[104] H. Oertel, M. Böhle, and T. Reviol. *Strömungsmechanik: für Ingenieure und Naturwissenschaftler*. Springer Vieweg, Wiesbaden, 2015.

[105] Office of Safety and Mission Assurance. Safety standard for hydrogen and hydrogen systems. *NASA Technical Memorandum NSS 1740.16*, 1997.

[106] B. Oreschko, M. Schultz, J. Elflein, and H. Fricke. Significant Turnaround Process Variations due to Airport Characteristics. *Air Transport & Operations Symposium 2010*, 2010.

[107] V. V. Osipov, M. J. Daigle, C. B. Muratov, M. Foygel, V. N. Smelyanskiy, and M. D. Watson. Dynamical model of rocket propellant loading with liquid hydrogen. *Journal of Spacecraft and Rockets*, 48(6):987–998, 2011.

[108] Parker Hannifin Corporation. Parker Industrial Hose Gold Label® Aircraft Fueling Hose, 2013.

[109] K. Pehr, P. Sauermann, O. Traeger, and M. Bracha. Liquid hydrogen for motor vehicles - the world's first public LH2 filling station. *International Journal of Hydrogen Energy 26*, 2001.

[110] W. Peschka. *Flüssiger Wasserstoff als Energieträger*. Springer-Verlag Wien, 1984.

[111] W. Peschka. The status of handling and storage techniques for liquid hydrogen in motor vehicles. *International Journal of Hydrogen Energy*, 12(11):753 – 764, 1987.

[112] W. Peschka. *Liquid Hydrogen Fuel of the Future*. Springer Wien New York, 1992.

[113] Pfeiffer Vacuum GmbH. Heptadry™, die trockene schraubenpumpe, 2016.

[114] E. Rame, J. W. Hartwig, and J. B. McQuillen. Flow visualization of liquid hydrogen line chill down tests. *AIAA 52nd Aerospace Sciences Meeting*, 2014.

[115] E. Ring. *Rocket Propellant and Pressurization Systems*. Prentice-Hall space technology series. Prentice-Hall, Englewood Cliffs, N.J., 1964. Fakultätsbibliothek Architektur und Stadtplanun.

[116] Rocketdyne. Space Shuttle Main Engine Orientation, 1998.

[117] H. M. Roder. Liquid Densities of Oxygen, Nitrogen,Argon and Parahydrogen. *National Bureau of Standards Technical Note 361*, 1974.

[118] ROHR Spezialfahrzeuge GmbH. AHD LF / HF HYDRANT DISPENSER, 2020.

[119] R. S. Ruggeri and R. D. Moore. Method for prediction of pump caviation perofrmance for various liquids, liquid temperatures, and rotaive speeds. *NASA Technical Note D-5292*, 1969.

[120] SAE International. *Compressed Hydrogen Surface Vehicle Fueling Connection Devices*. J2600, 2015.

[121] SAE International. *Fueling Protocols for Light Duty Gaseous Hydrogen Surface Vehicles*. J2601, 2020.

[122] S. Sanz de Vicente. Ground Handling Simulation with CAST. Master's thesis, Hamburg University of Applied Sciences, 2010.

[123] A. Schlegel. *Bodenabfertigungsprozesse im Luftverkehr*. Gabler Verlag, 2010. Eine statistische Analyse am Beispiel der Deutschen Lufthansa AG am Flughafen Frankfurt/Main.

[124] M. Schmidt. *Ground-Operational Assessment of Novel Aircraft Cabin Configurations*. PhD thesis, Technical University of Munich, 2018.

[125] M. Schmidt, M. Engelmann, T. Brügge-Zobel, M. Hornung, and M. Glas. Paxelerate - an open source passenger flow simulation framework for advanced aircraft cabin layouts. In *54th AIAA Aerospace Sciences Meeting*, 2016.

[126] T. Schwanekamp, C. Ludwig, and M. Sippel. *Cryogenic Propellant Tank and Feedline Design Studies in the Framework of the CHATT Project*. 2014.

[127] M. J. Sefain. *Hydrogen Aircraft Concepts & Ground Support*. PhD thesis, Cranfield University, 2000.

[128] A. Sera. Jet Fuel Pipelines And Storage Require Special Operation, Maintenance Considerations. *Pipeline & Gas Journal*, 236(12), 2009.

[129] D. Silberhorn, G. Atanasov, J.-N. Walther, and T. Zill. Assessment of Hydrogen Fuel Tank Integration at Aircraft Level. *Deutscher Luft- und Raumfahrtkongress 2019*, 2019.

[130] D. Silberhorn, J. Hartmann, N. M. Dzikus, G. Atanasov, T. Zill, U. Brand, J. C. G. Trillos, M. Oswald, T. Vogt, D. Wilken, and W. Grimme. The Air-Vehicle as a Complex System of Air Transport Energy Systems. *AIAA AVIATION 2020 FORUM*, 2020.

[131] A. J. Sobin and W. R. Bissell. Turbopump systems for liquid rocket engines. *NASA Special Publication 8107*, 1974.

[132] V. Sosounov and V. Orlov. Experimental Turbofan Using Liquid Hydrogenand Liquid Natural Gas as Fuel. *AIAA - 26th Joint Propulsion Conference*, 1990.

[133] Space Is Kind Of Cool. Why the Falcon 9 Uses Subcooled Liquid Oxygen. https://www.youtube.com/watch?v=gHwZk_qEeAY. Accessed: 12.01.2021.

[134] Space Program Operations Contract. Shuttle crew operations manuel. United Space Alliance, 2008.

[135] D. Steiner and J. Taborek. Flow boiling heat transfer in vertical tubes correlated by an asymptotic model. *Heat Transfer Engineering*, 13(2):43–69, 1992.

[136] W. G. Steward, R. V. Smith, and J. A. Brennan. Cooldown transients in cryogenic transfer lines. In K. D. Timmerhaus, editor, *Advances in Cryogenic Engineering, Volume 15*. Springer, 1969.

[137] W. F. Stewart. Refueling considerations for liquid-hydrogen fueled vehicles. *5th Intersociety Cryogenics Symposium*, 1984.

[138] H. P. Stinson and R. J. Strickland. Experimental findings from zero-tank net positive suction head operation of the j-2 hydrogen pump. *NASA Technical Note D-6824*, 1972.

[139] K. Stolzenburg, D. Berstad, L. Decker, A. Elliott, C. Haberstroh, C. Hatto, M. Klaus, N. Mortimer, R. Mubbala, O. Mwabonje, P. Nekså, H. Quack, J. Rix, I. Seemann, and H. Walnum. Efficient Liquefaction of Hydrogen: Results of the IDEALHY Project. *XXth Energie Symposium*, 2013.

[140] R. O. Stroman, M. W. Schuette, K. Swider-Lyons, J. A. Rodgers, and D. J. Edwards. Liquid hydrogen fuel system design and demonstration in a small long endurance air vehicle. *International Journal of Hydrogen Energy*, 39(21):11279 – 11290, 2014.

[141] D. E. Stuck. Liquid rocket disconnects, couplings, fittings, fixed joints, and seals. *NASA Special Publication 8119*, 1976.

[142] D. Surek and S. Stempin. *Angewandte Strömungsmechanik*. Vieweg+Teubner, 2007.

[143] G. P. Sutton and O. Biblarz, editors. *Rocket Propulsion Elements*. A Wiley Interscience publication. John Wiley & Sons, New York, 7. ed. edition, 2001. Includes bibliographical references and index.

[144] S. Tamhankar. Terminal Operations for Tube Trailer and Liquid Tanker Filling: Status, Challenges and R&D Needs. *DOE Hydrogen Transmission and Distribution Workshop*, 2014.

[145] H. Tatsumoto, Y. Shirai, M. Shiotsu, K. Hata, Y. Naruo, H. Kobayashi, Y. Inatani, and K. Kinoshita. Forced convection heat transfer of subcooled liquid hydrogen in horizontal tubes. *AIP Conference Proceedings*, 1434(1):747–754, 2012.

[146] Tesla. Charger prototype finding its way to Model S. https://www.youtube.com/watch?v=uMM0lRfX6YI. Accessed: 13.12.2020.

[147] The Boeing Commercial Airplane Company. An Exploratory Study to Determine the Integrated Technological Air Tranportation Sytem Ground Requirements of Liquid-Hydrogen-Fueled Subsonic, Long-Haul Civil Air Transports. *NASA Contrator Report 2699*, 1976.

[148] J. Thorbeck. DOC-Assessment Method. https://www.fzt.haw-hamburg.de/pers/Scholz/Aero/TU-Berlin_DOC-Method_with_remarks_13-09-19.pdf. Accessed: 18.03.2021.

[149] H.-R. Tränkler and L. M. Reindl. *Sensortechnik: Handbuch für Praxis und Wissenschaft*. Springer Vieweg, Berlin, Heidelberg, 2., völlig neu bearb. aufl. 2014 edition, 2014.

[150] U.S. Geological Survey. Mineral commodity summaries 2020, 2020.

[151] Verein Deutscher Ingenieure. *VDI-Wärmeatlas*. Springer Vieweg, 2013.

[152] D. Verstraete. *The Potential of Liquid Hydrogen for long range aircraft propulsion*. PhD thesis, Cranfield Unversity, 2009.

[153] D. Verstraete, P. Hendrick, P. Pilidis, and K. Ramsden. Hydrogen fuel tanks for subsonic transport aircraft. *International Journal of Hydrogen Energy*, 35(20):11085 – 11098, 2010. Hyceltec 2009 Conference.

[154] M. B. Vietze. *Gekoppelte aerothermodynamische und strukturmechanische Optimierung kryogener Raketenoberstufen*. PhD thesis, Universität der Bundeswehr München, 2018.

[155] L. Wang, Y. Li, F. Zhang, F. Xie, and Y. Ma. Correlations for calculating heat transfer of hydrogen pool boiling. *International Journal of Hydrogen Energy*, 41(38), 2016.

[156] F.-J. Wetzel. Improved handling of liquid hydrogen at filling stations: Review of six years' experience. *International Journal of Hydrogen Energy*, 23(5):339–348, 1998.

[157] J. Wilken, M. T. Scelzo, and L. Peveroni. System Study of Slush Propellants for Future European Launch Vehicles. *Space Propulsion 2018*, 2018.

[158] C. Winnefeld, T. Kadyk, B. Bensmann, U. Krewer, and R. Hanke-Rauschenbach. Modelling and designing cryogenic hydrogen tanks for future aircraft applications. *Energies*, 11:105, 2018.

[159] J. Wolf. Liquid hydrogen technology for vehicles. In *Handbook of Fuel Cells*. John Wiley & Sons, 2010.

[160] World Economic Forum. Clean Skies for Tomorrow: Sustainable Aviation Fuels as a Pathway to Net-Zero Aviation, Nov. 2020.

[161] R. Wurster and U. Schmidtchen. Wasserstoff-Sicherheits-Kompendium. Technical report, Deutschen Wasserstoff- und Brennstoffzellenverband (DWV), 2011.

[162] K. Yuan, Y. Ji, and J. Chung. Cryogenic chilldown process under low flow rates. *International Journal of Heat and Mass Transfer*, 50(19):4011 – 4022, 2007.

[163] N. Zuber. *Hydrodynamic Aspects Of Boiling Heat Transfer*. PhD thesis, University of California, 1959.

Statutory declaration and copyright for student works[1]

Herewith I, Jonas Mangold, 2940456, Karl-Stirner-Str. 17, 73494 Rosenberg, grant the University of Stuttgart, Institute of Aircraft Design, a free, temporally and spatially unlimited, simple right of use for the master's thesis or other student work with the title

Economical assessment of hydrogen short-range aircraft with the focus on the turnaround procedure

and the results of this work. I declare to have written this work independently and to have complied in the preparation of this work with the relevant terms, in particular with the copyright protection of third-party contributions. As far as my work contains external contributions (e.g. pictures, drawings, text passages), I declare that these contributions are marked as such (e.g. quotation, indication of source) and that I have obtained any necessary author's consent for the use of these contributions in my work. In the event of infringement of the rights of third parties through my work, I agree to compensate the University of Stuttgart for any resulting damage or to indemnify the University of Stuttgart against any third-party claims.

The right of use hereby granted to the University of Stuttgart extends to all known types of use and, in addition, the right to use the work results in research, teaching and study. This includes in particular the right of duplication and distribution, the right to process, modify and use of modified results as well as the right to make them publicly accessible on the internet and the right to transfer them to a third party without my renewed consent.

I am aware that granting the right of making my work publicly accessible also means that my name can be mentioned in connection with the title of the above-mentioned work on the websites of the University of Stuttgart. I am also aware that - if my work itself is not made accessible on the internet - the granting of the right to use public access also means that the University of Stuttgart can mention my name on its websites in connection with the title of the above-mentioned work (e.g. in lists of student work completed at the institute).

In addition, I transfer the ownership of a copy of my above-mentioned work to the University of Stuttgart, which I make available to the library of the Institute of Aircraft Design free of charge and grant the University of Stuttgart the above-mentioned rights of use for this copy as well.

Stuttgart, 04.05.2021 Jonas Mangold

Place, date, signature

[1] Based on the document "Einräumung von Nutzungsrechten an einer studentischen Arbeit" of the central administration of the University of Stuttgart from 29 September 2016.